# Inaugural Dissertation

**submitted to the**
**Combined Faculties for the Natural Sciences and for Mathematics**
**of the Ruperto-Carola University of Heidelberg, Germany**

**for the degree of**
## Doctor of Natural Sciences

**presented by**

## Katharina Hammer
**Diplom-Biochemikerin**
**Born in Arnstadt, Germany**


Date of oral examination: November 4th, 2014

# Engineering of oncolytic adenoviruses for delivery by mesenchymal stem cells to pancreatic cancer

**First referee:** **Prof. Dr. Martin Müller**

**Second referee:** **PD Dr. Dirk Nettelbeck**

# 1. Summary

Alternative treatment strategies for pancreatic cancer are urgently needed as all available therapies fail to work efficiently. Oncolytic adenoviruses are promising agents as they can be engineered to specifically replicate in tumor cells and subsequently lyse them (oncolysis). Oncolytic adenoviruses have shown an excellent safety profile in phase 1 and 2 clinical trials. However, these studies revealed a need for improvement of the therapeutic efficiency of the viral agents. The critical issues were the limited efficiency of tumor cell lysis and the poor delivery of the virus to the tumor site after systemic administration due to clearance by neutralizing antibodies and liver sequestration. The delivery problem was approached by using mesenchymal stem cells (MSCs), isolated from human bone marrow, as carrier cells to shield the virus from nonspecific uptake and neutralization. MSCs are established carriers to mediate targeted delivery of oncolytic adenoviruses to tumor sites in animal models. In this study, genetic modifications of oncolytic adenovirus were explored for improvement of the viral agent in the context of MSC delivery. The overall aim of the study was to identify those modifications, which mediated optimized adenovirus transduction and replication in MSCs, allowed unimpeded migration of infected MSCs for the time required for tumor homing, and mediated improved killing of the pancreatic cancer cells.

From a set of capsid variants, performed transduction experiments identified the fiber chimera 5/3, derived from adenovirus serotype 5 fiber with the cell binding domain of serotype 3, to consistently mediate most efficient transduction in MSCs as well as in established and low-passage pancreatic tumor cells. Ad5/3 served as capsid background in the subsequently investigated set of modified, replication-competent, oncolytic adenoviruses. The modifications included: i. the deletion of the viral gene *E1B19K* aiming at improved virus replication and release kinetics, ii. the transgene insertions of the shedded death ligand TRAIL to mediate bystander killing, and iii. the transgene insertion of the prodrug-converting enzyme FCU1, which mediates conversion of the systemically administered prodrug 5-Fluorocytosine to the chemotherapeutic agent 5-Fluorouracil, for additional tumor cell killing. Infection of MSCs with the *E1B19K*-deleted or TRAIL-modified viruses resulted in dramatically improved virus replication and release kinetics compared to a matching control virus. Further, it was shown that MSCs infected with the *E1B19K*-deleted or TRAIL-modified viruses maintained their migration properties over 2 days. This time span corresponds to the reported time MSCs need *in vivo* to home to a tumor after systemic administration. From these observations it was concluded that the investigated modifications have the potential to improve MSC-mediated virus delivery. Subsequently, the *E1B19K*-deleted, TRAIL-expressing, and FCU1-expressing viruses were tested in established pancreatic tumor cell lines for improved killing. All modified viruses showed enhanced tumor cell killing in a subset of cell lines. Further, virus spread and killing was investigated in low-passage pancreatic tumor cell cultures, as a clinically relevant model, and in MiaPaCa-2 spheroids, to mimic viral behavior in a 3D tumor structure. Also in these models, the results indicated that the analyzed virus modifications are suited to achieve more efficient tumor cell killing.

In the course of this study, virus mutants were identified, which possessed improved replication and release kinetics in MSCs, allowed unimpeded MSC migration, and showed enhanced pancreatic tumor cell killing abilities. Therefore, strategies to improve oncolytic adenoviruses for MSC-mediated delivery to pancreatic tumor sites were derived, which can contribute to improve clinical efficiency of adenovirotherapy.

# 2. Zusammenfassung

Behandlungsalternativen für Pankreastumore sind dringend notwendig, da derzeitige Therapien keinen ausreichenden therapeutischen Nutzen zeigen. Onkolytische Adenoviren sind hier vielversprechend, da sie so spezifisch modifiziert werden können, dass sie bevorzugt in Tumorzellen replizieren und sie anschließend töten (Onkolyse). In Studien der klinischen Phase 1 und 2 haben onkolytische Adenoviren ein gutes Sicherheitsprofil bewiesen. Es wurde jedoch die Notwendigkeit einer Effizienzverbesserung der viralen Vektoren aufgezeigt. Als kritisch erwiesen sich hierbei die Effizienz der Tumorzelllyse, sowie der Weg der Viren zum Tumor nach systemischer Applikation, da die meisten Viren entweder von Antikörpern neutralisiert oder von der Leber aufgenommen wurden. Der ungewünschte Verlust wurde durch die Verwendung von aus menschlichem Knochenmark isolierten mesenchymalen Stammzellen (MSCs) als Transportzellen umgangen, die das Virus vor ungewünschter Aufnahme und Neutralisation schützen. MSCs sind in Tiermodellen als spezifische Transportzellen von onkolytische Adenoviren zu Tumoren etabliert. In der vorliegenden Studie wurden genetische Modifikationen von onkolytische Adenoviren untersucht, die auf die Verbesserung der Viren im Kontext des MSC-Transports abzielten. Das Ziel des Projekts war, diejenigen Modifikationen zu identifizieren, die Virustransduktion, -replikation und -transport in MSCs, sowie anschließende Tumorzelltötung optimierten.

Aus einer Auswahl von Kapsidvarianten konnte in durchgeführten Transduktionsexperimenten die Fiberchimäre 5/3, die sich aus Adenovirus Serotyp 5 Fiber mit der zellbindenden Domäne von Serotyp 3 zusammensetzt, als am besten transduzierende Kapsidvariante bestimmt werden, sowohl in MSCs als auch in etablierten und niedrig-passagigen Pankreaskrebszellen. Das Ad5/3 Kapsid wurde für die anschließend untersuchten modifizierten, replikations-kompetenten, onkolytischen Adenoviren verwendet. Diese Modifikationen waren: i. die Deletion des viralen *E1B19K* Gens, um eine verbesserte Virusreplikation und -freisetzung zu erreichen, ii. die Insertion des Gens des Todesliganden TRAIL, für die Zerstörung benachbarter Tumorzellen, und iii. die Insertion des Gens *FCU1*, das die Prodrug 5-Fluorocytosin nach systemischer Applikation in das Chemotherapeutikum 5-Fluorouracil umwandelt, das zusätzlich Tumorzellen tötet. Die Infektion von MSCs mit den *E1B19K*-deletierten oder TRAIL-modifizierten Viren zeigte deutlich verbesserte Virusreplikations- und Virusfreisetzungs-Kinetiken. Ferner wurde gezeigt, dass die Migrationseigenschaften der MSCs über 2 Tage beibehalten wurden, auch wenn MSCs mit den *E1B19K*-deletierten oder TRAIL-modifizierten Viren infiziert waren. Diese Zeitpanne entspricht der Zeit, die MSCs *in vivo* benötigen, um den Tumor zu erreichen. Demzufolge waren die analysierten Modifikationen zur Verbesserung des Transports der Viren zum Tumor potentiell geeignet. Anschließend wurden die modifizierten Viren hinsichtlich ihrer Fähigkeit zur verbesserten Tumorzelltötung in etablierten Pankreaskrebszelllinien getestet. Alle modifizierten Viren zeigten verbesserte Lyse in einem Teil der Zelllinien. Weiterhin wurde Virusausbreitung und Zelltötung in niedrig-passagigen Zellkulturen, als ein klinisch relevantes Modell, und in MiaPaCa-2 Spheroiden, um das Virusverhalten in einer 3D-Tumorstruktur nachzustellen, analysiert. Auch in diesen Modellen wiesen die Ergebnisse darauf hin, dass die analysierten Modifikationen geeignet sind, um die Tumorzellzerstörung zu verbessern.

Im Laufe dieser Studie wurden Virusmutanten identifiziert, die verbesserte Replikations- und Freisetzungs-Kinetiken in MSCs zeigten, die Migration von infizierten MSCs zuließen, sowie eine verbesserte Tumorzelltötung aufzeigten. Daraus lassen sich Strategien ableiten, die zur verbesserten klinischen Effizienz der Adenovirotherapie beitragen können.

# 3. Table of Contents

# 4. Abbreviations

| | |
|---|---|
| 5-dUMP | 5-Fluorodeoxyuridine monophosphate |
| 5-FC | 5-fuorocytosine |
| 5-FU | 5-flurouracil |
| 5-FUMP | 5-Fluorouridine monophosphate |
| ADP | adenovirus death protein |
| ALDH | aldehyde-dehydrogenase |
| Amp | ampicillin |
| AMP | adenosine 5'-monophosphate |
| ANOVA | analysis of variances |
| Apo-1 | apoptosis antigen 1 |
| APS | ammounium persulfate |
| AraC | arabinosyl cytosine |
| ATP | adenosine 5'-triphosphate |
| Bcl-2 | B cell lymphoma 2 protein |
| bp | base pair |
| BPSA | human beta globin splice acceptor |
| BSA | bovine serum albumin |
| CAR | coxackie and adenovirus receptor |
| CD | cytosine deaminase |
| CDKN2A | cyclin-dependent kinase inhibitor 2A |
| CDx | cluster of differentiation |
| CMV | cytomegalovirus |
| CsCl | caesium chloride |
| DKFZ | German Cancer Research Center |
| DMEM | Dulbecco's Modified Eagle's Medium |
| DMSO | demethyl sulfoxide |
| DNA | deoxyribonucleic acid |
| dNTP | deoxyribonucleotide triphosphates |
| DTT | dithiothreitol |
| $EC_{50}$ | effective concentration 50 |
| EDTA | ethylenediaminetetraacetic acid |
| EGTA | ethylene glycol tetraacetic acid |
| ESA | epithelial surface antigen |
| EtOH | ethanol |
| FBS | fetal bovine serum |
| FCU1 | yCD-UPRT gene |
| fw | forward |
| GFP | green fluorescent protein |
| GM-CSF | granulocyte-macrophage colony-stimulating factor |
| HCl | hydrochloric acid |
| HEK | human embryonic kidney |

| | |
|---|---|
| HNSSC | head and neck squamous cell carcinoma |
| HR1/2 | homologous region 1/2 |
| HRP | horseradish peroxidase |
| HSV | herpes simplex virus |
| i..p. | intra-peritoneal |
| i.a. | intra-arterial |
| i.t. | intra-tumoral |
| i.v. | intra-venous |
| IFN-β | interferon-β |
| IL | interleukin |
| IMDM | Isocove's modified Dulbecco's medium |
| IRES | internal ribosomal entry site |
| Kan | kanamycin |
| kb | kilo base pairs |
| KCl | potassium chloride |
| kDa | kilo Dalton |
| K-Ras | Kirsten rat sarcoma viral oncogene homolog |
| LB | Luria Bertani medium |
| LB | Luria Broth medium |
| LDH | lactate dehydrogenase |
| LiCl | lithium chloride |
| LITR | left inverted terminal repeat |
| Luc | firefly luciferase |
| $MgCl_2$ | magnesium chloride |
| $MgSO_4$ | magnesium sulfate |
| min | minutes |
| MLP | major late promoter |
| mRNA | messenger ribonucleic acid |
| MSC | mesenchymal stem cell |
| n.s. | not significant |
| NaCl | sodium chloride |
| NDV | newcastle disease virus |
| NF-κB | nuclear factor kappa-light-chain-enhancer of activated B cells |
| NH medium | nonhematopoietic stem cell expansion medium |
| NSC | neuronal stem cell |
| OD | optical density |
| p.i. | post-infection |
| pA | polyadenylation |
| Pb | Polybrene |
| PBS | phosphate buffered saline |
| PCR | polymerase chain reaction |
| PMSF | phenylmethylsulfonyl |
| pRb | retinoblastoma protein |
| RITR | right inverted terminal repeat |
| RLU | relative luminescence units |
| rpm | rounds per minute |

| | |
|---|---|
| RPMI | Roswell Park Memorial Institute medium |
| rv | reverse |
| s.c. | subcutaneously |
| SA | splice acceptor site |
| SD | standard deviation |
| SDS | sodium dodecyl sulfate |
| SDS-PAGE | discontinuous sodium dodecyl sulfate polyacrylamide gel electrophoresis |
| sn | supernatant |
| SV40 | simian virus 40 |
| $TCID_{50}$ | tissue culture infectious dose 50 |
| TEMED | N,N,N',N'-tetra-methylethylenediamine |
| TNF | tumor necrosis factor |
| TRAIL | TNF-related apoptosis-inducing ligand |
| Tris | trizma base |
| Tris-HCl | trizma hydrochloride |
| T-VEC | Talimogene Laherparepvec |
| UPRT | uracil phosphoribosyltransferase |
| UV | ultraviolet |
| v/v | volume per volume |
| vp | viral particles |
| VSV | vesicular stomatitis virus |
| w/v | weight per volume |
| XTT | 2,3-bis(2-methoxy-4-nitro-5-sulfophenyl)-2H-tetrazolium-5-carboxanilide |

# 5. Introduction

## 5.1. Pancreatic Adenocarcinoma

### 5.1.1. The Pancreas and Pancreatic Cancers

The pancreas is a gland in proximity to the duodenum and behind the stomach. It is anatomically subdivided into tail, body, and head and traversed by a duct system (**Figure 1**). Histologically, the pancreas is composed of gland tissue that can be distinguished into an endocrine and an exocrine part. The exocrine gland cells produce fluids containing digestive enzymes, which are transported via the drainage duct system into the duodenum [2]. The endocrine gland cells of the pancreas are clustered in the Langerhans islets and produce a variety of hormones, including insulin and glucagon, which after release into the blood are responsible for regulating the blood glucose level [3].

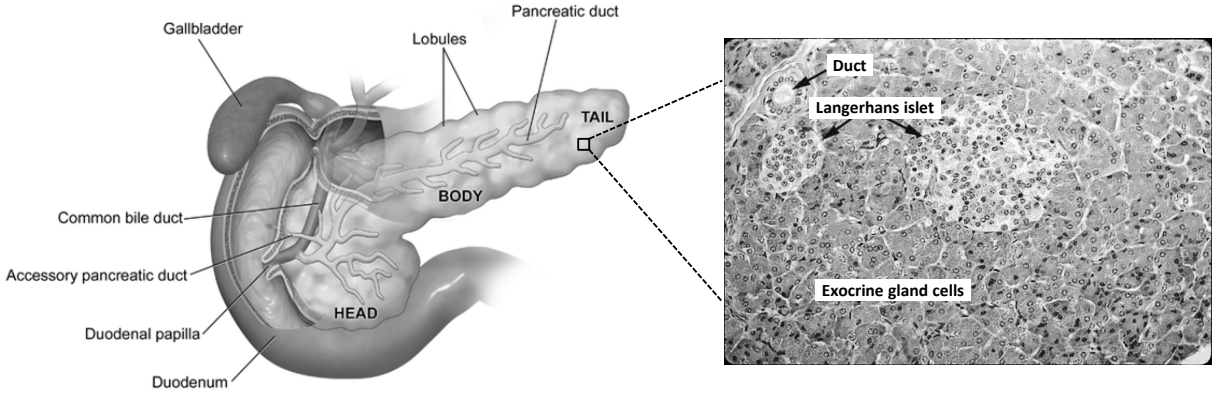


**Figure 1: Anatomy of the Pancreas and its Surroundings.** The pancreas is structurally subdivided into tail, body, and head, traversed by a duct system which ends in the pancreas head into the duodenum. The right panel shows a histological image of a duct and Langerhans islets surrounded by the exocrine gland cells. (Adapted from http://upload.wikimedia.org and http://www.siumed.edu)

Malignant transformation of cells in the pancreas leads to pancreatic cancer. Pancreatic cancer accounts for 3% of all newly detected cancer cases and is the 10$^{th}$ most frequently occurring cancer [4]. Due to a 5-year-survival rate of only 6%, it accounts for 6% of cancer death cases. It is therefore the 4$^{th}$ most frequent cause of cancer death in the US [4]. However, a differentiation of the pancreatic cancer cases is necessary as the pancreas is composed of many different cell types which lead to a variety of tumors with different prognoses and treatment requirements.

The by far most frequent entity, with >85% of occurring pancreatic cancers, are adenocarcinomas [5], which arise from malignant transformation of the exocrine cells lining the ducts [5, 6]. These tumors are poorly treatable and the reason for the bad prognosis for pancreatic adenocarcinomas [4]. Other exocrine cell types present in the pancreas, like acinar cells, giant cells, mucinous cells, or signet ring cells can also form tumors, but these are very infrequent [7]. Cancers of the endocrine pancreatic islet cells are very rare (1% of pancreatic cancer cases) [7]. These cancers are characterized by production of vast amounts of the hormones insulin or glucagon, but are often slow-growing, better treatable, and have a 5-year survival rate of 42% [8].

In public discussions, the term pancreatic cancer is usually used synonymously for pancreatic adenocarcinomas [7], as all other occurring tumors neither show a similar frequency nor similar

treatment difficulties. Long-term statistics show that survival for pancreatic adenocarcinoma patients has not significantly improved over the last three decades [4]. Therefore, this cancer is considered one of the most aggressive occurring cancers with urgent need for treatment improvement.

### 5.1.2. Pancreatic Adenocarcinoma Genetics and Risk Factors

Tumorigenesis is a multistep process that requires the accumulation of genetic mutations. Cancers of one cell type in different individuals can therefore be genetically very different. However, there are some common mutations which can be found in the majority of pancreatic adenocarcinomas. Common modifications are activating mutations of K-Ras (95%) [9] and inactivating mutations of p16 (CDKN2A, 98%) [5]. Furthermore, mutations in p53 are frequently occurring (70%) [10]. 97% of pancreatic adenocarcinomas show chromosomal instability [5]. Familial pancreatic cancer seems to be rare, though germline mutations of e.g. CDKN2A (p16) have been reported [11]. Identified risk factors include cigarette smoking, increased body mass index, and the consumption of red meat and dairy products, though the contribution of the dietary factors is controversially discussed [12, 13]. Also diabetes mellitus, alcohol intake, and chronic pancreatitis are considered to be risk factors [12].

### 5.1.3. Treatment of Pancreatic Adenocarcinomas

If pancreatic adenocarcinoma are detected in the early stages of tumor development, a resection is possible following the Whipple procedure (pancreaticoduodenectomy), where part of the pancreas, duodenum, gallbladder, and part of the bile duct are removed [12]. However, due to the lack of symptoms during the early stages of the tumor, 80% of the tumors are diagnosed in advanced stages, where resection is already impossible because of locally advanced disease and metastases [12]. Metastases often occur in abdomen, liver, lung, bone, and brain [14]. In this stage, chemotherapy is the method of choice. The most commonly used chemotherapeutics are gemcitabine and 5-Fluorouracil (5-FU) [14, 15] (**Figure 2**). However, both drugs do often not have a significant therapeutic effect, even though some studies suggest that gemcitabine has a slightly better effect than 5-FU [16, 17]. For treatment, both of them are combined with radiation (here, they function as sensitizers [18]) or other chemotherapeutic agents, such as cisplatin and oxaliplatin [19].

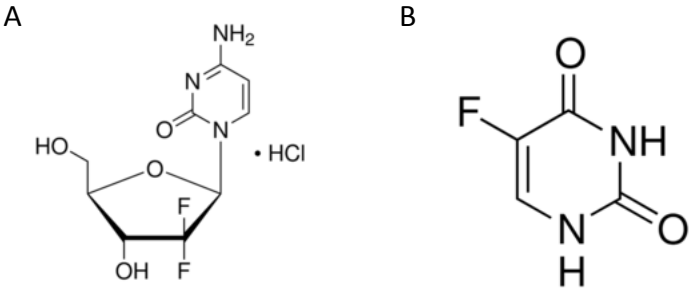


**Figure 2: Gemcitabine and 5-Fluorouracil. A:** Gemcitabine is a nucleoside analog and, when introduced instead of cytidine, during DNA replication, causes growth arrest and apoptosis. **B:** 5-FU is an antimetabolite of thymidine and an irreversible inhibitor of the thymidylate synthase. Thymidylate synthase converts 5-dUMP into dTMP and inhibition therefore leads to nucleotide shortage [1]. (Images taken from www.sigmaaldrich.com)

The median survival of the resectable pancreatic adenocarcinomas is between 15 to 19 months and the 5-year survival is around 20% [12]. For advanced disease, treatment usually only aims for palliative care and prolonged survival. Even with treatment, the median survival after diagnosis is less than 12 months [12].

## 5.2. Cancer Stem Cell Theory

The theory that tumors are composed of a heterogeneous mass of cells was first published in 1976 [20]. The theory that every cancer cell can equally acquire genetic alterations that lead to improved growth and metastatic behavior (stochastic model), is today complemented by the theory of a hierarchical order in cancer tissue similar to normal tissue (hierarchical model) [21]. According to the hierarchical model, a distinct subpopulation of tumor cells has the ability for tumor initiation, progression, persistence, and development of metastasis [22]. Referring to the parallels of the function of stem cells in normal tissue, these cells are termed cancer stem cells. The origin of these cells is discussed controversially. They could either rise from somatic stem cells and acquire genetic alterations or from lineage-committed cells that re-acquire stem cell-like characteristics [23].
Previous studies have described the cancer stem cells as highly resistant to chemotherapy due to high expression of membrane transporters, distinct DNA repair mechanisms, reduced immunogenicity, increased expression of anti-apoptotic genes, low proliferation rate, and high levels of telomerase [23]. Due to the predominantly quiescent state of cancer stem cells [24] the impact of cell cycle-dependent chemotherapeutics, like gemcitabine and 5-FU, is very limited [25]. Chemotherapy often even led to selective killing of non-stem-cell-like cancer cells and consequently to an enrichment of the cancer stem cell population, which can lead to tumor reoccurrence [26] and re-establishing of a tumor with a similar morphology than the original tumor [27, 28]. As a consequence, a successful cancer therapy should aim to target these tumor-initiating cells with a new generation of therapeutic agents, which do not depend on replication of the cancer cells and overcome the described resistance mechanisms.
In pancreatic adenocarcinomas, cancer stem cells were first described in 2007. Li et al. [28] identified a small subpopulation of cancer cells, which after subtransplantation in mice could undergo self-renewal and could re-establish the tumor with a morphology similar to the primary tumor. This subpopulation with tumor-renewal capacity was identified to have a characteristic surface marker pattern of CD44+/CD24+/ESA+. This population of cells made up <1% of the entire cancer cells population, but had a 100-fold increased tumorigenic potential than the bulk tumor cells [28]. In the same year, CD133+ was reported to be another cancer stem cell marker [29] and later, c-Met was added to the list of potential marker candidates to identify cancer stem cells [27, 30]. The identification of these cells is not only possible based on surface marker profile, but characteristics as K-Ras/p53 mutation, colony/spheroid formation ability, ALDH activity, E-cadherin expression, and Vimentin overexpression [31] are also used.
These characteristics and the variety of possible markers indicate that the cancer stem cells might not be an exclusive subpopulation of cells, but subject to clonal evolution themselves [32].

## 5.3. Virotherapy

A very promising approach to overcome chemotherapy resistance of cancers and targeting the cancer stem cells is virotherapy. Virotherapy uses a replication-competent virus that selectively infects, replicates, and kills the tumor cells through oncolysis. The released progeny viral particles lyse in the following replication rounds initially uninfected tumor cells (**Figure 3**). The key advantages of these therapeutical agents are that: i. the viral agent is propagating itself and producing progeny therapeutic material, ii. it is specific for cancer cells and has therefore limited side effects in normal tissue, iii. killing by some viruses (e.g. oncolytic adenovirus) does not depend on replication of the cancer cell and therefore stem cells cannot escape the treatment.

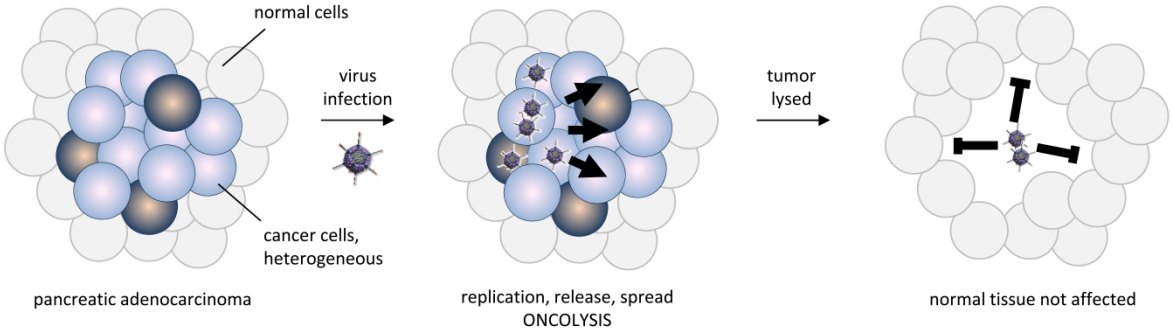


**Figure 3: Principle of Virotherapy.** The virus infects the tumor cells and replicates. The host cell is killed through oncolysis and viral progeny is released, which spreads to the initially uninfected tumor cells. Non-malignant cells are not able to propagate the virus. Therefore, virus spread is aborted with the complete lysis of the tumor.

In the past years, several viruses have been investigated as oncolytic agents. These included viruses with inherent pathogenicity towards tumors, as NDV (newcastle disease virus), VSV (vesicular stomatitis virus), or reovirus [33]. Their selectivity for tumor cells as hosts is due to the similarity of the cellular modifications during virus infection and carcinogenesis, e.g. Ras-pathway activation, and IFN-pathway deregulation [33]. These viruses therefore preferentially replicate in cells featuring these mutations. Other viruses were specifically engineered to target tumor cells, as adenovirus, vaccinia, influenza, polio, measles, or herpes simplex virus [34]. Some of the engineering strategies for oncolytic adenoviruses are explained in **section 5.5**.

So far, performed clinical trials with oncolytic viruses resulted in low toxicity and very few adverse side effects, which disproved safety concerns of uncontrolled virus effects in non-target regions [34]. However, therapeutic efficiency still needs to be improved for most viruses. The first clinical approved oncolytic virus is the oncolytic adenovirus H101 in China [35]. Several viruses are in advanced phases of clinical trials in Europe and the USA. T-VEC, an oncolytic herpes simplex virus expressing GM-CSF, is close to approval. With this virus, several clinical trials in head and neck cancer (NCT01161498) and melanoma (NCT00769704 and NCT01368276) were successfully completed. In a clinical Phase 3 trial of intralesional injection of melanoma with T-VEC compared to GM-CSF alone (NCT00769704), the virus was superior to the single treatment with GM-CSF and reached the primary endpoint (6 months durable response) [36, 37]. Further viruses, which are also in Phase 3 trials, are CG0070, an oncolytic adenovirus expressing GM-CSF against bladder cancer (NCT01438112), oncolytic herpes simplex virus HSV1716 against glioblastoma (UK-0177 and UK-0136), and an oncolytic reovirus, Reolysin, in combination with chemotherapy against head and neck cancer (NCT01166542).

Besides the direct oncolysis, other mechanisms were shown to contribute to tumor cell killing. First, oncolytic viruses where shown to have antivascular function by either anti-angiogenic properties (e.g. downregulation of VEGF by oncolytic adenovirus) [38] or infection and lysis of tumor endothelial cells (e.g. vaccinia virus, HSV) [39]. In clinical trials, antivascular activity has been shown for the oncolytic vaccinia virus JX-594 [40]. Second, oncolytic viruses were shown to induce the adaptive immune system [34, 41]. The infection and lysis by the oncolytic viruses causes the releases of danger signals and tumor cell proteins, which function as tumor-associated antigens. Following presentation, they elicit a tumor-specific immune response [41]. The presence of tumor-specific T-cells following infection with oncolytic viruses was shown in clinical studies with the modified

oncolytic adenovirus Ad5/3-Δ24-GM-CSF [42], oncolytic HSV T-Vec [43], and the oncolytic vaccinia virus JX-594 [44]. However, these alternative targeting strategies were not pursued in the course of this thesis.
In summary, the outcome of the clinical trials was very promising. However, the viral agents need to be further modified to gain specific and improved oncolytic activity.

## 5.4. Adenovirus

### 5.4.1. Structure and Serotypes

Adenoviruses are classified in four genera. The human adenoviruses belong to the genera Mastadenovirus and are subdivided into 52 serotypes. Diseases caused by adenoviruses in humans include infections of the upper respiratory track, conjunctivitis, and pneumonia. In immuno-competent individuals, all serotypes cause relatively mild infections [45].
The adenoviral capsid has an icosahedral structure with a diameter of 80-110 nm and is non-enveloped. The capsid contains three major proteins: hexon, penton base protein, and fiber (**Figure 4A**). The sides of the surface areas are multimeres of hexons. Each corner is composed of a pentamer of penton base proteins, which are the anchor for the fiber. The fiber is a trimeric protein, which is structurally divided in a tail, shaft, and knob (**Figure 4B**). The tail mediates the binding of the fiber to the penton base. The central fiber shaft varies in lengths and flexibility dependent on the adenovirus serotype. The initial attachment to the host cell is mediated by the knob, the structure at the outer tip of the fiber. The knob binds to a receptor, which differs depending on the adenovirus serotype, e.g. for HAdV-3: Desmoglein-2 [46] and CD46 [47], for HAdV-5: Coxsackie and Adenovirus Receptor (CAR) [48]. Subsequently, internalization is mediated by binding of integrins of the host cell to the penton base (**Figure 4C**).

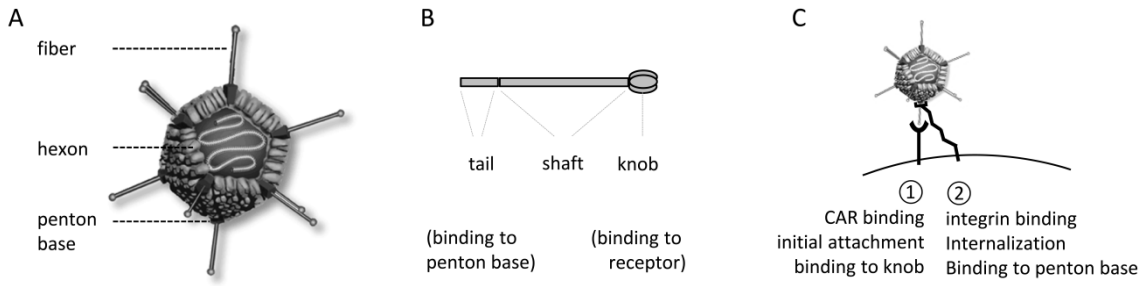


**Figure 4: Adenovirus Particle Composition and Description of Attachment. A:** Structure of the viral particle. The core is composed of hexon proteins and the corners of the icosahedron of penton base proteins, which are the anchor for the fiber. **B:** Detailed structure of the fiber. The tail is mediating the contact to the penton base. **C:** Two-step process of viral attachment and internalization.

### 5.4.2. Replication Cycle

The adenovirus replication cycle can be subdivided into several steps [45] (**Figure 5**). First, the adenovirus knob binds to the primary receptor on the host cell surface (HAdV-5: CAR, HAdV-3: Desmoglein-2, CD46). Following this first attachment, a second interaction is mediated via an RGD motif in the penton base with integrins $\alpha_v\beta_3$ or $\alpha_v\beta_5$ on the host cell. This interaction results in internalization of the surface-bound viral particles via clathrin-coated vesicles. In the endosome, the pH falls, the viral particles dissociate from the endosome membrane, and subsequently the endosomes are lysed. After shedding of capsid-associated proteins, the remaining capsid parts with

the viral DNA bind to dynein and are transported into the nucleus via the nuclear pores. In the nucleus, the virus DNA is replicated and transcribed in the following order: i. transcription of immediate early genes, ii. transcription of early genes, iii. DNA replication, iv. transcription of late genes. Following translation, several proteins, including hexon, penton base, and fiber, assemble into capsomeres with the help of chaperones, and the viral DNA is integrated into the particle. Finally, through induction of host cell desintegration, release of progeny viral particles is initialized.

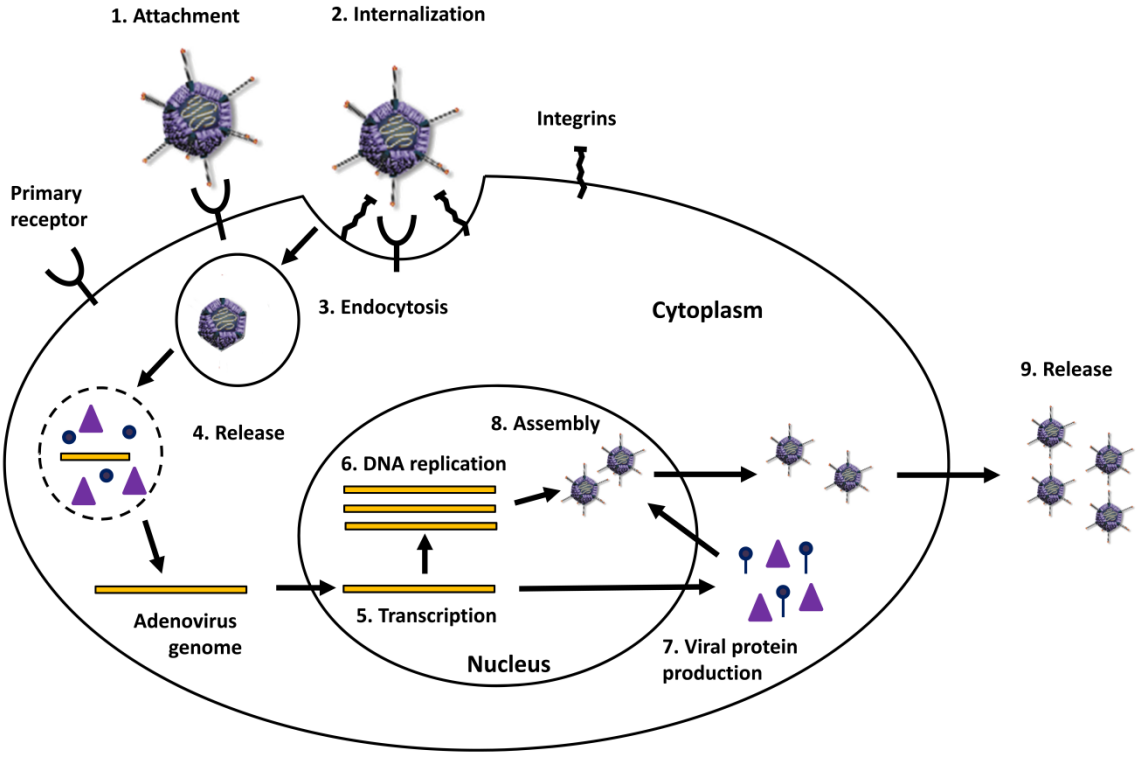


**Figure 5: Schematic Outline of the Viral Replication Cycle.** Binding to the primary receptor (1) and to integrins (2) triggers clathrin-dependent endocytosis (3). After acidic endosomal escape (4), the genome is translocated into the nucleus. Transcription is initiated (5), following adenoviral genome replication (6) and adenoviral protein synthesis (7). Finally, the progeny viral particles are assembled (8) in the nucleus and are released from the cell by host cell lysis (9). (Modified from http://ssg-adenovirus.blogspot.de/)

### 5.4.3. Genome Organization and Viral Proteins

The genome of adenoviruses is a linear, double-stranded DNA with both strands having coding function. The genome is structurally subdivided into 5 areas (**Figure 6**) [45]: Four for early expressed gene regions (*E1-E4*) and one for late gene expression (L, encoding mainly structural proteins). The genome is flanked on each site by inverted terminal repeats, which have a function in the initiation of virus replication. The order of transcription initiation is progressive, starting with the immediate early *E1* genes, *E1A* and *E1B*. The *E1* gene products mediate the activation of the transcription factor E2F. The products of E2F-mediated transcription activate the viral DNA polymerase which leads to transcription of the other early genes in the order *E2* to *E4*. Finally the major late promoter (MLP) is activated, starting the transcription of the late genes (*L1-L5*). The transcription of *E1* itself depends on host cell proteins.

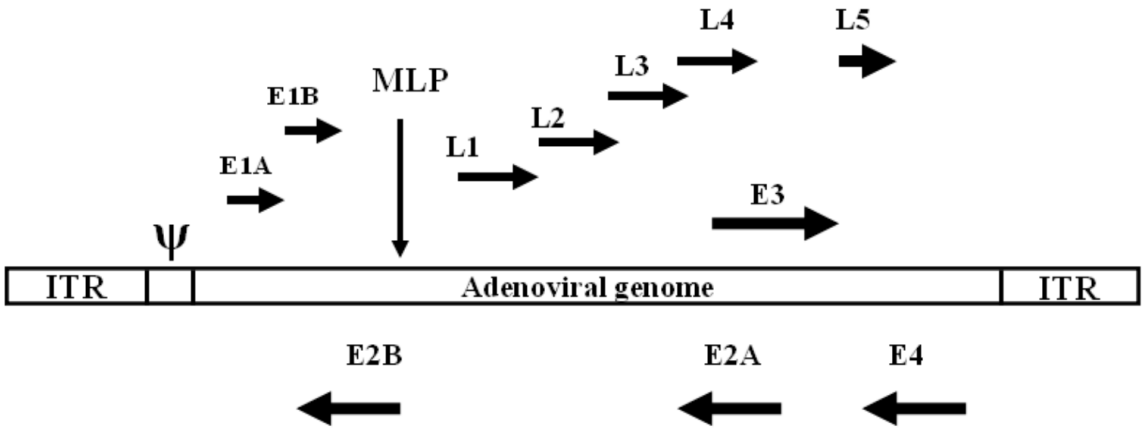


**Figure 6: Scheme of the Adenovirus Genome.** ITR: inverted terminal repeat, Ψ: packaging signal, *E1* to *E4*: early genes, *L1* to *L5*: structural genes, MLP: major late promoter. Modified from [49]

Key functions of viral proteins are i. the modification of cell cycle factors to support virus replication and ii. the regulation of host cell death to allow a full viral replication cycle. This is achieved through the interaction of viral proteins with apoptosis and cell cycle-regulating proteins of the host cell.
The E1A proteins are the key players for transforming the host cell from a quiescent into a proliferating state. Through binding of E1A to the retinoblastoma protein (pRb), the E2F transcription factor is released and mediates cell cycle progression [50, 51].
The regulation of host cell death is mediated by a variety of viral proteins. On the one hand, the viral life cycle kinetics aim for efficient viral replication and progeny release, but on the other hand viral replication needs to be regulated in a way that the host cell integrity is maintained until the progeny viral particles are fully developed. Release of premature virus particles would not support maximal further spread and is therefore evolutionary unreasonable. Several viral proteins featuring pro- and anti-host cell survival functions regulate this process. The key players featuring anti-apoptotic functions are the two *E1B* gene products, E1B55K and E1B19K. E1B55K binds to p53, therefore abrogates the normal apoptotic mechanisms of the cell [52], and inhibits the induction of apoptosis [53]. E1B19K is a Bcl-2 analog [54]. It can bind and therefore neutralize the action of pro-apoptotic Bax protein [55], and thus interferes with the intrinsic apoptosis pathway. Additionally to the two E1B proteins, products of the *E3* gene block the extrinsic induction of apoptosis. Proteins encoded by the *E3B* gene region (E310.4K/14.5K) down-modulate apoptosis by inducing internalization of the apoptosis receptor Fas/Apo-1 [56].
The key player featuring pro-apoptotic function is the E1A protein. The E1A protein can induces apoptosis via accumulation of p53 through inhibition of p53-degrading processes [57], but also through p53 independent processes [58]. Additionally, the virus expresses a protein which is necessary for efficient lysis, called the adenovirus death protein, ADP [59], encoded in the *E3* region. In summary, all these proteins regulate a fine tuned balance to achieve optimal virus replication and release kinetic for optimized progeny spread.

The following summary of adenoviral genes and proteins (**Table 1**) is not complete but explains the proteins' functions with importance for this project:

**Table 1: Adenoviral Genes, Gene Products, and Function.**

| Immediate early genes | | Protein functions |
|---|---|---|
| *E1* | | Responsible for modification of the host cell |
| | ***E1A*** | 3 strongly conserved regions (CR1-CR3), induces transcription of E2 - E4: CR1 and CR2 interact with tumor suppressor **pRb**, abolishes pRb binding to the E2F transcription factor, E2F initiates transcription<br>Mediates apoptosis induction |
| | *E1B* | **E1B19K**: inhibits the intrinsic apoptosis pathway through binding of the Bax proteins and therefore counteracts the pro-apoptotic function of E1A<br>**E1B55K**: interaction with the transactivation domain of **p53**, leads to ubiquitinylation and therefore proteolytic degradation of p53 |
| Early genes | | |
| *E2* | *E2A, E2B* | Codes for proteins with function in replication of viral DNA and viral DNA-polymerase |
| *E3* | | 7 proteins, not essential for viral replication but for persistent virus infection |
| | *gp19K* | Reduces concentration of MHCI proteins on host cell surface |
| | *E3B* | Reduce sensitivity towards TNFα-induced apoptosis via Fas receptor internalization |
| | *ADP* | Responsibilities in cell lysis and release of virus progeny from host cell |
| *E4* | | ORF 1-7, various functions in transcription control, regulation of splicing of late genes |
| | *ORF6* | binds p53 like E1B55K |
| Late genes | | |
| *L1-L5* | | Structural proteins, transcription under control of the **major late promoter**, 30 kb pre-transcript |

## 5.5. Oncolytic Adenoviruses

Adenoviruses are frequently used as oncolytic tools. Historically, adenoviruses can be considered as a prototype for virology research. Several aspects of early basic virology studies have been elucidated with adenoviruses, including host cell transformation mechanisms [60, 61]. This early research resulted in a good genomic and functional characterization, which made it possible that adenovirus genomes can be easily manipulated and that the virus can be purified to high-titers [62]. These were prerequisites for their use as oncolytic agents. Early clinical studies in the 1950's started to test wild type adenoviruses of different serotypes for treatment of cancer patients [63]. The results showed that the viruses were generally safe, as no severe side effects were observed, but not sufficient to induce durable effects [63]. In the 1990's, the next generations of oncolytic viruses had modifications for cancer cell specificity as well as improved oncolysis [63]. Still, no severe adverse side effects were observed whereas the oncolytic efficiency still needed to be improved in terms of effective infection, effective replication, and effective lateral spread [62, 63]. The means to improve these features are modifications of the viral capsid for improved entry, modification of viral genes for improved replication kinetics, and the insertion of transgenes for improved killing. The following paragraphs describe the most common modifications and primarily the ones that were employed in this study.

### 5.5.1. Capsid Engineering for Improved Infection

Historically, oncolytic adenoviruses are typically based on human Adenovirus Serotype 5 (HAdV-5), as were all the viruses used for this study. The receptor of HAdV-5, CAR (Coxsackie- and Adenovirus Receptor), was demonstrated to be poorly expressed on tumor cells in previous studies [64, 65]. Therefore, alteration of the fiber in order to re-target virus entry to proteins that are more abundantly expressed on tumor cells is essential.

A promising modification is the substitution of the knob region of HAdV-5 by the knob of HAdV-3, resulting in a fiber Ad5/3 chimera [66]. The initial host cell contact is then retargeted to Desmoglein-2 [46], which is part of the desmosomes and ubiquitously expressed on normal and cancer cells. As the penton base and the fiber shaft remain unaltered, the secondary interaction for internalization is still mediated by integrin binding (as explained in **Figure 4C**). An alternative modification is the introduction of an RGD peptide into the HI-loop in the virus HAdV-5 knob, resulting in the Ad5RGD variant [67]. In this case, the initial and the secondary binding are depending on integrins, which are also ubiquitously expressed on cancer cells. Studies reported that both capsid modifications have resulted in improved transduction of tumor cells [66, 68-70]. It is important to note that these modifications improve tumor cell targeting, but they are not tumor specific. Tumor specificity is achieved by targeted delivery and transcriptional regulation, which are explained below.

### 5.5.2. Viral Gene Modification for Selective Replication

The safety of the viral agents has always been an issue in oncolytic virotherapy. It has to be assured that cancer cells are targeted while normal cells remain unaffected by exploiting molecular differences between these cells. In order to make viral replication specific for cancer cells, the immediate early genes *E1A* and *E1B55K* have been altered. *E1A* and *E1B55K* bind to pRb and p53 respectively, and mediate cell cycle progression and inhibition of apoptosis induction ([51, 52] and **section 5.4.3**). These functions are crucial for the performance of the virus life cycle. Modifications that abrogate the functionality of these proteins would promote viral replication selectively in cells, where these pathways are otherwise deregulated, namely in cancer cells. The functional E1A and E1B55K proteins are then not necessary to initiate viral replication or to inhibit apoptosis. Therefore, *E1A* and *E1B55K* modified viruses would preferentially replicate in cancer cells and not in normal cells.

Binding of the viral protein E1A to pRb releases the transcription factor E2F, which then initiates S-phase entry of the host cell cycle. This is a prerequisite for viral DNA replication (**Figure 7A, B**). Whyte et al [71] reported that the binding of E1A to pRb is mediated by two regions (amino acids 30-60 and 120-127 of E1A) and deletion of either one abrogates binding to pRb. Heise et al. [72] and Fueyo et al. [73] were the first to report an adenovirus mutant with a deletion in *E1A* (24 bp, which refer to amino acids 121-128). The mutated gene is referred to as *E1AΔ24*. Through this mutation, the viral E1A protein is unable to bind to pRb, E2F is not activated, S-phase entry is not triggered, and therefore viral replication is not induced in untransformed quiescent cells (**Figure 7C**). Consequently, the *E1AΔ24* mutation makes viral replication selective for cancer cells with mutated pRb and constitutively active E2F, where the S-phase entry initiation through the virus E1A protein is not necessary for induction of virus replication (**Figure 7D**). Previous publications showed that the *E1AΔ24* deletion does not interfere with virus replication in various cancer types [73, 74]. All of the described oncolytic viruses in this project have the *E1AΔ24* deletion.

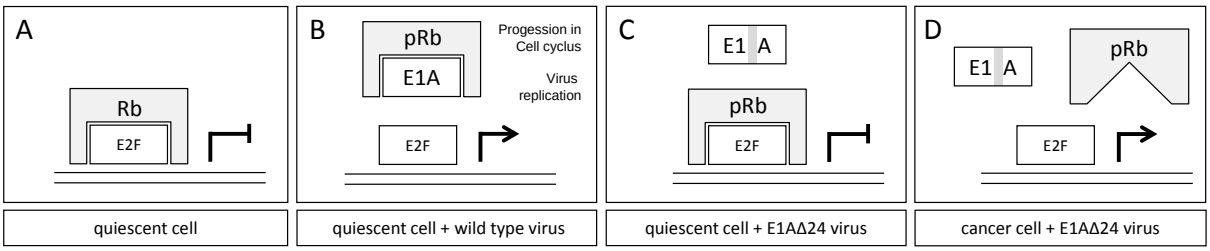


**Figure 7: Mechanistic Overview of E1A / E1AΔ24 and S-Phase Induction. A:** In untransformed, quiescent cells, pRb binds to the E2F transcription factor. In order to enter the S-phase, pRb needs to be phosphorylated by cyclin-dependent kinases, which releases its binding to E2F. E2F can then acts as a transcription factor and initiate replication. **B:** When adenoviral E1A protein is present, E1A binds to pRb, which therefore releases E2F. This initiates cell cycle progression as well as viral replication. **C:** When the amino acids responsible for E1A-binding to pRb are deleted (Δ24), binding is inhibited and therefore S-phase entry and initiation of viral replication is abrogated. **D:** In cancer cells with mutated pRb, the progression of the cell cycle is not anymore controlled by the interaction of pRb and E2F and cell cycle progression is continuous. Therefore, viral replication of an E1AΔ24 virus can be initiated without an interaction of E1A and pRb.

Through deletion of *E1B55K*, which was first described by Bischoff et al. [75], viral replication was supposed to take place in p53-mutated cells only, where the p53 function is already deregulated. However, studies showed that this selectivity was not achieved due to several mechanisms as reviewed in Everts et al. [33]. The strategy of Δ*E1B55K* modification was not investigated during this project.

### 5.5.3. Viral Gene Modification for Improved Replication and Release

As already mentioned above, adenovirus has evolved mechanisms to ensure the completion of the viral life cycle via proteins with anti-apoptotic functions. These are, beside E1B55K, E1B19K and E3B. Deletion of these anti-apoptotic genes aims for improvement of the oncolytic properties and therefore tumor lysis. The mechanistic rationale behind this strategy is that the pro-apoptotic function of the E1A protein is more pronounced when the anti-apoptotic proteins E1B19K and/or E3 are deleted [76]. Therefore, the virus life cycle kinetics could be enhanced and therefore the viral agent improved for virotherapy. Concerns that the deletion of anti-apoptotic genes could lead to premature abrogation of the viral life cycle proved to be untrue in cancer cells [77]. The outcomes of performed studies are summarized in the following.

Several studies have analyzed viruses with deleted *E1B19K* and/or *E3B* [76, 78-81]. Deletion of *E1B19K* resulted in enhanced viral replication and release in a variety of tumor cell lines including pancreatic adenocarcinoma [76, 79]. The therapeutic effect was even more increased in combination with chemotherapeutics and was sufficient to overcome chemotherapy-resistance in cell lines [76, 82]. These studies also reported that the observed phenotype was greatly impaired in normal cells compared to cancer cells [76, 79, 80]. It was suggested by Liu et al. [78] that this can possibly be explained with the regulation state of the apoptosis pathways. In normal cells, infection with a virus without a functional *E1B19K* and, therefore, with a pronounced pro-apoptotic phenotype, causes abrogation of viral replication due to increased apoptosis induction. In cancer cells, the apoptosis pathways are deregulated. Infection with the same virus cannot induce apoptosis and the viral replication cycle is thus maintained. While the detailed mechanisms are not fully understood, it seems that deletion of *E1B19K* can contribute to tumor cell-specific viral replication [80].

The deletion of E3B was also shown to enhance viral replication [79]. However, all the oncolytic viruses used in this study are E3 deleted. In order to generate oncolytic viruses with additional

transgenes in the genome, inherent genome parts need to be deleted. The total adenovirus genome size cannot be enlarged much as capsid capacity is limited. Some studies advised the retention of the wild type E3 [79], as deletion of E3B was shown to enhance clearance, and the ADP protein promotes viral spread [83]. Yet, the E3 protein is not essential for viral replication. Therefore, deletion of E3 is a strategy which is widely used for transgenes carrying adenoviruses in ongoing clinical trials and was the strategy of choice in this project.

### 5.5.4. Transgene Insertions for Improved Lateral Killing

One challenge of efficient oncolytic adenovirus therapy is the limited spread of the virus through the tumor mass. Due to the strong stromal reaction in pancreatic adenocarcinomas [84], which is not permeable for viral particles, some parts of the tumor might not be reached by the virus [85, 86]. As a consequence, the insertion of transgenes into the virus genome, which induces bystander killing of neighboring, non-infected cells, has been exploited. One possible “arming” strategie is the insertion of genes encoding pro-apoptotic proteins, which are small enough to diffuse across the stromal barrier [87].

In this study, this problem was approached by the insertion of a gene, whose protein product induces tumor cell-specific apoptosis. The sheddable membrane protein TRAIL (TNF-related apoptosis inducing ligand) binds to death receptors and induces the extrinsic apoptosis pathway [88]. Clinical trials have shown its cancer cell-specific toxicity [89] compared to non-malignant cells. Further, the feasibility of TRAIL delivery by a replication-deficient viruse was shown [90]. In a mouse model, a therapeutic benefit was achieved through the combination of oncolysis and TRAIL killing by i.t. injection of a replication-competent, TRAIL expressing adenovirus, compared to virus treatment alone in bladder cancer xenografts [91]. These studies indicate that improved tumor cell killing by arming oncolytic adenoviruses with TRAIL is feasible.

A critical point of arming viruses with genes encoding toxic proteins is to not interfere with the viral replication cycle. The virus produces a toxic protein, which is shedded and kills the tumor cells, including the ones with ongoing viral replication. However, the virus needs a viable tumor host cell to perform the complete replication cycle. Premature apoptosis of an infected tumor cell could abort the virus life cycle and no functional progeny virus would be produced. Studies evaluating insertion strategies for transgenes have revealed that expression with the late viral genes under control of the major late promoter towards the end of the viral replication cycle allows both, efficient transgene expression as well as completion of the viral life cycle [92]. An identified successful strategy was to couple transgenes via an IRES (internal ribosomal entry site) to a late gene, like the fiber gene [93]. Further studies showed that transgene expression can also be successfully achieved by insertion via a splice acceptor site (SA) downstream of the E4 gene [93, 94].

Other possibilities to improve tumor killing via “arming” include degradation of the tumor stroma via insertion of genes encoding hyaluronidase [95] or metalloproteinases [96] for improved viral spread. Further, genes encoding antiangiogenic proteins such as endostatin [97], immunomodulators like GM-CSF [98] or interleukins (reviewed in [99]) to induce a tumor-specific immune response have been investigated. One of the most widely used methods of arming is the insertion of genes encoding prodrug converting enzymes, which was used in this study and is discussed in the following section.

## 5.6. Prodrug Activation System

Common chemotherapeutics have the disadvantage that after being applied systemically, they do not specifically target tumor cells but all dividing cells in the body, which causes severe side effects. Further, due to various reasons including drug dose limitations, the tumor cannot be completely eradicated and the treatments are therefore insufficient. The principle of a prodrug activation system is that a non-endogenous enzyme is delivered to the tumor site, which can convert a non-toxic, systemically-applied prodrug into a tumor-toxic drug. If the drug is diffusible, an effective bystander killing can be accomplished at the tumor site. Therefore, this strategy avoids systemic side effects, as occurring during treatment with standard chemotherapeutics, and achieves higher concentration of the drug at the tumor site.

Oncolytic viruses armed with genes encoding prodrug activating enzymes mediate the expression of the enzyme in a virus replication- and location-dependent manner. As the viruses are engineered to specifically target tumor cells, the prodrug activating enzyme expression is restricted to the tumor site. Following prodrug administration and conversion, cancer cell are being killed. As the prodrug application can be timed, interference of toxic therapeutics after prodrug conversion with viral replication can be avoided.

One of the best studied prodrug activation systems is CD/5-FC (**Figure 8**). CD (cytosine deaminase) converts the prodrug 5-FC (5-Fluorocytosine) into the active chemotherapeutic 5-FU (5-Fluorouracil), which can freely diffuse without using gap junctions [100]. Feasibility of CD expression by an adenoviral vector, leading to efficient prodrug conversion, was shown *in vivo* [101]. However, it was reported that some pancreatic cancer cells have intrinsic or acquired resistance against 5-FU, which was correlated with overexpression of 5-FU degrading enzymes in patients [102]. This resistance can be overcome through expression of UPRT (uracil phosphoribosyltransferase), a pyrimidine salvage enzyme originating from yeast, which converts 5-FU into 5-FUMP and 5-dUMP [103]. The adenoviral delivery of UPRT in combination with 5-FU was shown to be able to sensitize or enhance the cytotoxic effect in some cancer cells [104, 105]. This was due to increased levels of 5-dFUMP and subsequently increased inhibition of the thymidylate synthase and DNA synthesis [103] (**Figure 8**). An optimized enzyme comprising the activities of yeast CD and yeast UPRT, called FCU1, was developed in the context of adenovirus-mediated gene therapy [106].

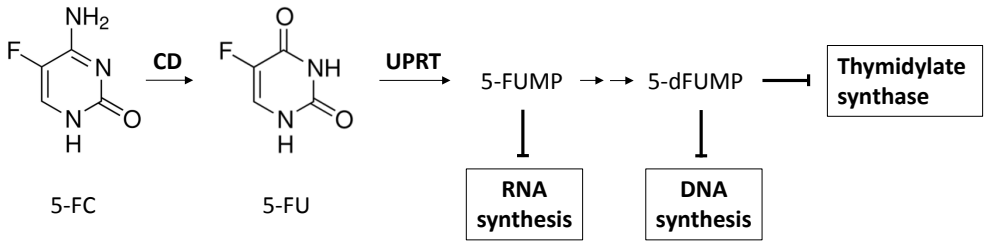


**Figure 8: Mechanism of CD/UPRT (FCU1) Prodrug Conversion.** 5-FC is converted by cytosine deaminase (CD) into 5-FU. 5-FU is diffusible and further converted by the salvage enzyme UPRT in the active metabolites 5-FUMP and 5-dFUMP.

This prodrug activation system was further shown to be promising in experiments with FCU1-expressing oncolytic adenoviruses [107]. As 5-FU is one of the standard chemotherapeutic treatments for pancreatic adenocarcinomas, the insertion of FCU1 in an improved oncolytic adenovirus was chosen for a combination therapy in this thesis.

## 5.7. Performed Clinical Trials with Oncolytic Adenoviruses

Several oncolytic adenoviruses are currently tested in clinical studies and are listed in **Table 2**.
The first oncolytic virus that went into clinical studies was Onyx-015, an *E1B55K*-deleted adenovirus [108]. For this virus, clinical data was acquired in a variety of tumor entities and via different application routes [109-112]. However, the Onyx-015 project showed that safety and tumor selectivity was well reproducible, although therapeutic efficiency of solely the virus agent was very limited [111]. The Onyx-015 project was stopped and the rights sold to a Chinese company, which developed it to the first approved oncolytic virus, now named H101 or Oncorine, in China [35]. However, it has no approval in Europe or the US for patient treatment.
Therefore, the challenge remains to improve the potency of oncolytic viruses by gene modifications or arming with transgenes. Several trials, mostly in Phase 1 are testing further modified oncolytic viruses. These viruses feature a variety of modifications (**Table 2**), as capsid modifications (Ad5RGD, Ad5/3), transgene insertions (GM-CSF, Hyaluronidase), and different promoters for tumor specific viral replication (E2F-1). Some of these viruses are tested in combination with standard treatment chemotherapeutics, as cisplatin, 5-FU, or gemcitabine, as possible future combination approaches (see references and clinical trials registry numbers in **Table 2**).

**Table 2: Oncolytic Adenoviruses Tested in Clinical Trials**

| Phase | virus | virus genetics | tumor entity | Admin. route | combination | reference |
|---|---|---|---|---|---|---|
| Phase 1 and 2 | Onyx-015 | HAdV-5, E1B 55K deletion, | lung metastasis | i.v. | - | PMID11420638 |
| Phase 2 | Onyx-015 | E3B deletion, | HNSSC | i.t. | cisplatin, 5-FU | PMID 10932224 |
| Phase 1/2 | Onyx-015 | Ad5 wild type capsid | pancreatic cancer | i.t. | Gemzar | PMID 12576418 |
| Phase 2 | Onyx-015 | | pancreatic cancer | i.a. | - | PMID 12414631 |
| Phase 1 | Ad5Delta24RGD | E1AΔ24 deletion, Ad5RGD fiber | ovarian cancer | i.p. | - | NCT00562003 |
| Phase 1 | DNX-2401 | former Ad5Delta24RGD | recurrent malignant glioma | i.t. | - | NCT00805376 |
| Phase 1 | DNX-2401 | former Ad5Delta24RGD | recurrent glioblastoma | i.t. or i.m. | temozolomide | NCT01956734 |
| Phase 1 | CGTG-102 | Ad5/3-d24-GMCSF<br>E1AΔ24 deletion, GM-CSF is in the place of deleted gene for gp19k/6.7K in the E3 region, Ad5/3 fiber | malignant solid tumors | i.t. | cyclophos-phamide | NCT01598129 |
| Phase 1 | ICOVIR-5 | Ad-DM-E2F-K-Δ24RGD<br>E1A transcpription under E2F promoter, E1AΔ24 deletion, Ad5RGD fiber | advanced or metastatic melanoma | endo-venous | _ | NCT01864759 |
| Phase 1 | VCN-01 | encoding human PH20 hyaluronidase downstream E4 via SA site, Ad5RGD fiber | advanced pancreatic adenocarcinoma | i.t. | gemcitabine | NCT02045589 |
| Phase 2/3 | CG0070 | E2F-1 promoter, expresses GM-CSF replacing E319K, Ad5 wild type capsid | bladder cancer | intra-vesical | gemcitabine | NCT01438112 |

Most of the clinical trials are in Phase 1, testing safety or dosage. The oncolytic adenovirus CG0070 has recently entered a Phase 2/3 trial (NCT01438112), looking for improvement of therapeutic efficiency compared to the available standard treatments of bladder cancer.

## 5.8. Virus Shielding and Targeted Delivery

After systemic application, only a very small fraction of the adenoviruses reaches the tumor sites. Causes for this limitation are liver sequestration and antibody neutralization. In mice, two minutes after i.v. injection of adenoviruses, the majority of virus particles is cleared from the blood stream [113]. This is due to recognition of hexon, to binding to blood components (coagulation factors IX, X, and complement factor C4 [62, 114, 115]), and to heparan sulfate proteoglycans [116], which mediates or leads to hepatocyte transduction. Further, viruses can transduce Kupffer cells by direct binding to scavenger receptors [117].
Additionally, most adults have neutralizing antibodies against HAdV-2 and HAdV-5, or undergo seroconversion after the first viral application.
Therefore, strategies were investigated to limit the delivery problem of oncolytic adenoviruses, especially the liver sequestration. The most straightforward approach is to shield the virus from uptake by the liver cells, which can be done in several ways [62]:

i. Chemical shielding: polymers, such as polyethylene glycol, which become chemically cross-linked to the virus surface. The method was shown to shield virus from neutralizing antibodies without inhibiting infectivity [118].
ii. Biological shielding: changing the virus tropism by modifying the capsid can inhibit specific binding processes, but not unspecific, receptor-independent uptake as described above.
iii. Carrier cells: see **section 5.8.1**.

There are also possibilities to circumvent neutralization by the immune system, which are:

i. Change the capsid an therefore switch the serotype of the virus [119]
ii. Temporary immune suppression: cyclophosphamide, a DNA-alkylating agent with chemo-therapeutic and immunosuppressive functions [87].

### 5.8.1. Carrier Cells for Oncolytic Adenovirus Delivery

In order to overcome the challenges of virus delivery, cells with tumor-homing properties are used as carriers for the virus. The viruses, bound or incorporated in these cells are therefore protected from neutralizing antibodies or unspecific sequestration on their way to the tumor. A variety of cells are utilized as carrier cells for oncolytic viruses to tumor sites.
i. Some studies have investigated tumor cells themselves to deliver oncolytic viruses (example: irradiated osteosarcoma cells as cell carrier for canine oncolytic adenovirus, [120]). The rationale behind this strategy is that tumor cells of the same kind will find the same niche and therefore deliver the virus to the tumor. Further, it was suggested that a cancer cell vehicle would propagate the virus best on the way to the tumor, as oncolytic viruses are designed to selectively replicate in tumor cells. However the difficulty here is that the targeted tumor and the cancer cell used for delivery need to be highly similar [121], which is difficult in a clinical setting.
ii. Cells like tumor-associated macrophages, endothelial progenitor cells, or mesenchymal stem cells (MSCs) do not target directly the tumor cells, but follow stimuli produced by the tumor stroma. They follow, according to their natural tropism to wounded tissue, tumor-induced gradients of angiogenic factors (endothelial progenitor cells), released inflammatory cytokines (MSCs, neuronal stem cells

[122]) or hypoxic factors [123]. The virus is therefore transported into the direct vicinity of the tumor. For all these cells, the isolation procedures are established and they can be expanded *in vitro*. Further, they allow productive infection and therefore propagate the virus on their way to the tumor. Several studies have investigated the delivery of oncolytic adenoviruses by macrophages [123], MSCs [124-126], and neuronal stem cells [122].

iii. Immune cells, e.g. tumor patient's T-cells with specificity for tumor-associated antigens, have a natural tumor tropism and can serve as a Trojan horse for the virus to be transported to the tumor site [127]. Studies have shown that the virus does not infect but just hitchhikes on the surface of these cells [127]. Therefore, virus propagation during migration is not possible. The disadvantage of this system is the difficulty of isolation of T-cells against highly tumor-specific antigens and the possibility of autoimmunity [121]. This approach has not been utilized for oncolytic adenoviruses.

### 5.8.2. MSCs as Carrier Cells for Oncolytic Adenovirus

In this study, mesenchymal stem cells were used as carrier cells since they have obvious advantages compared to other possible carriers as mentioned above. MSCs can be easily isolated from almost every tissue in the body [128]. For clinical and research purposes, they are mostly isolated from bone marrow, as for this study, or adipose tissue [129]. In bone marrow aspirates, they only account for <0.1% of the nucleated marrow cells and need to be expanded *in vitro* to obtain sufficient amounts ([130] and references therein). The isolation is based on surface markers and plastic adherence [131]. The expansion is well described and established [132]. Further, the identity of the cells is confirmed through the differentiation into chrondogenic, adipogenic, and osteogenic lineages [131, 133].

The natural tropism of MSCs is to follow a chemotactic gradient to inflamed or wounded tissue and to mediate repair [128]. MSCs express a number of growth hormone receptors, chemokine receptors, adhesion molecules, and toll-like receptors, which were identified to be associated with cell migration [128]. Tissue repair capacity of MSCs has been investigated in clinical trials for various diseases (reviewed in [134]). For their application as carriers of chemotherapeutic agents, the same characteristics are utilized. Dvorak et al. [135] compared tumor tissue to a chronic wound that constantly releases inflammatory mediators. Especially the tumor stroma is a source of continuous release of growth factors, hypoxic factors, and inflammatory mediators [130]. MSCs follow these gradients to the tumor stroma, as they would to wounded tissue [128, 136]. Therefore, they were used as vehicle to deliver therapeutic agents to the vicinity of the tumor, including TRAIL [137-139] and oncolytic adenoviruses. After an initially study of MSCs loaded with an IFN-β expressing replication-deficient adenovirus [140], the concept was studied with a variety of differently altered oncolytic adenovirus targeting different tumor entities including breast, ovarian, melanoma, glioma, and neuroblastoma [125, 141-144]. These studies provided the proof-of-principle that oncolytic adenoviruses are able to infect MSCs, are amplified in MSCs, and are delivered to the tumor site after i.t. [125], i.v [126], or i.p [124] administration in *in vivo* mouse models. It was further shown that MSC homing was unaltered by viral infection [145] and that the virus was handed-on to tumor cells [144].

In view of possible treatment options of cancer patients later on, MSCs can be transplanted allogeneically, meaning that donor and recipient are from different individual, i.e. healthy donors. This is possible, because MSCs have intrinsic immunomodulatory functions [130] that inhibit rejection, inhibit innate and adapted immunity, but also actively induce immune tolerance. This is of special interest as it was reported that the quality of MSCs decreases with age in humans [146]. Therefore in this study, MSCs from 4 different healthy donors were used, who were between 20 and 30 years old. **Figure 9** summarizes the advantages of MSCs as carriers compared to virus i.v. injection.

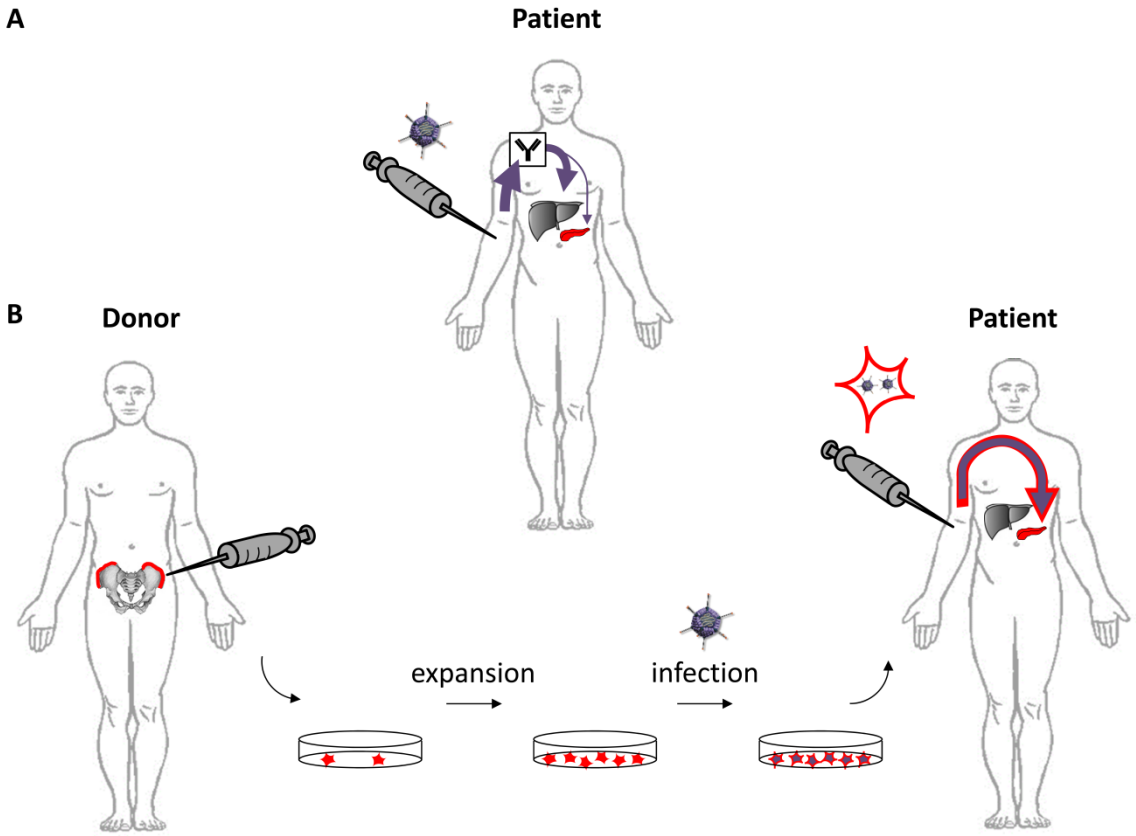


**Figure 9: Systemic Effects of Direct Virus Injection Versus Virus Delivery by MSCs for Pancreatic Adenocarcinoma in Human. A:** After systemic injection of the virus, the majority of viral particles are cleared by neutralizing antibodies or sequestered by the liver. Only the minority of virus particles reaches the pancreatic tumor (red). **B:** MSCs are isolated (e.g. from the bone marrow of the iliac crest) and after purification, expansion, and infection are administered systemically. The MSCs home to the tumor site, protecting the virus particles from sequestration by the liver and neutralizing antibodies. (Elements taken from: www.clipartbest.com**,** blog-static.hellomagazine.com/thenakednutritionist/files/2012/05/liver3.jpg, www.sign-lang.uni-hamburg.de/glex/illusgr/l74290.jpg)

### 5.8.3. The Delivery System

The delivery approaches for oncolytic adenoviruses by MSCs, all underlie the same principle, which is described schematically in (**Figure 10**).

MSCs are isolated from bone marrow donations of healthy donors and expanded. Afterwards, they become infected *ex-vivo* and systemic applied to a tumor patient. The MSCs home to the tumor site, while the virus is replicating. At the end of the viral life cycle, the progeny virus particles are released at the tumor site and infect a subset of the tumor cells. The virus then replicates in the tumor cells, performs oncolysis, and the progeny viruses further spread through the tumor.

The critical factors for the kinetics of the system are viral replication and release in MSCs and tumor cells. Premature virus release in the bloodstream during delivery would subvert the system. Therefore, the system required that virus release kinetic is accordant with the time the MSCs need to reach the tumor site in an *in vivo* setting. The same virus needs subsequently to efficiently replicate in and lyse the tumor cells.

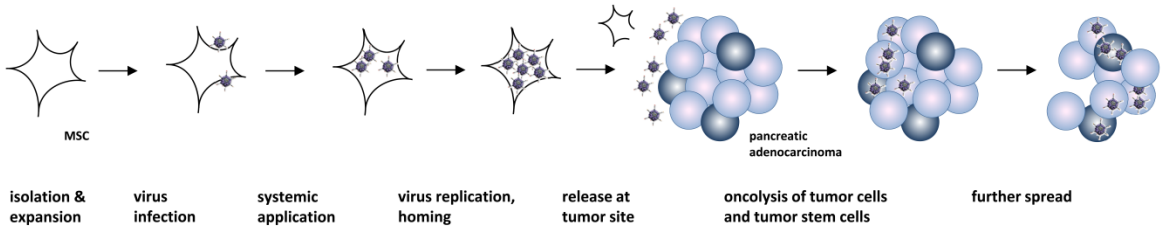


**Figure 10: Summary of The Delivery System of Oncolytic Adenovirus by MSCs.** MSCs are loaded with virus *ex vivo* and are systemically applied. The virus is replicating in MSCs during homing. After being delivered to the tumor site, the virus is released and infects the tumor cells including tumor stem cells and subsequently spreads through the tumor.

An exploratory clinical trial was performed using CELYVIR (MSCs loaded with the oncolytic adenovirus ICOVIR-5) [147]. This clinical trial used a similar delivery approach as the one described above. Autologous MSCs were infected ex vivo. Four children with metastatic neuroblastoma were treated with 2-4 i.v. infusions of CELYVIR. In 3 out of 4 children, relapse occurred after a first complete response. In the fourth child, after a progression phenotype, complete remission occurred after 36 months. The data suggests that the immunological response correlates with the good outcome. Another clinical trial has been opened testing CELYVIR and is recruiting patients currently (NCT01844661).

### 5.8.4. Optimizing Oncolytic Adenoviruses for Delivery in MSCs

A major advantage of this system is the propagation of the viral agent during transport. Therefore, two approaches for optimization are rational: i. optimization of transduction in order to have a high initial titer to start with and ii. the optimization of the replication and release kinetics of the virus in MSCs.

Several studies have analyzed transduction of oncolytic viruses in MSCs. It was reported that the receptor for the HAdV-5 wild type virus CAR is lowly expressed on MSCs [125, 136, 148], which resembles the situation in cancer cells described in **section 5.5.1**. In cancer cells, adenoviruses capsid variants Ad5/3 and Ad5RGD showed improved transduction by retargeting the virus to Desmoglein-2 and integrins, respectively. Several studies investigated whether transduction with Ad5/3 and Ad5RGD could improve transduction of MSCs and which capsid variant resulted in best transduction. At least for integrins, studies confirmed their expression on undifferentiated MSCs [125, 136, 148]. The outcomes of the transduction experiments showed, that the mentioned modifications improved transduction in almost all studies. However they did not accord on which capsid variant transduced best [124, 125, 136, 149].

Optimization of viral replication and release in MSCs for optimized delivery has not been analyzed so far and is the topic of this thesis.

# 6. Aim of the study

Alternative treatment procedures for pancreatic cancer are urgently needed. Oncolytic adenoviruses have a great potential for tumor treatment and have shown an excellent safety profile. However, virus mediated oncolysis still needs to be improved. Further, neutralizing antibodies and liver sequestration presented a major roadblock for efficient virus delivery to the tumor site after systemic application. In this study, the problems of virus delivery and efficiency were approached. Mesenchymal stem cells (MSCs), isolated from human bone marrow, are established as carrier cells and would be utilized for targeted and therefore more efficient virus delivery to the tumor site. Modified oncolytic viruses, which carry modifications that aimed for improved tumor cell killing, would be investigated. The overall aim was to identify the virus modifications, which best improved virus delivery and tumor cell killing, including the tumor stem cells, in the context of the delivery system.

The first specific aim of this study was to identify the best transducing virus capsid variant. Optimized viral cell entry would be needed for MSCs, to optimize the amount of viral particles delivered by MSCs, and for tumor cells, to optimize tumor cell killing efficiency. Therefore, Ad5, Ad5/3, and Ad5RGD capsid variants were going to be tested on MSCs as well as on established pancreatic tumor cell lines and low-passage pancreatic tumor cell cultures. The capsid variant, which would be identified as best transducing, was aimed to be used as capsid background for the further investigated modified oncolytic adenoviruses.

For the second aim, a set of further modified viruses should be tested for improved replication and release kinetics in MSCs as well as for maintenance of migration capacity of virus-infected MSCs. Three virus modifications were aimed to be investigated: the deletion of the early gene *E1B19K* for improved virus kinetics, TRAIL expression for bystander killing, and FCU1 expression for prodrug conversion. A set of replication-competent viruses carrying the modifications had to be generated. Virus replication and release kinetic analysis in MSCs were planned. The more progeny virus particles would be produced and released, the more efficient the virus delivery would be. However, these improved kinetics needed to allow maintenance of migration properties of MSCs and further, viral release kinetics had to correspond to the time the MSCs needed to reach the tumor site. Therefore, a subsequent transwell migration assay was planned in which migration behavior had to be assessed over 2 days, as the *in vivo* relevant time span for MSC tumor homing. The combined information of the migration assay and the obtained release kinetics would give insight on which modifications allows unimpeded migration combined with optimized amount of virus progeny delivery.

For the third aim, the modified viruses should be tested on established pancreatic tumor cell lines, spheroids, and low-passage cultures in order to identify the virus modification resulting in best oncolysis performance. As it has been shown that the targeting of cancer stem cells was very important for successful cancer therapy, this would be a special focus of this aim. Here, the cell lines, which were planned to be used, were known to have cancer stem cell-like characteristics. Further, in order to analyze virus spread and killing in a 3D tumor structure, the modified viruses were aimed to be tested in pancreatic tumor cell line spheroids. Finally, the viruses should be investigated in low-passage pancreatic tumor cell cultures to obtain data in patient's tumor resembling material.

Combination of the obtained data of virus life cycle kinetics in MSCs, migration of infected MSCs, and oncolysis in pancreatic cancer cells, aimed to identify an optimized oncolytic adenovirus for delivery by MSCs.

# 7. Results

## 7.1. Defining the Best Adenovirus Capsid Variant for Transduction in MSCs and Tumor Cells

In order to improve delivery of oncolytic adenoviruses by MSCs, virus entry optimization was a first approach. It is critical for transduction of MSCs in order to optimize the amount of delivered viral particles as well as for transduction of tumor cells in order to optimize viral lysis. Therefore, the aim of this transduction experiment was to identify the best suited capsid variant for transduction of MSCs as well as pancreatic adenocarcinoma cell lines.

Oncolytic viruses are historically based on human adenovirus serotype 5 (HAdV-5). The physiological receptor of HAdV-5, CAR (Coxsackie- and Adenovirus Receptor), was demonstrated to be poorly expressed on tumor cells [64, 65, 150] as well as on MSCs [125, 136, 148, 151] in previous studies. In order to optimize transduction, viruses with altered capsid variants were tested. These were Ad5/3 (HAdV-5 shaft and HAdV-3 knob fiber chimera, mediating binding to Desmoglein-2 and CD46) [66] and (RGD peptide introduced in the HI loop of the knob, mediating binding to integrins) Ad5RGD [67]. Both capsid variants containing adenoviruses had been tested on MSCs [124, 125, 136, 149] and a variety of cancer cell lines, including pancreatic cancer, before [66, 68-70]. However, these studies did not consent to which virus variant led to best transduction. Therefore, the aim of this set of experiments was to define the best suited capsid variant for the MSCs and pancreatic cancer cells used in this study. Ad5/3, Ad5RGD, as well as unaltered wild type HAdV-5 (Ad5) were tested on MSCs isolated from healthy donors, established pancreatic adenocarcinoma cell lines, and low-passage pancreatic adenocarcinoma cultures. MSCs were isolated from bone marrow of healthy donors and characterized through their differentiation potential by the group of Ingrid Herr (University Hospital Heidelberg). They were used in passages 5-9. Low-passage pancreatic ductal adenocarcinoma cultures PacaDD-159 and JoPaca-1 were provided and characterized by the group Pilarsky [152] (University Hospital Mannheim) and the group Hoheisel [153] (DKFZ, Heidelberg), respectively.

### 7.1.1. Viruses Used for Transduction Experiments and Luciferase Assay

For the analysis of transduction efficiency, a set of replication-deficient, luciferase expressing viruses was used. For virus outlines see **Figure 11.**

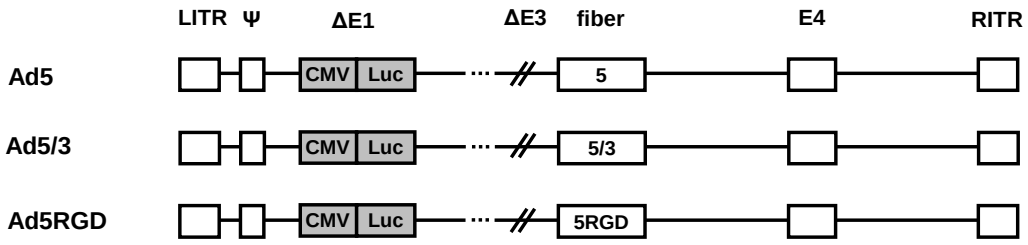


**Figure 11: A Schematic Genome Outline of Viruses Used for Transduction Experiments.** LITR/RITR: left/right inverted terminal repeat, Ψ: packaging signal, all viruses were *E1*- and *E3*-deleted, the firefly-luciferase gene (*Luc*) under CMV-promoter control was introduced replacing *E1*, capsid variants: Ad5 contained serotype 5 wild type capsid, Ad5/3 expressed a chimeric capsid composed of HAdV-5 shaft and HAdV-3 knob, while for Ad5RGD the CRCRGDCFC peptide was introduced into the Ad5 HI-loop.

In all viruses, the *E1* region was substituted by a firefly luciferase (*Luc*) gene under CMV promoter control. The viral genomes only varied in the fiber modifications (5, 5/3, 5RGD). The viruses were previously amplified and purified in our group (see Methods **section 10.3.2/10.3.3**), and prior to this study proof-characterized and titered. Physical virus particle concentrations of the preparations were measured by OD260 and infectious viral particles were determined by $TCID_{50}$ assay on HEK293 cells., HEK293 cells were used for $TCID_{50}$ determination for the replication-deficient viruses, since they are able to substitute the deleted *E1* gene and therefore enable virus replication (see Methods **section 10.3.5**). The ratios of physical and infectious viral particles were between 2 and 50.
In the performed reporter gene assay, cells were plated and transduced 24 hours later with the same amount of viral particles of Ad5, Ad5/3, Ad5RGD, or mock-transduced. Because transduction of viruses with identical virus backbones and different capsids was analyzed, physical virus particles (vp) were used for virus titer calculation. The use of vp is the standard in the field for transduction experiments analyzing capsid-modified viruses (capsid variations were shown to affect the infectious virus particles ($TCID_{50}$) titers). 2 days post-infection, the cells were lysed, luciferase substrate was added, and relative luminescence units (RLU) were measured. Measured RLU were proportional to the amount of expressed luciferase and further to the numbers of viral particles which had entered the host cell. This correlation was possible as all viruses carry the same CMV-*Luc* reporter cassette, making luciferase activity per transduced genome comparable between the virus variants. Observed differences in RLU intensities were correlated to the amount of transduced luciferase transgenes and therefore to differences in entry efficiency of the capsid modified viruses. The assay was used to define the best transducing capsid variant in MSCs and pancreatic tumor cells.

### 7.1.2. Capsid Variants Transduction Analysis in MSCs

The graphs in **Figure 12** show the results of the transduction experiments with the three virus capsid variants in MSCs from 4 different donors. RLU measured in Ad5-transduced MSCs were comparable to mock-infection levels and on average 2 RLU. Transduction with Ad5/3 resulted in measured RLU of 1029/ 130/ 3310/ 3922, respectively for Donor 1 to 4 and transduction with Ad5RGD in measured RLU of 144/ 117/ 74/ 34, respectively for Donor 1 to 4.

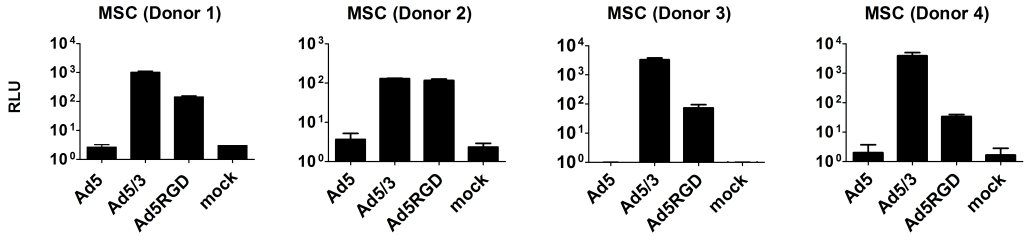


**Figure 12: Luciferase Activity Following Transduction of MSCs.** MSCs of 4 different healthy donors were transduced with 1,000 vp/cell of capsid-modified adenoviral vectors. Luciferase activity of cell lysates was determined 2 days post-infection. Columns show mean relative luminescence units. Error bars show SDs of triplicate transductions.

Comparing the measured RLU of the capsid variants, transduction with Ad5/3 resulted in the strongest measured luminescence signals. These were 386-/ 35-/ 3310-/ 1961-fold higher (respective Donor 1-4) than measured RLU levels for transduction with Ad5 and 7-/ 1.1-/ 45-/ 101-fold higher than measured RLU for transduction with Ad5RGD. Therefore, only for Donor 2 measured RLU for Ad5/3 and Ad5RGD were similar. For Donor 1, 3, and 4, transduction with Ad5/3 resulted in superior luciferase activity compared to Ad5RGD.

Assuming that measured luminescence units correlate with the amount of transduced viral particles as explained above, it can be concluded that transduction with Ad5/3 resulted in most efficient transduction compared to the other capsid variants. Noteworthy was that despite expected donor variation, the Ad5/3 could be identified as best transducing capsid variant accordantly.

### 7.1.3. Capsid Variants Transduction Analysis in Established Cell Lines and Low-Passage Pancreatic Adenocarcinoma Cultures

Further, established and low-passage pancreatic adenocarcinoma cell lines and cultures were transduced with the virus capsid variants. For the established pancreatic cell lines (**Figure 13A**), transduction with Ad5 led to measured RLU of 42/ 66/ 28/ 301 (for MiaPaCa-2/ BxPc-3/ AsPc-1/ Panc-1, respectively), which was above the mock-transduced level of 0 RLU. Transduction with Ad5/3 led to measured RLU of 311/ 897/ 39/ 494 and transduction with Ad5RGD to measured RLU of 26/ 84/ 14/ 209 (for MiaPaCa-2/ BxPc-3/ AsPc-1/ Panc-1, respectively). Therefore, RLU values following transduction with Ad5/3 were between 1.4 - 13.7-fold higher (AsPc-1 and BxPc-3, respectively) compared to Ad5 and for all cell lines higher than measured RLU for Ad5RGD.

For the low-passage pancreatic adenocarcinoma cultures, PacaDD-159 and JoPaca-1, transduction with Ad5 resulted in measured RLU of 589 and 25, respectively (**Figure 13B**). Transduction with Ad5/3 resulted in 7435 and 1527 and transduction with Ad5RGD in 1161 and 14 measured RLU for PacaDD-159 and JoPaca-1, respectively. Therefore, transduction with Ad5/3 led to 13.1-fold (PacaDD-159) and 61.9-fold (JoPaca-1) higher luminescence units compared to Ad5 and to 6.4-fold (PacaDD-159) and 111.7-fold (JoPaca-1) higher luciferase activity than Ad5RGD.

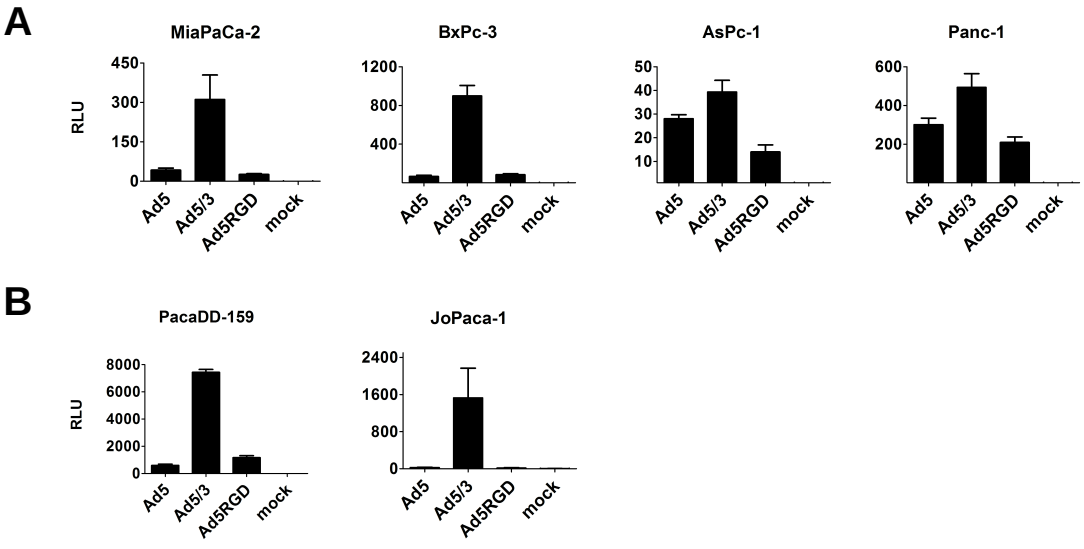


**Figure 13: Luciferase Activity Following Transduction of Established and Low-Passage Pancreatic Adenocarcinoma Cells.** 4 established pancreatic tumor cell lines **(A)** and 2 low-passage pancreatic ductal adenocarcinoma cultures **(B)** were transduced with 100 vp/cell of capsid-modified adenoviral vectors. Luciferase activity of cell lysates was determined 2 days post-infection. Columns show mean relative luminescence units. Error bars show SDs of triplicates.

Transduction with the Ad5/3 adenoviral vector resulted in superior luciferase activity compared to Ad5 and Ad5RGD in MSCs and pancreatic adenocarcinoma cells. Therefore, correlating the measured RLU to transduction efficiency of the capsid variant viruses, it can be concluded that Ad5/3 transduced the MSC carrier cells as well as the established and low-passage tumor cells best. Based

on this conclusion, the fiber 5/3 background was chosen for the generation or selection of improved oncolytic viruses in the next step.

## 7.2. Replication and Release Analysis of Modified Viruses in MSCs

Utilizing MSCs as carrier cells exploits two mechanisms to improve delivery of oncolytic adenoviruses. One aspect is the shielding function of the virus from the immune system and the prevention of viral particle sequestration by the liver. The second function involves the propagation of the replication-competent viral agent during the homing process. The aim of this thesis was to optimize this second function by developing modified oncolytic adenoviruses with optimized replication and release kinetics in MSCs. To this end, two modified viruses were tested. The aim was to identify the modifications which improved virus replication best. However, it is crucial to consider that the virus release kinetics from MSCs have to correlate with the time the MSCs need to reach the tumor site after systemic application. Therefore, the focus of the experiment lay on the influence of the introduced viral modifications on total infectious viral particle production as well as the kinetics of virus release into the supernatant. The obtained data was combined with a following migration study (see **section 7.5**) in order to identify the best suited virus variant for optimized delivery.

### 7.2.1. Modified Oncolytic Viruses

Two modified viruses were tested for improved replication in and release from MSCs. The viruses pursued two different strategies to improve kinetics: i. deletion of a viral gene with function in the viral life cycle (Ad-Δ19K-Luc) and ii. insertion of a transgene mediating bystander killing (Ad-TRAIL). For the virus outlines see **Figure 14**.

The *E1B19K* gene was shown to have anti-apoptotic function [154] and its deletion resulted in improved replication and release kinetics in tumor cells [76, 79, 81, 84]. In this study, an *E1B19K*-deleted adenovirus was tested for its replication and release behavior in MSCs, which had not been investigated before. The adenovirus that carried a deletion in the early gene *E1B19K*, Ad-Δ19K-Luc was generated in the Nettelbeck group and was described in Rohmer et al [81]. For the second strategy, the insertion of the full-length gene of the TNF-related apoptosis-inducing ligand (*TRAIL*) into the viral genome aimed for improved virus kinetics in MSCs as well as for bystander killing. Bystander killing is needed to overcome the strong stromal reaction in pancreatic adenocarcinomas [84], which present a diffusion barriers to the virus, with a diffusible toxic ligand. The effect of the expression of the death ligand on virus replication and release in MSCs was unknown and explored in this experiment. Ad-TRAIL was generated in the course of this study (described in **section 7.8.5**). TRAIL was inserted via an internal ribosomal entry site (IRES) downstream of the fiber5/3 gene. For the confirmation of TRAIL transgene expression by immunoblot see **Figure 22**. Ad-Luc was used as control for the modified viruses. It was generated in the Nettelbeck group and was described in Rohmer et al. [81]. Ad-Luc and Ad-Δ19K-Luc contained a firefly luciferase gene (Luc), which was introduced downstream of the fiber5/3 via an IRES, following the same strategy as used for Ad-TRAIL. The insertion via IRES downstream of the fiber was identified as the preferential strategy of choice for strong transgene expression in previous studies [92]. The consistent strategy of transgene insertion was allowing comparison of the viruses in terms of replication and release in MSCs.

All viruses were replication-competent in order to investigate replication in MSCs. Therefore, they carry a functional *E1A* gene. The 24 amino acid deletion in *E1A* (*E1AΔ24*) makes viral replication selective for proliferating cells (see Introduction **section 5.5.2**). In order to provide genome space to

introduce transgenes, the *E3* gene is deleted. All viruses further contain the fiber 5/3 chimera, as identified as best transducing fiber variant in **section 7.1**. All viruses were amplified and purified (see Methods **sections 10.3.1-10.3.3**). Further, they were proof-characterized, viral particles determined by OD260 measurement and infectious viral particles determined by $TCID_{50}$ assay on A549 cells (for details see Methods **section 10.3.4/10.3.5**). The ratios of physical and infectious viral particles were between 5 and 31, and therefore in the usual range, indicating proper virus preparations and virus vitality.

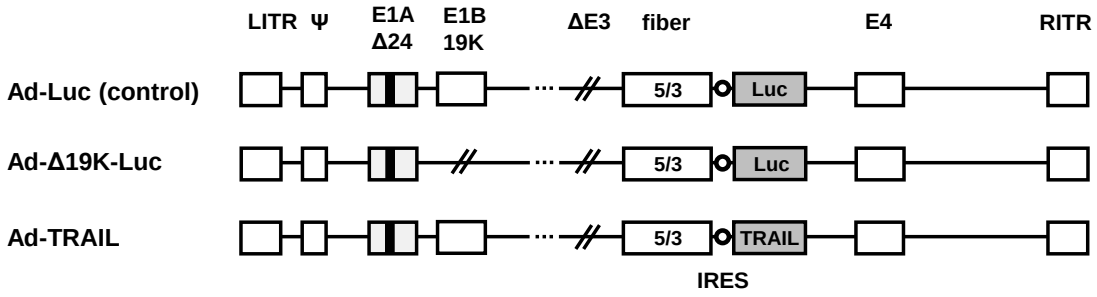


**Figure 14: Modified Oncolytic Adenoviruses Used for Replication/Release Experiments in MSCs.** Genome outlines of viruses used for the replication and release experiment in MSCs. LITR/RITR: left/right inverted terminal repeat, Ψ: packaging signal, *E1AΔ24*: deletion of pRb-binding region in *E1A* for cancer selective replication, *E1B19K*: early gene with anti-apoptotic features, *E3*-deleted, chimeric Ad5/3 fiber (5/3), *Luc*/*TRAIL*: firefly luciferase (*Luc*) and full-length *TRAIL* transgenes were inserted via IRES (internal ribosomal entry site) downstream of the fiber gene.

### 7.2.2. Replication and Release Kinetics Study of the Modified Viruses in MSCs

**Figure 15** shows the results of the performed burst assay to determine infectious particles in cells and supernatant of infected MSCs. For this assay, MSCs were seeded and 24 hours later infected with the respective virus, Ad-Luc, Ad-Δ19K-Luc, or Ad-TRAIL. For infection, the $TCID_{50}$ titers were used for infection titer calculation, as it is the standard in the field for experiments comparing viruses with identical capsids. Cells and supernatant of infected MSCs were harvested separately at 2, 4, 6, and 8 days post-infection and the amount of infectious viral particles was determined by $TCID_{50}$ assay on A549 cells for cells and supernatant separately. Here, the amount of infectious viral particle (and not physical viral particles) was determined, as only those contribute to further virus spread after release from MSCs. **Figure 15A** shows the development of infectious viral particle production in cells and supernatant of the virus-infected MSCs over time. The experiment was performed in MSCs from 3 different donors. The acquired data allows the comparison of replication (total viral particles over time) and release (virus particles in the supernatant over time) kinetics between the modified viruses Ad-Δ19K-Luc and Ad-TRAIL to the control virus Ad-Luc.

During infection with Ad-Luc the majority of viral particles were found in the cells throughout the experiment. In the case of Ad-Δ19K-Luc and Ad-TRAIL the amount of viral particles in the supernatant exceeds those in the cells at a certain time post-infection. The cross point was for Ad-Δ19K-Luc between day 3 to 4 and for Ad-TRAIL between day 5 to 8. The numbers included in each graph of **Figure 15A** describe total infectious virus particle in the supernatant at day 8 post-infection. For both viruses, an improvement in infectious viral particle release into the supernatant was observed. Compared to Ad-Luc, the release of infectious virus was for Ad-Δ19K-Luc factor 14/ 48/ 72 (for Donor 1/ 2/ 4, respectively) and for Ad-TRAIL factor 3/ 16/ 18 (for Donor 1/ 2/ 4, respectively) higher. In terms of total infectious viral particles, Ad-Δ19K-Luc infection yielded on average in 6-fold more infectious particles, infection with Ad-TRAIL in 2-fold more particles compared to Ad-Luc. Therefore,

it can be concluded that both modified viruses led to earlier and more efficient virus release from infected MSCs compared to the control virus Ad-Luc. Further, the numbers of total virus particles at day 8 indicate that more infectious virus particles were produced when MSCs were infected with Ad-Δ19K-Luc or Ad-TRAIL compared to Ad-Luc.

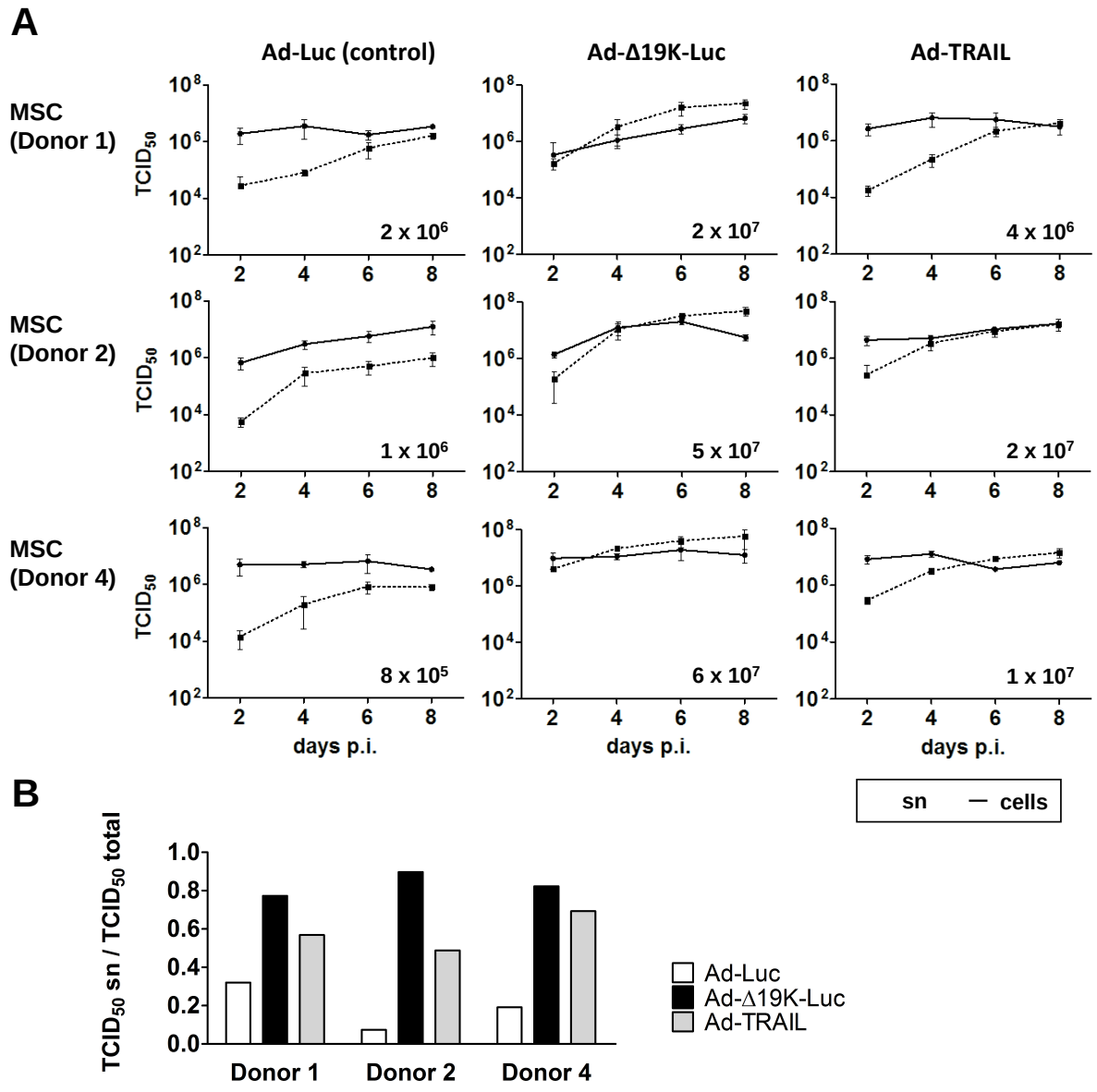


**Figure 15: Replication and Release Kinetics Analysis of Ad-Δ19K-Luc and Ad-TRAIL in MSCs. A:** Viral replication and release in MSCs of three different donors. Cells were seeded and transduced with 1,000 TCID50/cell of viruses shown in **Figure 14**. After 2, 4, 6, and 8 days, supernatant (sn) and cells were harvested separately and total infectious viral particles in cells and supernatant were determined separately by $TCID_{50}$ assay on A549 cells. The experiment was performed in triplicates. Symbols show mean infectious viral particle titers. Error bars show standard deviations of triplicate infections for cells and sn. Shown numbers in each graph indicate infectious viral particle amount in the supernatant at day 8 post-infection. **B:** The ratio of released to total infectious virus particles determined by the ratio of $TCID_{50}$ of sn to $TCID_{50}$ of total (cells + sn) at day 8 post-infection in MSCs of the three tested donors.

**Figure 15B** shows the ratios of released infectious virus particles to total (cell-bound and released) infectious virus particles at day 8 post-infection for each virus and MSC donor. The ratios were used to evaluate if increased release is proportional to the increase of viral particle production or if increased release is an additional contributing mechanism. The bars show that for both, Ad-Δ19K-Luc

and Ad-TRAIL, a much higher proportion of virus particles were released to the supernatant compared to Ad-Luc. This suggests that a mechanism, independent from increased total virus particle production, caused more efficient release.

In summary, infection of MSCs with both modified viruses, Ad-Δ19K-Luc and Ad-TRAIL, resulted in the increase of infectious particles production as well as increased release compared to Ad-Luc. Therefore, improved replication and release were complementing mechanisms for the observed improved kinetics for Ad-Δ19K-Luc and Ad-TRAIL. Further, the enhancement was most prominent for infection with Ad-Δ19K-Luc. Noteworthy was that for MSCs from all three donors the replication and release kinetics for each of the three viruses were strongly comparable.

The improved virus life cycle kinetics of Ad-Δ19K-Luc and Ad-TRAIL compared to Ad-Luc could also be confirmed microscopically (**Figure 16**). At day 6 post-infection, most of Ad-Luc infected MSCs were still attached and only few rounded-up cells were observed. In contrast, Ad-Δ19K-Luc-infected MSCs were almost completely detached and already started to disintegrate. For Ad-TRAIL, approximately half of the cells were detached. The observation that change in morphology was most progressed for Ad-Δ19K-Luc, was in line with the obtained data in **Figure 15**. However, note that rounded-up and floating cells do not necessarily indicate cell death, but progression of the viral life cycle and severe interference with host cell integrity/organization. The observations in **Figure 16** for Donor 4 are representative and were also observed during infections of Donor 1 and 2.

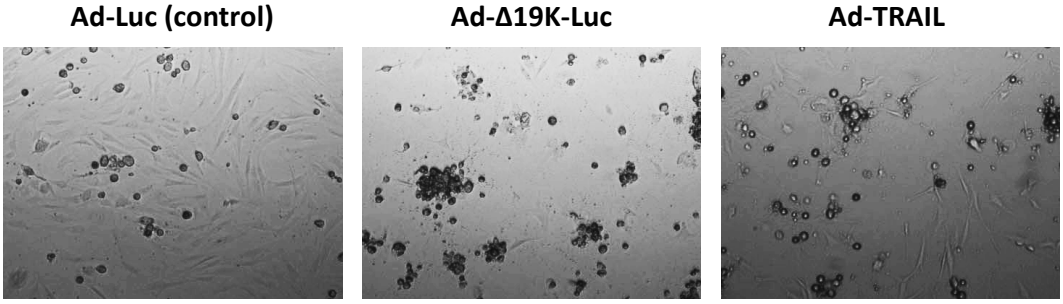


**Figure 16: Differences in Morphology of Infected MSCs at Day 6 Post-Infection.** During the burst assay shown in **Figure 15**, bright-field picture were taken of MSCs (Donor 4), infected with 1,000 $TCID_{50}$/cell at day 6 days post infection. Attached MSCs (mainly seen in pictures of infection with Ad-Luc) have a fibroblast-like morphology, whereas rounded-up cells were detached MSCs (mainly seen in pictures of infection with Ad-Δ19K-Luc).

### 7.2.3. Cytotoxicity Experiments of Modified Viruses in MSCs

To further confirm the improved replication and release kinetics of Ad-Δ19K-Luc and Ad-TRAIL in MSCs as seen in the burst assay (**Figure 15**), MSC lysis was tested in a long-term cytotoxicity assay (**Figure 17**). MSCs of Donor 1 and 4 were incubated with serial dilution of Ad-Luc, Ad-Δ19K-Luc, or Ad-TRAIL from 100 to 0.001 $TCID_{50}$/cell. At day 14 post-infection, the wells were stained with crystal violet. Adding of crystal violet simultaneously fixes and stains cells, which are attached in the well. When cells were killed or detached due to virus infection, wells appear clear; areas with intact cell layer appear dark. Therefore, stages of absent, starting, and complete cytopathic effect can be distinguished. By comparing the lowest concentrations at which the viruses were able to induce a starting or full cytopathic effect, the oncolytic efficiency of the viruses can be compared. Improved cytotoxic behavior of the modified viruses was present, if lysis at lower $TCID_{50}$/cell compared to the control virus Ad-Luc was observed.

As a replication-deficient control virus, Ad-CMV-GFP was used. The *E1A* gene was substituted by a *GFP* gene under CMV-promoter control. Further, the virus also had a 5/3 fiber. Ad-CMV-GFP was

kindly provided by Igor Dmitriev and David Curiel, and was purified, characterized, and titered in the course of this study (see Materials **section 10.3**). The virus was used to verify that no cell-detachment independent of viral replication took place and that observed loss of cells was due to lysis in case of the replication-competent viruses.

As shown in **Figure 17** (first lanes), Ad-CMV-GFP did not induce lysis in any of the infected wells. In the following lanes, the cytotoxic potential of the modified oncolytic viruses Ad-Δ19K-Luc, and Ad-TRAIL compared to Ad-Luc were tested. For MSC from both donors, infection with Ad-Δ19K-Luc led to about 100-fold increased lysis compared to Ad-Luc. In case of Ad-TRAIL, lysis was increased about 10-fold for Donor 1 and 100-fold for Donor 4. The results confirmed the hypothesized improvement of replication and release by the *E1B19K* deletion and indicate that MSCs of both donors are TRAIL-sensitive. The experiments also revealed a donor dependent susceptibility to virus infection, which was about 10-fold higher for Donor 4 than for Donor 1. Similar observations had already been made in the transduction experiments (**Figure 12**).

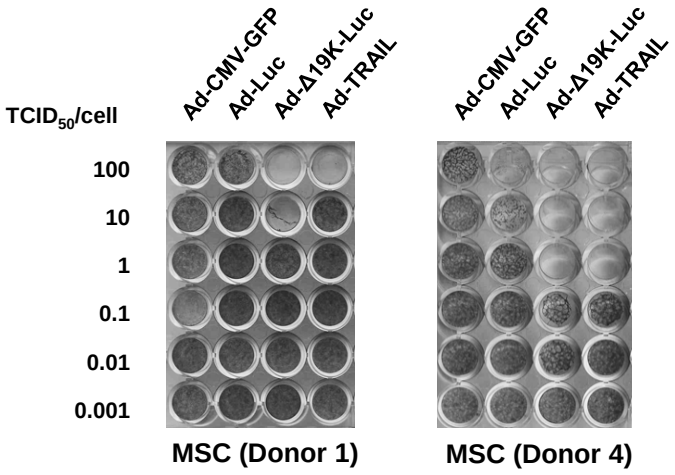


**Figure 17: Cytotoxicity of the Modified Oncolytic Viruses on MSCs.** Cytotoxicity experiment to analyze cytotoxic potential of generated viruses. Cells were infected with indicated serial dilutions of $TCID_{50}$/cell with indicated viruses. 14 days post-infection cells were stained with crystal violet. Plates were dried and scanned. Ad-CMV-GFP: replication-deficient control virus.

### 7.2.4. Characterization of Virus Progeny Produced in MSCs

After virus release from MSCs at the tumor site, the virus needs to efficiently infect tumor cells. To test whether the virus progeny produced in MSCs maintains the same oncolytic qualities than purified virus, the oncolytic potential of MSC-produced virus particles was analyzed in the established pancreatic adenocarcinoma cell line MiaPaCa-2. Equal amount of infectious viral particles from purified virus and virus progeny produced in MSCs (supernatant from **Figure 15A**, Donor 4, day 4) were tested. MiaPaCa-2 lysis was analyzed by XTT cell viability assay (see Methods **section 10.5.7**). Due to limited sample amount, the experiment was only performed once in triplicates. No significant difference in absorbance was observed between purified and MSC-produced virus for equal conditions for each of the viruses (**Figure 18**). This indicated that viruses from both sources were able to induce cell killing equally well, and therefore, that virus progeny produced in MSCs had the same vitality than the purified virus. Further, the result indicated that MiaPaCa-2 were sensitive to TRAIL as most efficient cell killing was seen following infection with Ad-TRAIL compared to other tested

viruses. However, to obtain statistically significant data, the experiments needs to be repeated with virus progeny produced in a different MSC donor.

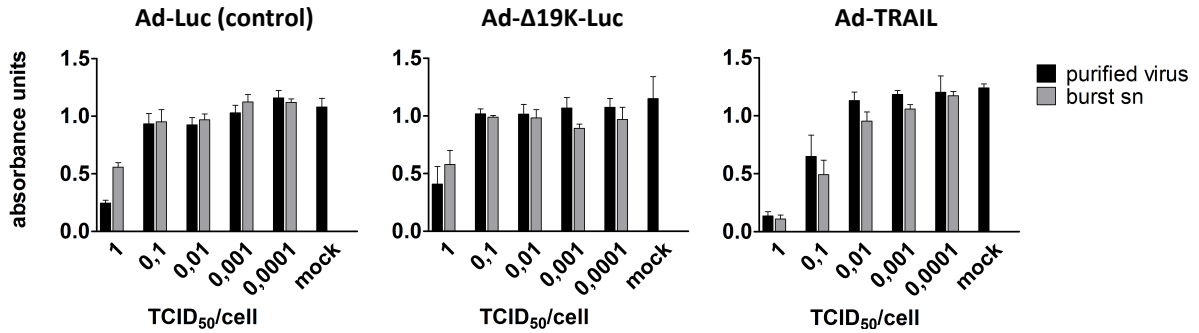


**Figure 18: Testing of Virus Progeny Produced in MSCs on MiaPaCa-2 for Maintenance of Virus Vitality.** 15,000 MiaPaCa-2 were infected either with purified virus or virus progeny produced in MSCs at indicated titers. Supernatant of virus-infected MSCs (Donor4) 4 days post-infection was obtained and titrated in the burst assay described in **Figure 15**. XTT assay of infected MiaPaCa-2 was performed 8 days post-infection. Columns show mean absorbance units. Error bars show SDs of triplicate infections.

## 7.3. Testing Polybrene as Adenovirus Transduction Helper for MSCs

### 7.3.1. Improving Adenovirus Transduction Efficacy for MSCs with Polybrene

Although the Ad5/3 capsid variant was the best in terms of transduction efficiency in MSCs (**Figure 12**), the measured RLU did not give information about the percentage of transduced cells. An oncolytic virus expressing GFP (Ad-GFP, **Figure 19A**) was generated to visualize infection.

Ad-GFP was generated by inserting the *GFP* gene via a splice acceptor site (SA) downstream of the adenovirus *E4* gene. By this means, GFP was expressed from the late viral transcription unit and therefore replication-dependent. Transgene expression had been shown to be efficient by this insertion strategy. [94]. For the cloning strategy see **section 7.8.2**. The virus genome was transfected, and viruses were amplified, purified, and proof-characterized. The physical viral particle titer was determined by OD260 measurement and infectious viral particles determined by $TCID_{50}$ assay on A549 cells (for details see Methods **section 10.4**). The ratio of physical and infectious viral particles was 30. Ad-GFP was a replication-competent virus, containing *E1AΔ24*, *E3* deletion, and a 5/3 fiber. Following MSC transduction, the GFP-signal started to appear after about 24 hours. Fluorescence pictures were taken 48 hours post-infection, when GFP expression was maximal but prior to the completion of the viral life cycle and cell lysis. The amount of green-fluorescent cells correlated with the amount of the initially infected cells.

The left set of pictures in **Figure 19B** shows images of MSCs from three donors, which were transduced with serial dilutions of virus. Transduction with 100 $TCID_{50}$/cell led to a very small fraction of GFP-positive cells (<5%). With 1,000 $TCID_{50}$/cell, transduction efficiency was increased (approximately 50%), but still not sufficient. 10,000 $TCID_{50}$/cell led to transduction of the majority of cells. As expected, some differences between the donors were observed. Donor 3 was better transducible, followed by Donor 1 and Donor 2 (this result is in accordance with the transduction experiments in **Figure 12)**. Transduction of Donor 3 with 10,000 $TCID_{50}$/cell led to a starting cytopathic effect. Therefore, the viral titers that were necessary for complete transduction were very high. In view of future *in vivo* experiments, when an initial infection of 100% is aimed for, these titers are problematic. Therefore, Polybrene, a cationic polymer, was tested as transduction helper. The

use of Polybrene had been shown in several studies to greatly improve adenovirus transduction of epithelial and endothelial cells [155] as well as in mouse MSCs [156].

The right part of **Figure 19B** shows transduction efficiency when Polybrene was used as transduction helper. MSCs were plated and 24 hours later infected with Ad-GFP in medium containing 8 ng/ml Polybrene for 2 hours. The fluorescent pictures were taken 48 hours post-infection. In pre-experiments (data not shown), Polybrene concentrations between 2 and 16 ng/ml were tested, and 8 ng/ml was identified as the optimal concentration. Now, 100 $TCID_{50}$/cell + Polybrene led in case of Donor 1 and 3 to transduction of a major fraction of cells and for Donor 2 to about 50% transduction. 1,000 $TCID_{50}$/cell + Polybrene led to almost complete transduction for all donors. It was estimated from this experiment that the use of Polybrene allows a 10-fold viral particle reduction needed for efficient MSC infection. Additionally, the differences in donor transducibility led to the conclusion that every donor needs to be tested prior to experiments in order to assure sufficient infection.

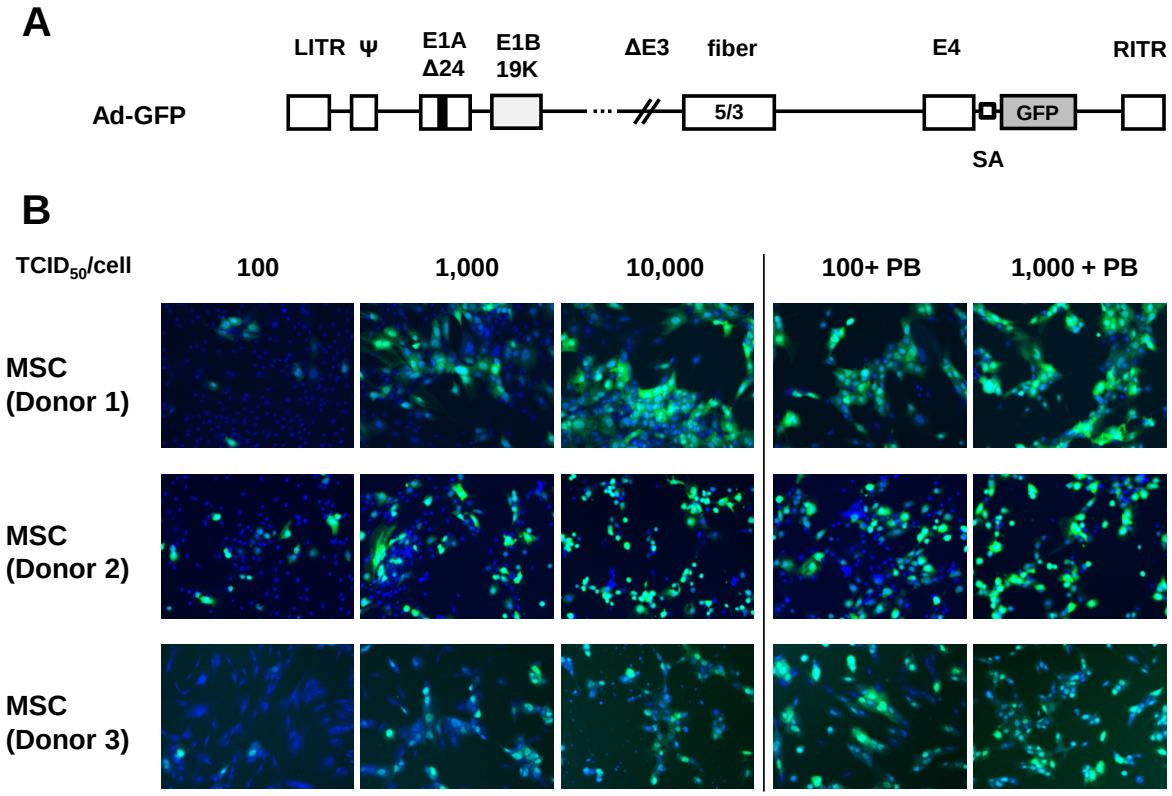


**Figure 19: Adenoviral Infection Efficiency of MSCs With and Without Polybrene. A:** Genome outlines of virus used for test infection of MSCs. LITR/RITR: left/right inverted terminal repeat, Ψ: packaging signal, *E1AΔ24*: deletion of pRb-binding region in *E1A* for cancer selective replication, *E3*-deleted, *GFP* was inserted via splice acceptor site (SA) downstream of *E4*. **B:** Fluorescence pictures to compare transduction with and without Polybrene (PB). MSCs of 3 different donors were transduced with 100, 1,000, or 10,000 $TCID_{50}$/cell or with 100 or 1,000 $TCID_{50}$/cell with 8 ng/ml PB. 48 hours post-infection cells were fixed with 4% paraformaldehyde, permeabilized with 0.5% Triton X-100 solution and stained with Hoechst 33258 (blue fluorescence of nuclei). Fluorescence pictures were taken with 10x magnification.

### 7.3.2. Virus Replication and Release Maintenance after Polybrene-Mediated Infection

To verify that the use of Polybrene as transduction helper does not subsequently interfere with viral replication and release, a burst assay was performed with MSCs from Donor 1. The burst assay procedure was explained in section **7.2.2** before. The aim of the experiment was to infect MSCs in a way that the number of cell-associated viral particles after infection with and without Polybrene was

comparable. Therefore, over the course of 4 days, the amount of produced and released progeny viral particles would allow conclusions whether the replication and release kinetics were altered with Polybrene. The viral titers needed for similar initial infection were estimated, based on the fluorescence pictures of **Figure 19B**. Here, infection with 1,000 $TCID_{50}$/cell without Polybrene and 100 $TCID_{50}$/cell with Polybrene resulted after 48 hours in comparable amount of transduced, green-fluorescence cells. Therefore, these two titers were used to obtain roughly comparable initial infection levels. MSCs were infected, with the modified viruses Ad-Luc, Ad-Δ19K-Luc, and Ad-TRAIL, with or without Polybrene and the determined titers. At day 0 (2 hours post-infection), the cells were harvested in order to analyze initial transduction titers. At day 4 post-infection, cells and supernatant were harvested separately to obtain information about replication and release. In all obtained samples, infectious viral particles amounts were determined by $TCID_{50}$ assay (see Methods **section 10.3.5.**)

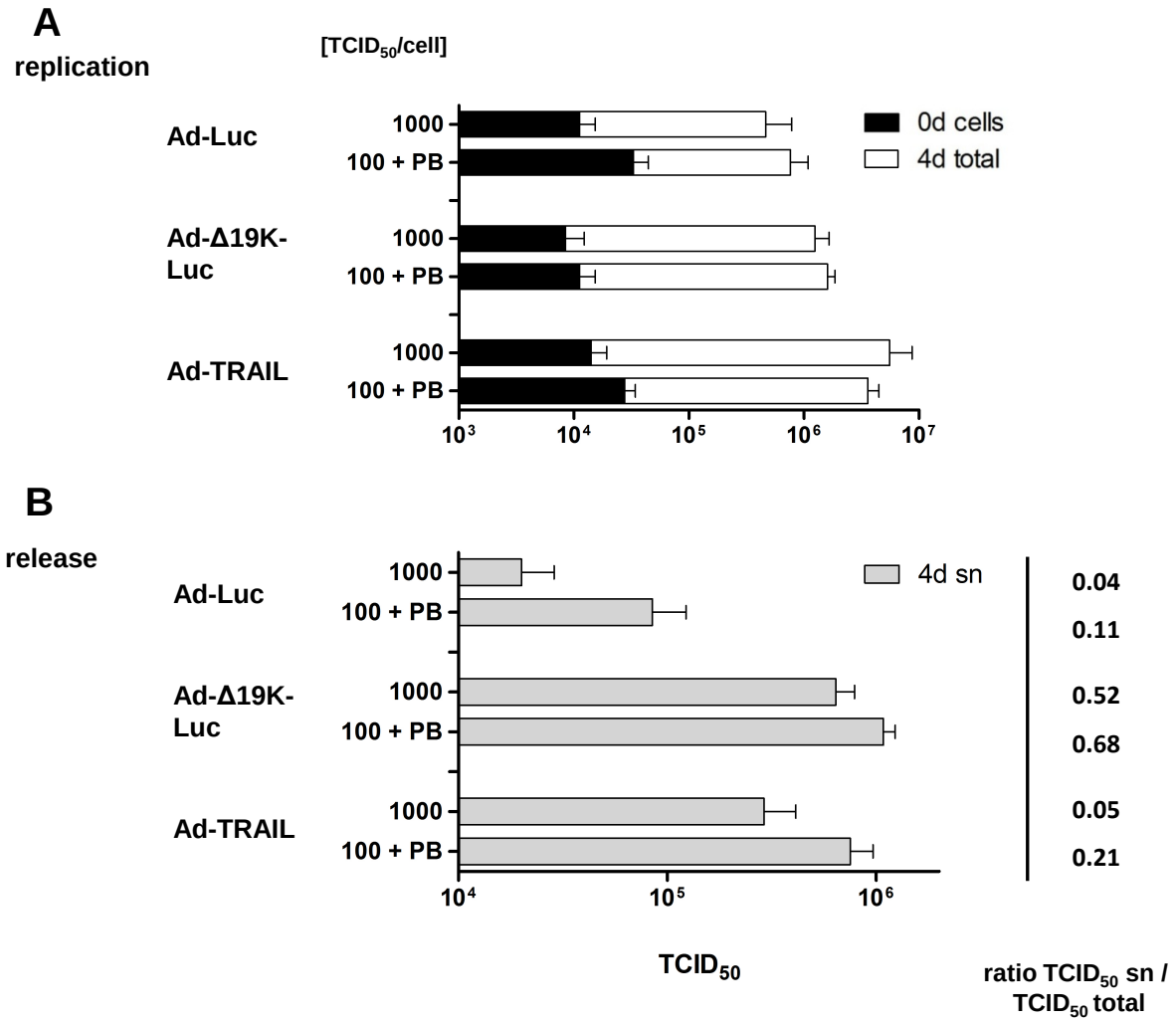


**Figure 20: Viral Replication and Release in MSCs After Polybrene-Mediated Infection.** MSCs (Donor 1) were transduced with 1,000 $TCID_{50}$/cell or with 100 $TCID_{50}$/cell + Polybrene (PB). At day 0 (2 hours post-infection), cells were harvested. At day 4 post-infection, cells and supernatant (sn) were harvested separately. In all samples, infectious virus particle titers were determined by $TCID_{50}$ assay on A549 cells. Bars show mean infectious viral particle titers and error bars SDs of triplicate infections. **A:** The graph shows infectious virus particles in cells at 0 days post-infection (black) and total viral particles at 4 days post-infection (white). **B:** The graph shows infectious virus particles in the supernatant (sn) at 4 days post-infection. The numbers shown on the right side of the graph describe the amount of released infection viruses, which was calculated from the ratio of $TCID_{50}$ sn / $TCID_{50}$ total (cells + sn) at day 4 post-infection.

The results shown in **Figure 20A**, describe the replication behavior of the modified viruses. The bars describe the amount of cell-bound viral particles at day 0 (black part) and total viral particles (cells + supernatant, white part) at day 4 post-infection. The experiment confirmed that viral infection titers of 1,000 $TCID_{50}$/cell and 100 $TCID_{50}$/cell + Polybrene at day 0 (black part of bars) resulted in roughly comparable amount of initially cell-associated virus. Titers for transduction with Polybrene were slightly higher, as already observed in the fluorescence pictures. The numbers of produced total infectious viral particles at day 4 post-infection (white part of bars) indicated no significant difference between samples with and without Polybrene in particle production. In accordance with the slightly higher starting viral particle amount, the numbers of produced viral particles were also slightly higher for 100 $TCID_{50}$/cell with Polybrene when infected with Ad-Luc and Ad-Δ19K-Luc. Only for Ad-TRAIL, produced viral particles were a bit less, though not significant. Further replication assays with different donors are necessary to draw a final conclusion.

**Figure 20B** describes infectious virus particles in the supernatant at day 4 post-infection and therefore the viral release behavior. As already shown in the burst assay over 8 days (**Figure 15A**), infection with Ad-Δ19K-Luc resulted in more efficient release, compared to Ad-TRAIL and Ad-Luc. For infections with Polybrene, this observation was recovered. Ad-Δ19K-Luc showed increased release compared to the other two viruses. Additionally, the graphs indicate that virus release was generally slightly improved compared to transduction without Polybrene. This was further analyzed by calculation of the $TCID_{50}$ ratios supernatant/cells. This ratio was used to judge if increased release is proportional to the increase of viral particle production. For all viruses transduced with Polybrene, higher release ratio was observed (between 1.5-fold for Ad-Δ19K-Luc and 4-fold for Ad-TRAIL). However, the experiments indicate that Polybrene is feasible as transduction helper for MSCs and no significant inhibition of viral replication and release kinetics were observed. Again, this experiment only provides preliminary data and has to be repeated with MSCs of other donors in order to conclude about an effect.

## 7.4. GFP-Transgene Viruses Generation and Characterization

### 7.4.1. Genome Outlines and Verification of Transgene Expression

For monitoring reasons, a set of replication-competent viruses expressing GFP additionally to *E1B19K*-deletion or *TRAIL*-insertion was generated (**Figure 21**). Further, an FCU1-expressing virus was added to the panel. The conversion of the prodrug 5-FC to the antimetabolite 5-FU aimed for an additionally killing effect. As long as the prodrug 5-FC was not added, virus properties of Ad-FCU1-GFP were expected to be comparable with those of Luc-expressing control virus. In view of *in vivo* settings, the prodrug administration can be timed and would be added when the virus has reached the tumor site and the virus has spread at the tumor site. Therefore, the converted prodrug does not interfere with any processes while the virus is affiliated with MSCs and the virus was analyzed in combination with the prodrug 5-FU only in the context of pancreatic adenocarcinoma cells lines.

In all viruses, the first transgene (*Luc*, *TRAIL*, or *FCU1*) was introduced via an IRES (internal ribosomal entry site) downstream of the fiber. The rational of the insertion strategy was described in **section 7.2.1**. All viruses contained as second transgene *GFP*, which was introduced via a SA (splice acceptor site) downstream of the viral *E4* gene. These strategies were chosen based on previous studies for optimized transgene insertions [92, 93]. They were shown to lead to efficient transgene expression but, due to late expression in the viral life cycle, did not interfere with viral replication. This was especially relevant in the case of infection of TRAIL-sensitive MSCs and cancer cells with Ad-TRAIL-

GFP, as completion of the virus life cycle and therefore efficient production of viral progeny had to be ensured. Early expression of TRAIL might abrogate the viral life cycle in these cells. Further, all viruses contained a 24 amino acid deletion in *E1A* (*E1AΔ24*) for cancer cell-selective replication (see Introduction **section 5.5.2**), the deletion of *E3* for genome size reduction in order to introduce transgenes, as well as the fiber5/3 chimera, as identified as best transducing fiber variant in **section 7.1**. For cloning strategies see **section 7.8.3**, **7.8.4**, **7.8.6**, and **7.8.7**. Virus genomes were transfected and viruses were amplified and purified (see Methods **section 10.3.1-10.3.3**). Further, they were proof-characterized, viral particles determined by OD260 measurement and infectious viral particles determined by $TCID_{50}$ assay on A549 cells (for details see Methods **section 10.3.4/10.3.5**). The ratios of physical and infectious viral particles were between 16 and 65.

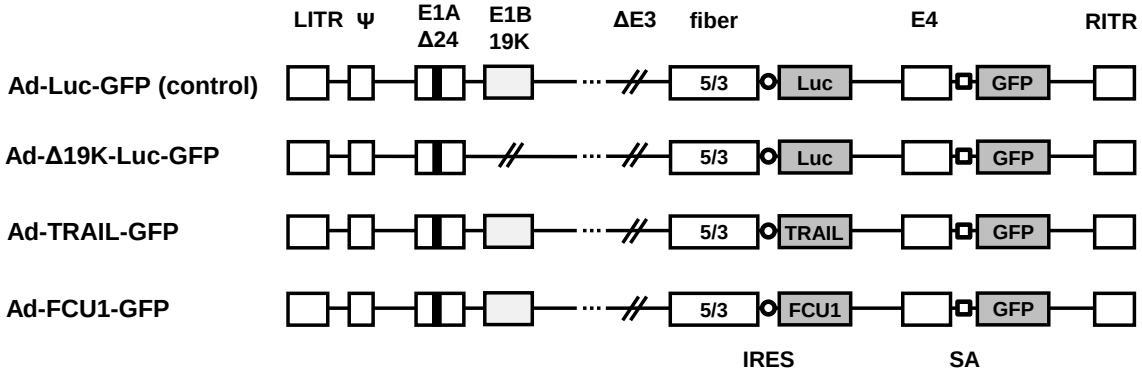


**Figure 21: A Schematic Outline of the Generated Virus Genomes.** LITR/RITR: left/right inverted terminal repeat, Ψ: packaging signal, *E1AΔ24*: deletion of pRb-binding region in *E1A* for cancer selective replication, *E1B19K*: early gene with anti-apoptotic features, *E3*-deleted, chimeric Ad5/3 fiber (5/3). The viruses contain 2 transgenes cassettes inserted via two different strategies; Firefly-Luciferase (*Luc*), *TRAIL*, and *FCU1* genes via internal ribosomal entry site (IRES) downstream of the fiber and *GFP* via splice acceptor site (SA) downstream of *E4*.

Transgene expression of FCU1 and TRAIL were confirmed by immunoblots of infected cells (**Figure 22**). To generate immunoblot samples, MiaPaCa-2 were infected with the indicated viruses, cells were harvested 48 hours post-infection and lysates were prepared and analyzed (for details see Methods **section 10.5**).

For the TRAIL immunoblot, the two viruses generated in the course of this study, Ad-TRAIL-GFP and Ad-TRAIL, were analyzed for TRAIL transgene expression. In order to analyze if virus infection itself caused intrinsic TRAIL expression, Ad-Luc-GFP was used as control. recTRAIL was a recombinant, purified TRAIL (recombinant Super Killer TRAIL, AXXORA, Farmingdale, NY) including only amino acid 95-281 (24 kDa) of the wild type sequence and was used as a positive control. In order to analyze intrinisic TRAIL background expression of the cells, a mock-infection control (medium only) was included. The TRAIL immunoblot shows two bands for virus-expressed TRAIL, correlating with the membrane-bound and shedded form. The loaded amount of purified TRAIL (recTRAIL) was 10 ng. The comparison of the band intensities of purified and virus-produced TRAIL allows only a rough estimation of TRAIL protein produced by the virus, however it indicates that TRAIL protein production by the virus is efficient. For Ad-Luc-GFP and mock-infection, no TRAIL signal was observed, indicating that no significant background TRAIL expression was present.

For the FCU1 immunoblot, the replication-deficient Ad-CMV-FCU1 virus, described in [106], was used as positive control. In both blots, Ad-Luc-GFP was included as negative, virus-infected control. Mock refers to uninfected, medium only-treated cells. For Ad-FCU1-GFP and Ad-CMV-FCU1 a band for FCU1 was seen. β-Actin blots confirmed equal sample loading for both immunoblots.

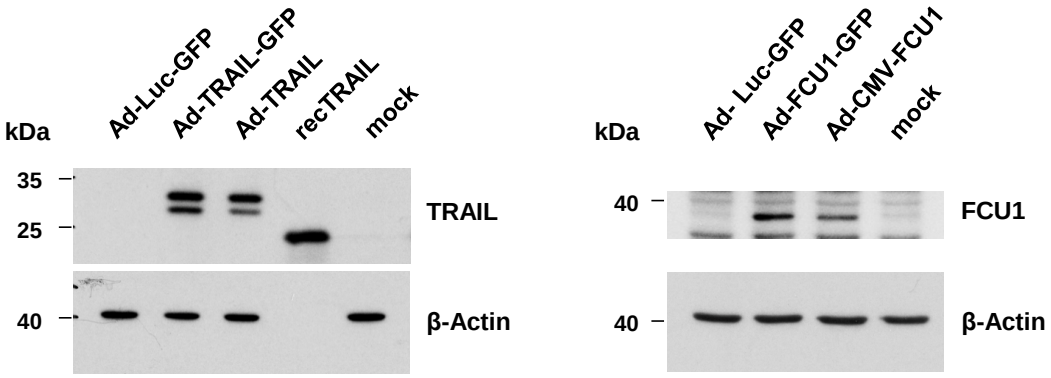


**Figure 22: Confirmation of TRAIL and FCU1 Transgene Expression by Immunoblotting.** MiaPaCa-2 were infected with 10 $TCID_{50}$/cell or mock-infected. 48 hours post-infection, lysates were prepared and TRAIL (left panel) and FCU1 (right panel) were detected by immunoblot. β-Actin was used as loading control. Ad-Luc-GFP: control virus, recTRAIL: KillerTRAIL™, soluble/human/recombinant (AXXORA), Ad-CMV-FCU1: replication-deficient, FCU1-expressing control virus; full-length TRAIL: 32 kDa, soluble TRAIL: 28 kDa, recTRAIL: 24 kDa.

### 7.4.2. Analyzing Differences in Transgene Expression

In subsequent infection experiments, A549 cells were infected with the viruses described in **Figure 21** and GFP expression was monitored. It was observed that GFP-intensities of infected A549 cells differed between the generated viruses. The pictures in the upper panel of **Figure 23A** show that GFP intensities for cells infected with Ad-TRAIL-GFP, Ad-FCU1-GFP, or Ad-GFP were stronger than for cells infected with Ad-Luc-GFP or Ad-Δ19K-Luc-GFP at 30 hours post-infection. PCR analysis confirmed that no sequence irregularities were present. To further confirm proper functionality of the viruses, the same set of images was taken, adding the antimetabolite AraC to the medium. AraC blocks cell and viral replication and therefore viral transgene expression, including GFP. 48 hours post-infection, fluorescence images were taken (**Figure 23A**, lower panel). In all virus-transduced wells, GFP expression was significantly reduced after adding of AraC, confirming that GFP transgene expression was under viral late promoter control and not irregularly independently expressed. Some observed residual GFP expression was most probably due to incomplete viral replication suppression because of the high virus input titers.

In order to analyze whether differences in GFP intensities could possibly be explained with differences in amounts of synthesized GFP protein, a Western blot was performed to quantify GFP protein in cells infected with the generated viruses (**Figure 23B**). It was observed that less GFP protein was expressed in Ad-Luc-GFP and Ad-Δ19K-Luc-GFP-infected cells, which correlates with the weaker GFP intensity seen in the pictures of **Figure 23A**. Control blots of hexon and fiber using the same samples, however, resulted in comparable band intensities of all samples, suggesting that there was no general problem with viral infection, replication, or synthesis of virus proteins.

As the genetic background was accurate and infectious viral particle production was not affected, experiments were continued and differences in GFP intensities were considered in fluorescence picture settings.

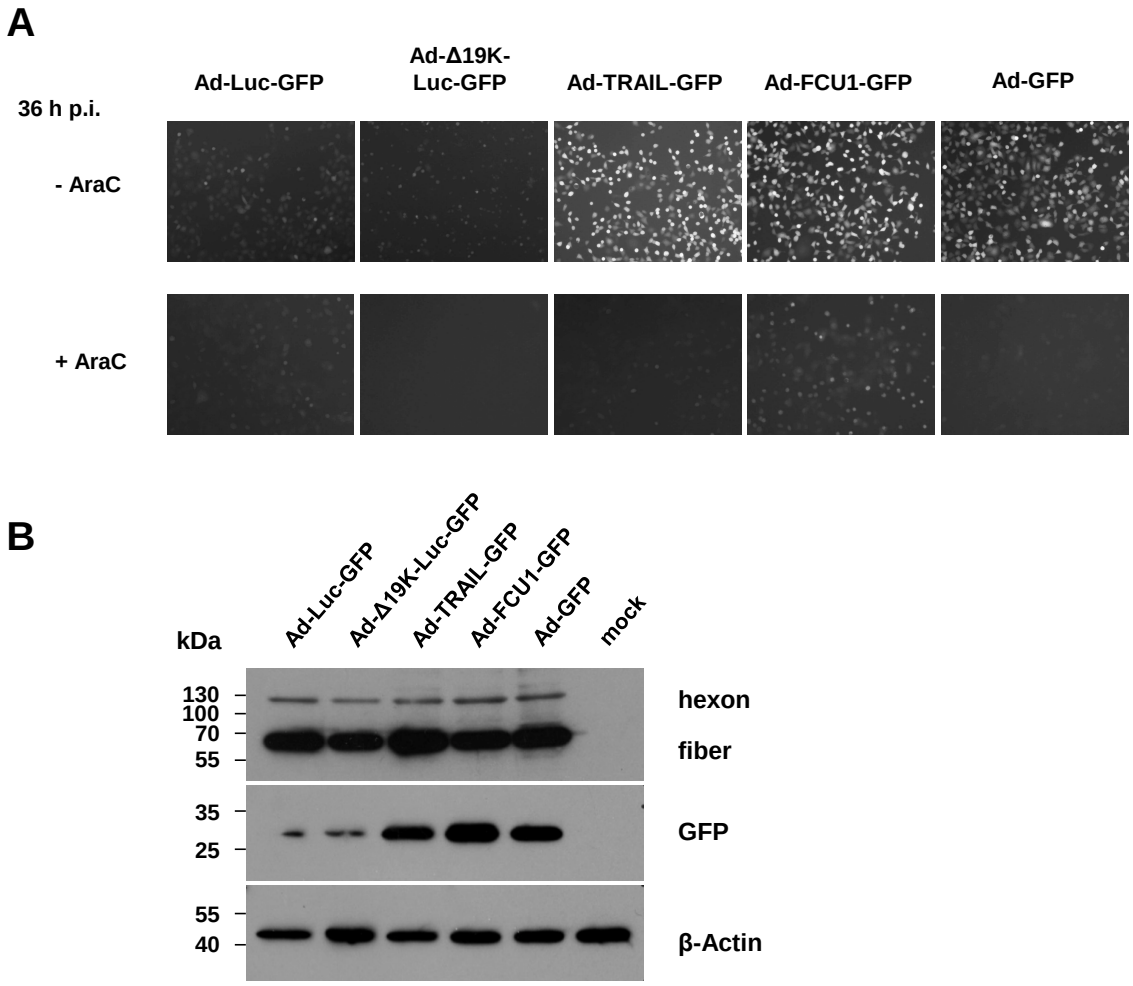


**Figure 23: Analyzing Differences in GFP Expression of the Generated Oncolytic Viruses. A:** Infection experiment utilizing AraC as viral replication inhibitor. A549 cells were infected with 100 $TCID_{50}$/cell of the indicated virus. 2 hours post-infection medium containing 25 µg/ml AraC or medium without AraC was added as indicated. AraC was replenished every 12 hours. 30 hours post-infection, fluorescence pictures were taken to monitor GFP intensities. **B:** Analysis of GFP, hexon, and fiber expression by immunoblotting. A549 cells were infected with 10 $TCID_{50}$/cell, 48 hours post-infection lysates were prepared and hexon/fiber and GFP were detected by immunoblot. β-Actin was used as loading control. Ad-Luc-GFP: control virus. Molecular weights: hexon: 130 kDa, fiber: 70 kDa, GFP: 27 kDa.

## 7.5. Migration Assay of Virus-Infected MSCs

A transwell migration assay (12 µm pore size) was performed to analyze whether MSCs migration capacity was affected by infection with the modified viruses. The aim was to analyze whether virus infection itself affected the migration behavior of MSCs and especially, whether the deletion of *E1B19K* or insertion of TRAIL affected MSC migration. The modifications showed improved replication and release kinetics from MSCs (**Figure 15**). Following, it was crucial to analyze whether they allow MSC migration maintenance for the length of time the MSCs need to reach the tumor. Transduced MSCs were allowed to migrate towards 10% FBS as chemoattractant for 38 hours (for procedure overview see **Figure 24A**). 38 hours correlates to the time reported in the literature that the MSCs need to home to a tumor *in vivo* after systemic application [142-144]. Further, this time period was reasonable since it was prior to virus release but guaranteeing sufficient GFP-transgene expression for monitoring.

The day before the experiment, MSCs were stained with PKH26 Red Fluorescent Cell Linker Kit (Sigma). 2 hours prior to the initiation of migration, MSCs were transduced with 2,500 $TCID_{50}$/cell of Ad-Luc-GFP, Ad-Δ19K-Luc-GFP, Ad-TRAIL-Luc, or Ad-FCU1-GFP or were mock-infected. The infectious titer was determined in a pre-experiment to sufficiently transduce MSCs of this donor without inducing an unspecific cytotoxic effect caused by an excess of physical viral particles. MSCs were added into the inside of the transwell insert (migration) or were plated in one well of a 24-well plate (controls).

At the end of the migration time the inserts were removed, non-migratory cells were removed from the upper side of the transwell membranes and fluorescence pictures of the lower side of the membranes were taken (**Figure 24B**, upper panel). The pictures show red-fluorescent cell membranes of all MSCs as well as a population of green-fluorescent virus-infected MSCs. The fraction of infected, migrated cells was determined by counting green and red fluorescent cells. However, this was not easily done for the transwells due to focusing problems of the sloping membrane surfaces, identification of cells which are still partly stuck in one of the pores, and high background fluorescence due to auto-fluorescence of the membranes. The counting resulted in approximately 80% infected migrated cells for all infections. The same analysis was done with the infected control MSCs, which had been plated in the 24-well plate (**Figure 24B**, middle panel). Here, green and red fluorescent cells were easily identifiable. After counting, the transduction rate was determined to be about 80%. The results showed that the ratio of uninfected to infected MSCs was the comparable, namely 80%, for migrated MSCs and MSCs plated in the 24-well plate (control). Therefore, the ratio of uninfected to infected cells remained the same after migration. This indicates that infected and uninfected cells migrated equally well. This was observed for infections with all modified viruses.

The control fluorescent pictures further show that Ad-Δ19K-Luc-GFP and (to lesser extend) Ad-TRAIL-Luc infected MSCs differed in morphology and were more rounded-up, while Ad-Luc-GFP and Ad-FCU1-GFP infected MSCs appeared morphologically similar to uninfected MSCs. This was according to the observations during the burst assay described in **Figure 16**. However, the fluorescence pictures suggest that these morphological differences had no effect on migratory competency.

Further, to determine the number of migrated cells quantitatively, a colorimetrical assay was performed. The transwell membranes were stained with crystal violet. Prior to dye extraction, pictures of the stained membranes were taken (**Figure 24B**, lower panel). Here again, the mentioned morphological differences were seen, especially in the picture of Ad-TRAIL-GFP-infected MSCs, where most of the cells were rounded-up. The dye was extracted and OD at 560 nm was measured. The colorimetrical evaluation resulted in no significant difference of infected MSCs compared to uninfected MSCs (**Figure 24C**), which indicates that the same total number of MSCs migrated in case of all samples.

Overall, it can be concluded that the infection of MSCs with the modified viruses retained unimpeded migration during the first 2 days post-infection. Therefore, neither the infection with oncolytic adenovirus itself (Ad-Luc-GFP) nor the effects of further viral modifications (deletion of *E1B19K*, the insertion of TRAIL, or the insertion of FCU1) affected the migration behavior of MSCs.

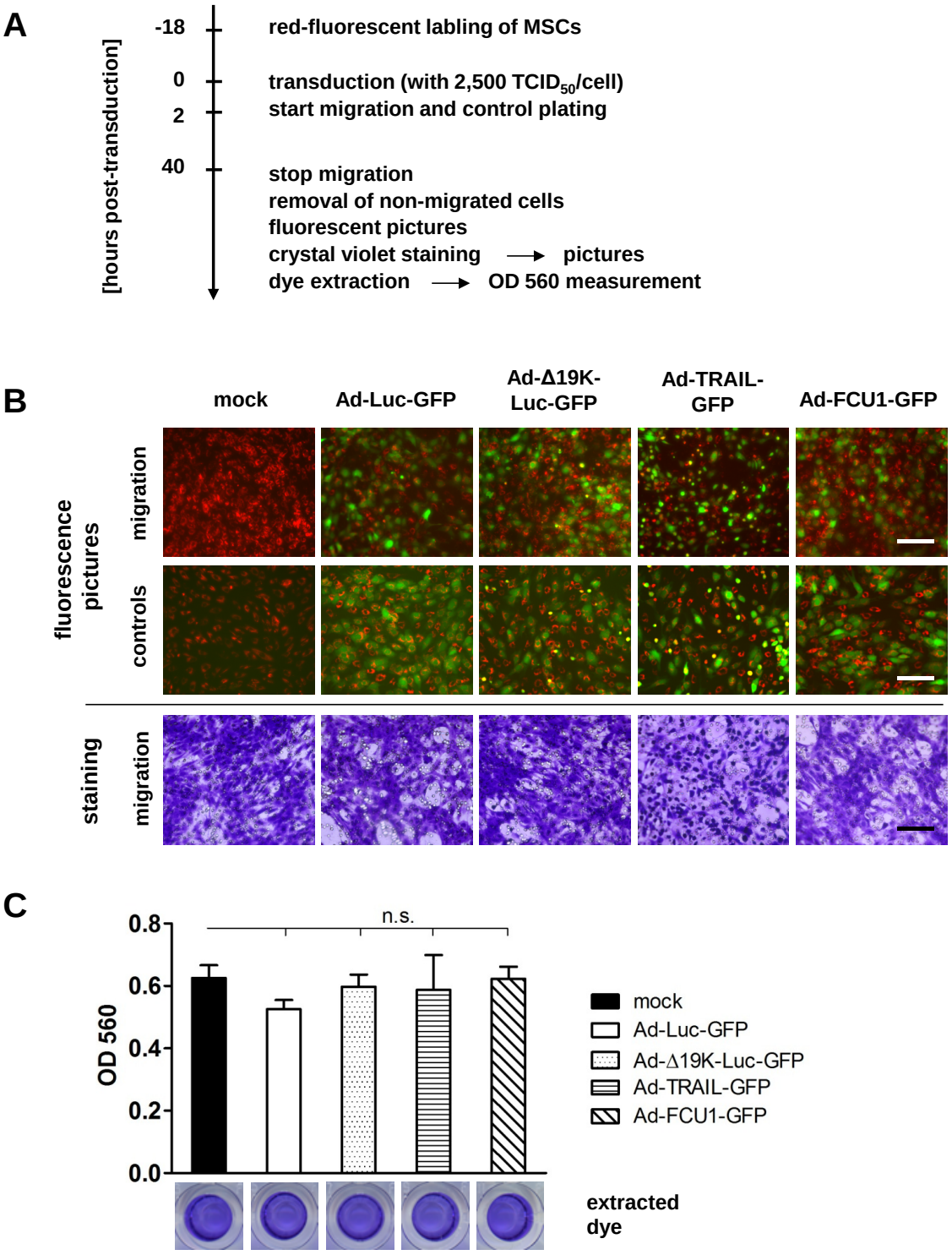


**Figure 24: Migration Analysis of MSCs Infected With the Modified Oncolytic Viruses. A:** Outline of the procedure of the MSC migration assay. MSCs were labeled with a red-fluorescent dye, infected, and allowed to migrate for 38 hours towards medium containing 10% FBS. The assay was evaluated qualitatively by fluorescent and bright-field pictures as well as quantitatively by colorimetrical measurement of the extracted dye solution. **B:** Qualitative evaluation of migration assay. Fluorescence pictures: overlay of red (MSCs) and green (virus-transduced MSCs) fluorescence images of migrated cells. For controls of transduction efficiency, half of the cells used for migration were plated in wells of a 24-well plate to determine transduction efficiency. Blue staining: MSCs on the membranes were stained with blue dye and bright-field pictures were taken prior to dye extraction. Scale bar = 200 µm. **C:** Quantitative evaluation of migration assay. Extracted dye solutions from the stained membranes were transferred to a 96-well plate, scanned, and OD560 was measured. Columns show mean OD readings, error bars show standard deviations of triplicate migrations. n.s.: no significant difference compared to mock-infected cells determined by one-way ANOVA.

## 7.6. Cytotoxicity Experiments in Established Pancreatic Adenocarcinoma Cell Lines

Following the proposed delivery model (**Figure 10**), the viruses need to infect and lyse the pancreatic tumor cells, including the tumor stem cells after being delivered at the tumor site by MSCs. Therefore, the killing properties of the generated oncolytic viruses, Ad-Δ19K-Luc-GFP, Ad-TRAIL-GFP, and Ad-FCU1-GFP/5-FC, were tested on established pancreatic adenocarcinoma cell lines MiaPaCa-2, BxPc-3, AsPc-1, and Panc-1. The investigated established pancreatic tumor cell lines can be associated with the different subpopulations of a tumor. In previous studies of our cooperation partner (group Ingrid Herr, University Hospital Heidelberg), the cell lines were characterized in terms of their stem cell resemblance based on the degree of differentiation, mutations in KRas/p53, colony/spheroid formation, ALDH activity, tumorigenicity in mice, and E-cadherin/Vimentin expression [31]. Based on this study, MiaPaCa-2 and AsPc-1 had been categorized as stem cell-like with the majority of the population showing stem cell characteristics; in contrast, BxPc-3 had been categorized as non-stem cell-like [31]. For Panc-1 it was reported, that a subpopulation with stem cell-like features was present (characterized by CD24+/CD44+, Vimentin, E-Cadherin,[157]). The provided data in the two publications did not allow a comparative grading of the stem cell-likeness. However, the oncolytic behaviour of the modified oncolytic viruses may give a first indication, whether tumor stem cells can be efficiently killed by oncolysis or bystander effects.

### 7.6.1. Cytotoxicity Assay in Pancreatic Adenocarcinoma Cell Line Monolayers

The generated viruses (**Figure 21**) were tested on established pancreatic adenocarcinoma cell lines to analyze, whether the modifications improved killing behavior compared to the control virus Ad-Luc-GFP. The aim of the study was to test whether improved oncolysis could be mediated by the *E1B19K*-deleted virus and whether improved tumor cell killing by bystander effects of TRAIL and the FCU1/5-FC prodrug system. Cells were plated and infected 24 hours later with serial dilution of viruses. The plates were incubated for 6 or 8 days. Afterwards, crystal violet was added to each well, which fixed and stained the remaining viable cells. Plates were dried and scanned (**Figure 25**). The wells, where the virus was able to lyse the cells, appear clear, whereas the wells, which were not affected by the virus, show an intact, stained cell layer (experiment was previously explained in **section 7.2.3**). Improved killing was defined by lysis at lower virus concentrations compared to the control virus Ad-Luc-GFP.

In the left lane of each plate in **Figure 25**, Ad-CMV-GFP was used as replication-deficient control virus (described in **section 7.2.3**). For BxPc-3 and AsPc-1, cells detached when they were infected with 100 $TCID_{50}$/cell Ad-CMV-GFP. As Ad-CMV-GFP was a replication-deficient virus, this effect was due to toxicity induced by the excess of physical viral particles. Starting at 10 $TCID_{50}$/cell, no cell loss was observed anymore. This replication-deficient virus control validated for the oncolytic replication-competent viruses that observed lysis with 10 $TCID_{50}$/cell or lower virus concentrations was due to oncolytic or bystander killing activity and not to unspecifically induced cell death. In the second lane of **Figure 25**, the control oncolytic virus Ad-Luc-GFP was administered followed by the modified oncolytic viruses. The following listing summarizes the killing behavior of the improved oncolytic viruses compared to Ad-Luc-GFP:

- Ad-Δ19K-Luc-GFP improved lysis in Panc-1 about 10-fold; in MiaPaCa-2, BxPc-3 and AsPc-1 killing was about 10-fold poorer compared to Ad-Luc-GFP.
- Ad-TRAIL-GFP improved lysis in Panc-1 (about 10-fold), strongly in AsPc-1 (about 100-fold), weakly in MiaPaCa-2 (<10-fold), but not in BxPc-3 compared to Ad-Luc-GFP.

- Ad-FCU1-GFP without the prodrug 5-FC was tested to confirm that the oncolytic behavior is similar to Ad-Luc-GFP; this was the case for all analyzed established pancreatic adenocarcinoma cell lines.
- Addition of 5-FC improved toxicity of Ad-FCU1-GFP in BxPc-3 and AsPc-1, and slightly in MiaPaCa-2; no improvement was seen in Panc-1.

In the last two lanes, 5-FU and 5-FC were tested independently from Ad-FCU1-GFP combination treatment. These controls were used to estimate 5-FU sensitivity of each cell line as well as to rule out unspecific effects of 5-FC prodrug background toxicity. The 5-FU sensitivity was shown to be different in the cell lines. The $EC_{50}$, estimated from the cytotoxic effect seen on the plates, varied between 0.01 (BxPc-3), 0.05 (MiaPaCa-2 and Panc-1), to 0.001 (AsPc-1) $TCID_{50}$/cell. Finally in the last lane, it was verified that 10 µM of 5-FC, which was the concentration used in combination with Ad-FCU1-GFP, was not toxic itself to any of the cell lines. In Lane 6, the combination treatment, Ad-FCU1-GFP + 10 µM 5-FC was tested. In BxPc-3 and AsPc-1, cytotoxicity was increased 10-100-fold compared to the control virus Ad-Luc-GFP. Therefore, the prodrug was efficiently converted and was contributing to the cytotoxic effect in addition to viral oncolysis in responsive cells. In MiaPaCa-2 and Panc-1, no or a very little beneficial effect was observed.

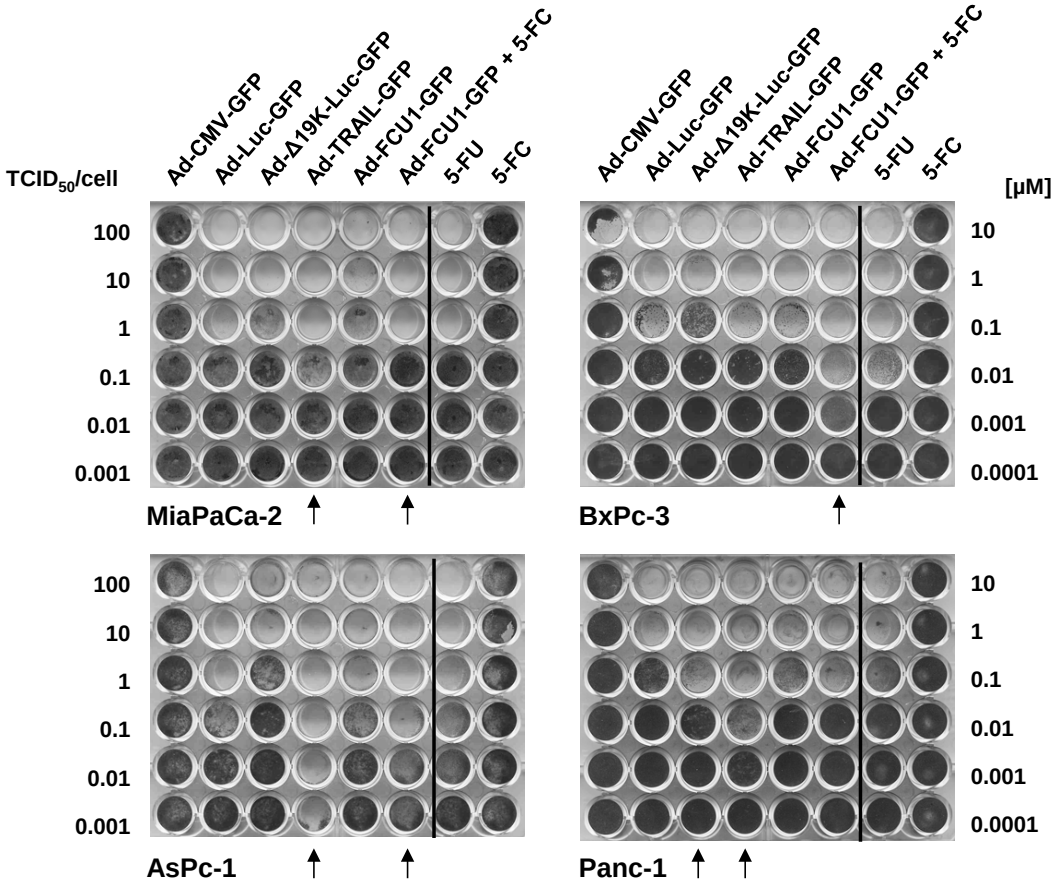


**Figure 25: Cytotoxicity of the Modified Viruses on Pancreatic Adenocarcinoma Cell Lines.** Cells were infected with serial dilutions of $TCID_{50}$/cell with the indicated viruses. 5 days prior to staining, 5-FC and 5-FU were added in concentrations indicated on the right side of the picture panel. 10 µM 5-FC was added to wells of lane 6 (Ad-FCU1-GFP + 5-FC). 6 days (MiaPaCa-2 and AsPc-1) or 8 days (BxPc-3 and Panc-1) post-infection cells were stained with crystal violet. Plates were dried and scanned. Ad-CMV-GFP: control virus, 5-FC: 5-Fluorocytosine, 5-FU: 5-Fluorouracil.

In conclusion, the cytotoxicity experiment revealed that the modified oncolytic viruses were able to improve killing in a subset of tumor cells: 2 established pancreatic tumor cell lines were TRAIL-sensitive, 1 cell line showed improved killing for Ad-Δ19K-Luc-GFP, and 2 were sensitive for the effects of the prodrug activation system Ad-FCU1-GFP/5-FC. They also revealed variations in sensitivity between cell lines to the different killing strategies.

### 7.6.2. Analysis of Transduction, Spread, and Cytotoxicity in MiaPaCa-2 Spheroids

Next, viral spread and cytotoxicity was aimed to be monitored in a 3D tumor-mimicking model. Further, the experiment was aimed to give indications if tumor stem cells can be targeted with the improved viruses in a 3D model. Therefore, MiaPaCa-2 cells grown in spheroids were chosen. MiaPaCa-2 cells had been characterized as tumor-stem-cell-like with spheroid forming capacity [31]. The spheroids were provided by the Herr group (University Hospital Heidelberg). 5,000 MiaPaCa-2 cells were seeded in 100 µl medium containing 0.25 % methylcellulose in a well of a round-bottom 96-well plate. Within 24 hours, the cells gathered at the well bottom and formed the spheroid. The methylcellulose was adding viscosity to the medium and therefore improving spheroid cell cohesion.
Spheroids were infected 24 hours after seeding with the modified viruses Ad-Luc-GFP, Ad-Δ19K-IL-GFP, Ad-TRAIL-GFP, and Ad-FCU1-GFP (described in **Figure 21**). Virus spread was monitored via GFP fluorescence imaging. Fluorescent pictures were taken for 8 days in 2 day intervals (**Figure 26**). Since the spheroids were cultivated separately in 96-wells, each spheroid could be monitored in a steady position over the whole time span.

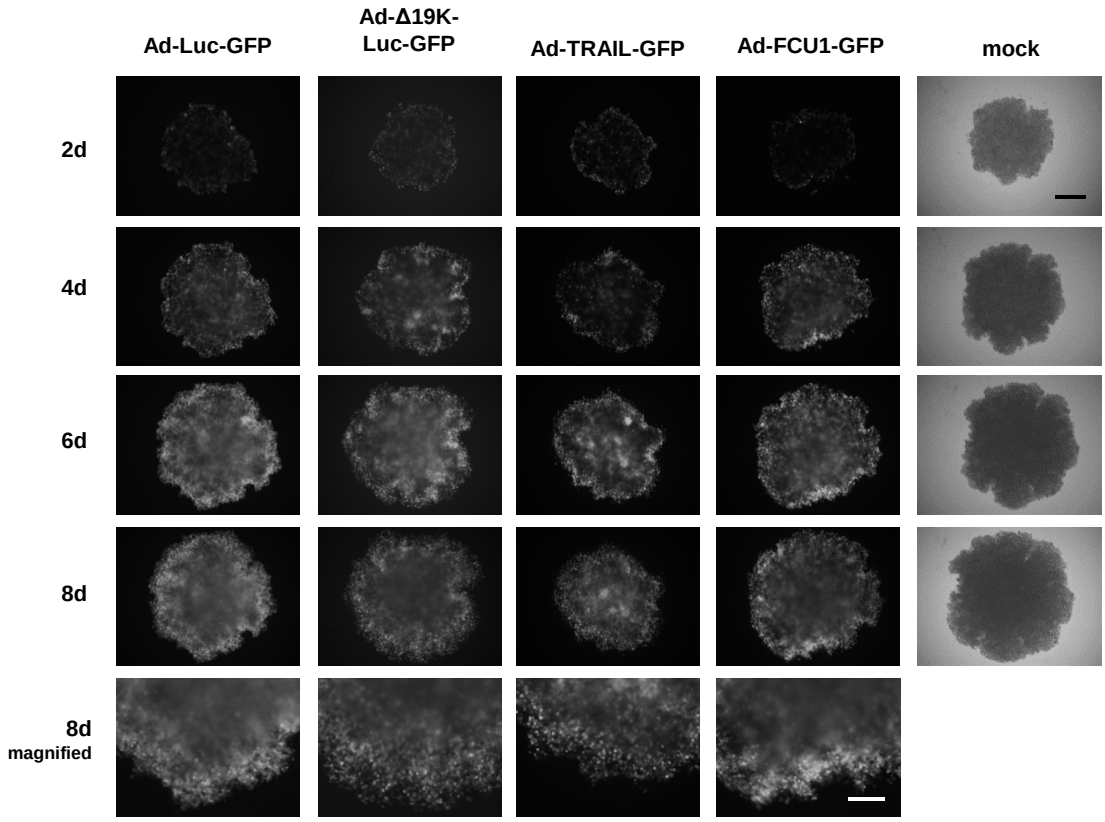


**Figure 26: Monitoring and Analysis of MiaPaCa-2 Spheroids Following Infection With the Modified Viruses.** MiaPaCa-2 spheroids were infected with 100 $TCID_{50}$/cell of indicated viruses or mock-infected. Virus spread was monitored via GFP expression at 2, 4, 6, and 8 days. Fluorescence and bright-field pictures were taken. Scale bar = 600 µm, magnified picture scale bar = 300 µm.

Increase in fluorescence intensity was observed until day 6 for all viruses. At day 8, fluorescence decreased probably due to progressing oncolysis, but also to nutrition depletion in the spheroid core [158]. Noticeable was that spheroid shapes differed depending on the virus variant. Ad-Luc-GFP and Ad-FCU1-GFP did not differ in size and shape from the mock-infected control spheroids throughout the experiment. The Ad-Δ19K-Luc-GFP and Ad-TRAIL-GFP-infected spheroids lost integrity around the outer rim loose, where cells were observed that made the rim seemed diffuse (**Figure 26**, 8d). For the Ad-TRAIL-GFP-infected spheroids, the images suggest that spheroids remained smaller in size compared to Ad-Luc-GFP and mock starting from day 4 post-infection.

This observation was quantitatively investigated by measuring the spheroid surface area. For this, the program Histo® was provided by the Herr group (University Hospital Heidelberg), with which the spheroid size was determined in pixels in the taken images. The results of two independent experiments are shown in **Figure 27**. The results show a significantly smaller spheroid size for Ad-TRAIL-GFP-infected spheroids compared to Ad-Luc-GFP in both experiments and compared to mock in experiment 2.

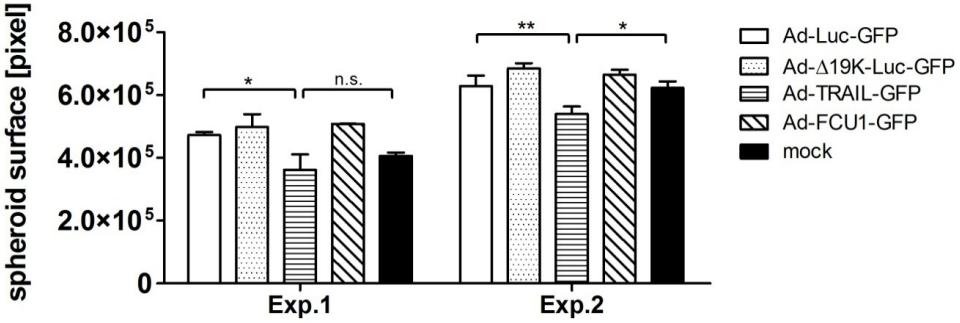


**Figure 27: Surface Area Determination of Infected and Mock-Infected MiaPaCa-2 Spheroids.** The spheroid sizes were determined from images at 4x magnification at day 6 post-infection. Spheroid sizes were determined in pixels (see Methods section 10.5.9). Columns show mean values and error bars show standard deviations of three spheroids per group. n.s.: not significant, *: $p < 0.05$, **: $p < 0.01$ determined by one-way ANOVA.

The disintegration of the spheroid rim seen during spheroid infection with Ad-Δ19K-IL-GFP and Ad-TRJAIL-GFP in **Figure 26** was further pursued. One assumption was that these diffuse layers were the remains of cells lysed by the virus and therefore were not attached to the spheroid body anymore. An LDH assay was performed to assay possible differences of spheroid integrity. In viable cells, LDH is only found intracellularly. Measuring LDH activity in the medium therefore gave an indication about the number of disintegrated, dead cells. LDH activity was measured in the supernatant of infected spheroids at day 4 and day 6 post-infection. In correlation to LDH activity measured in mock-infected and complete lysis controls, the amount of dead cells for virus-infected spheroids was determined (also see Methods **section 10.5.8**).

Consistent observations in two independent experiments (**Figure 28**) showed that at day 4, LDH release of Ad-TRAIL-GFP-infected spheroids was greatest followed by Ad-Δ19K-Luc-GFP. Vice versa at day 6, Ad-Δ19K-Luc-GFP-infected spheroids showed the greatest LDH release followed by Ad-TRAIL-GFP. Infections with Ad-Luc-GFP and Ad-FCU1-GFP led to lower, but above mock-infected levels of LDH release. Comparing the two experiments, it was noticed that the background LDH activity levels of the mock-infected controls were significantly different. Looking at day 6 post-infection for mock-infected control spheroids, in experiment 1 about 45% of spheroid cells were dead cells, while in experiment 2 only about 8% of cells were dead. This difference also translated into the increase of

dead cells caused by virus infection. In experiment 1 on day 6, the difference of mock- and Ad-Δ19K-Luc-GFP-infected samples was 1.4-fold (mock: 45.19% dead cells, Ad-Δ19K-Luc-GFP: 63.64% dead cells). For experiment 2, the factor was 4-fold (mock: 7.65% dead cells, Ad-Δ19K-Luc-GFP: 30.78% dead cells). This outcome suggests that critical conditions, e.g. the quality of spheroids, varied between experiments. However, while the background killing was different, the toxicity induced by the virus was very similar (absolute differences mock and Ad-Δ19K-Luc-GFP: 18% in experiment 1 and 23% in experiment 2). Further, examination of the measured LDH activity and therefore the amount of dead cells over time revealed an overall tendency, which was a fast onset-killing by Ad-TRAIL-GFP and the best longer-term killing by Ad-Δ19K-Luc-GFP.

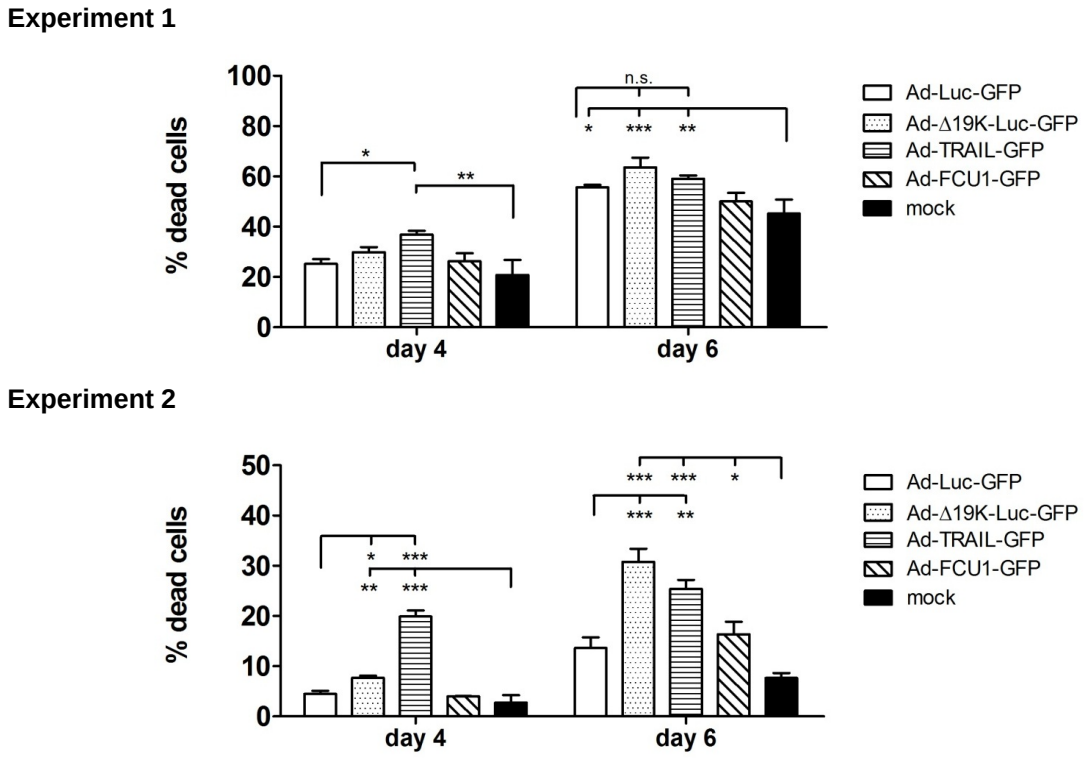


**Figure 28: Determining the Amount of Dead Cells Following MiaPaCa-2 Spheroid Infection With the Modified Viruses.** MiaPaCa-2 spheroids were infected with 100 $TCID_{50}$/cell of indicated viruses or mock-infected. LDH release was monitored in infected MiaPaCa-2 spheroid supernatants at day 4 and day 6 post-infection. Graphs shows means of % of dead cells compared to total lysis control; error bars show standard deviations of three spheroids per condition. n.s.: not significant, *: $p < 0.05$, **: $p < 0.01$, ***: $p < 0.001$ determined by one-way ANOVA.

In conclusion, Ad-Δ19K-Luc-GFP and Ad-TRAIL-GFP changed morphology of tumor spheroids and caused enhanced LDH release from the spheroid cells, indicating improved oncolysis. Interestingly, oncolysis experiments in MiaPaCa-2 monolayers (**Figure 25**) did indicated weak sensitivity for TRAIL and even a poorer oncolytic activity of Ad-Δ19K-Luc-GFP compared to the Ad-Luc-GFP control virus. The effects of the viruses on the tumor cells were apparently different when MiaPaCa-2 were grown as spheroids.

## 7.7. Experiments in Low-Passage Pancreatic Ductal Adenocarcinoma Cell Cultures

Two low-passage pancreatic ductal adenocarcinoma cell cultures, which were established from tumor material of patients, were tested for transduction and oncolytic capacity.

JoPaca-1 cells were described in Fredebohm et al. [153] and were isolated from poorly differentiated pancreatic ductal adenocarcinoma. The authors reported that they identified three different cell subpopulations by shape and spreading behavior. Further, FACS analysis revealed that a large fraction of cells in the culture expressed stem cell markers (CD133+/ALDH1+: 21%; CD44+/CD24+/ESA+: 10%, capability of tumor sphere formation). PacaDD-159 cells were described in Rückert et al. [152, 159]. These cells were also isolated from pancreatic ductal adenocarcinoma. qPCR analysis revealed that the amount of stem cell marker mRNA is similar to those of Capan-1, which had been reported to be stem cell-like [31]. Therefore it can be concluded that both cell cultures contained a heterogeneous subpopulation of cells, including a fraction which was expressing tumor stem cell markers. This subpopulation can be claimed to mirror the tumor-initiating cells in pancreatic adenocarcinomas and analysis of these cell lines therefore gave strong indications for *in vivo* situations.

Transduction experiments were already shown in **Figure 13B**, which identified the Ad5/3 capsid variant virus to perform best transduction. To gain information about transducibility, both cell lines were infected with serial dilutions of Ad-GFP (virus and experiment described in **section 7.3.1**). 48 hours post-infection images were taken and GFP-positive cells were correlated with transduction efficiency. Fluorescence pictures are shown in **Figure 29**.

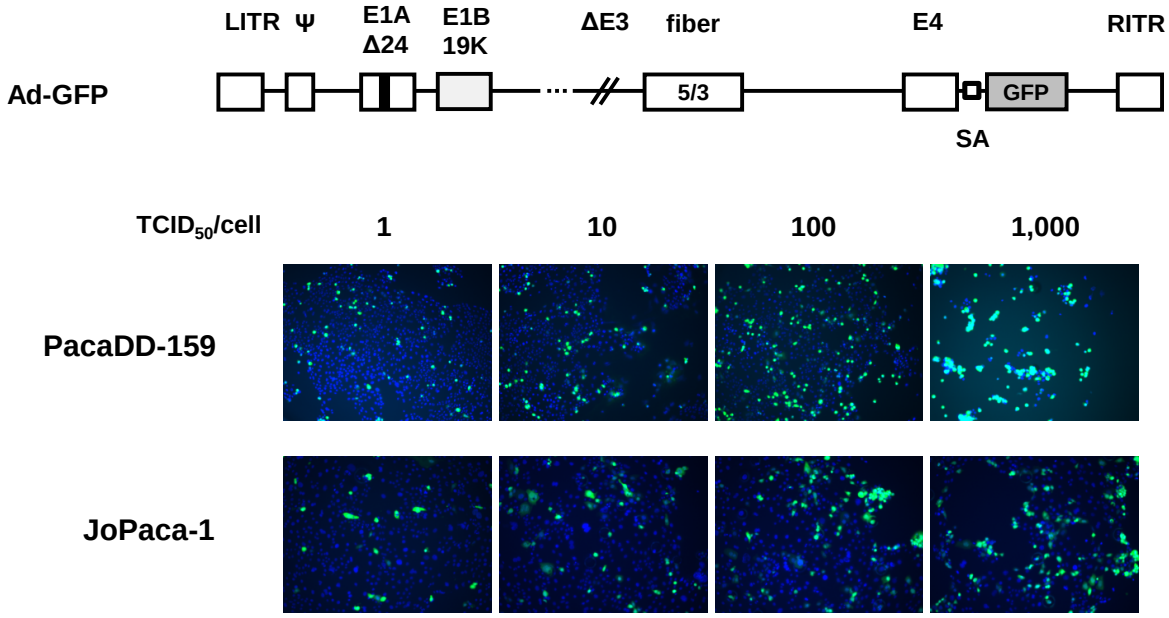


**Figure 29: Adenoviral Infection Efficiency of Low-Passage Pancreatic Adenocarcinoma Cell Cultures.** Fluorescence pictures to determine infection efficiency. Low-passage pancreatic ductal adenocarcinoma cell lines PacaDD-159 and JoPaca-1 were infected with 1, 10, 100, or 1,000 $TCID_{50}$/cell of Ad-GFP. 48 hours post-infection cells were fixed with 4% paraformaldehyde, permeabilized with 0.5% Triton-X 100 solution and stained with Hoechst 33258. Fluorescence pictures were taken with 10x magnification.

For PacaDD-159 it was observed that transduction with 1 $TCID_{50}$/cell led to very few infected, GFP-positive cells. As the viral titer was increased up to 1,000 $TCID_{50}$/cell, transduction rates as well as

the cytopathic effect were increasing. Even with the highest tested titer of 1,000 $TCID_{50}$/cell, not all cells were GFP-positive. Therefore full transduction was not reached even though all cells, including the non-GFP-positive ones, were rounded up and apparently affected by virus infection. In JoPaca-1 cells, the observations were similar. Here, it was remarkable that infected cells seem to cluster, which could indicate that there might be a difference in infectibility of the reported subpopulation of cells.

A cytotoxicity assay was performed testing the improved oncolytic viruses on the two cell cultures (**Figure 30**). The experimental set-up was described in **section 7.6.1** before. In PacaDD-159, Ad-Δ19K-Luc-GFP showed no improvement in killing compared to the control virus Ad-Luc-GFP. Ad-TRAIL-GFP as well as Ad-FCU1-GFP + 5-FC led to an about 10-fold increased cytotoxicity compared to Ad-Luc-GP. JoPaca-1 showed about 100-fold better infectibility. Though here, no improvement in lysis was observed for infection with Ad-TRAIL-GFP or Ad-FCU1-GFP + 5-FC. Infection with Ad-Δ19K-Luc-GFP led to an about 10-fold reduced induction of oncolysis.
Compared to the cytotoxicity assay performed with established pancreatic adenocarcinoma cell lines in **Figure 25**, it was observed that the overall infectibility was lower. While infection with 1 $TCID_{50}$/cell of control virus Ad-Luc-GFP was sufficient to lyse 3 out of 4 established cells within 6 or 8 days, 100 $TCID_{50}$/cell were needed for PacaDD-159.

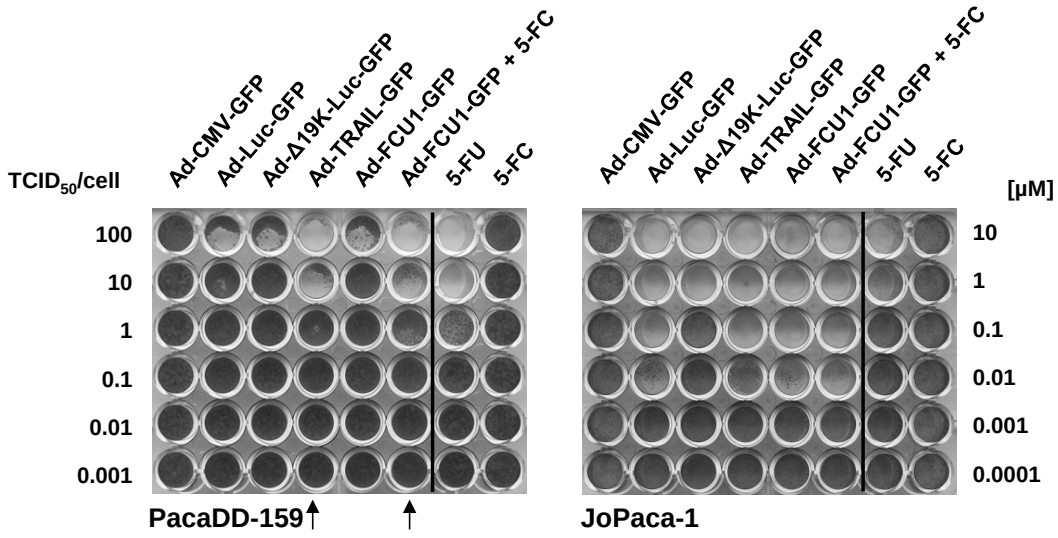


**Figure 30: Cytotoxicity of the Modified Viruses on Low-Passage Pancreatic Ductal Adenocarcinoma Cultures.** Cells were infected with serial dilutions of $TCID_{50}$/cell of indicated viruses. 5 days prior to staining, 5-FC and 5-FU were added in concentrations indicated on the right of the picture panel. To lane 6 (Ad-FCU1-GFP + 5-FC) were 10 µM 5-FC added. 12 days post-infection cells were stained with crystal violet. Plates were dried and scanned. Ad-CMV-GFP: control virus, 5-FC: 5-Fluorocytosine, 5-FU: 5-Fluorouracil.

In conclusion, variations between low-passage pancreatic adenocarcinoma cell lines were observed. In PacaDD-159, the infection with the improved oncolytic viruses resulted in improved cytotoxicity through the additional effect of TRAIL- or 5-FU-mediated killing, while in JoPaca-1 cells the improved viruses could not perform improved oncolysis. This indicates that a subset of pancreatic ductal adenocarcinomas was susceptible to improved lysis by the tested, modified viruses.

## 7.8. Virus Cloning

This section describes the cloning of the viruses which were generated during the course of this project. For the origin of the other viruses, see the references in the previous sections or Materials **section 9.9**.

### 7.8.1. General Cloning Strategies

The principle strategy, which was followed for cloning, was first described by He et al [160]. The complete adenovirus genome size with approximately 36 kbp is too big to introduce modifications directly into the genome by restriction enzyme digestions. Therefore, a system of shuttle plasmids was used. The shuttle plasmids had a size of about 10 kb and contained the parts of the viral genome, where modifications needed to be introduced. The genes were modified in the shuttle plasmid and subsequently introduced into the full viral genome via homologous recombination of the modified shuttle plasmid with a viral backbone plasmid.

**Figure 31** describes the general cloning strategies, which were used for this project. Modifications were introduced into three different areas of the viral genome:

i. Into the *E1* region (deletion of *E1B19K*)
ii. Transgene insertion via IRES downstream of the fiber5/3 (*Luc*, *TRAIL*)
iii. Transgene insertion via SA downstream of *E4* (*GFP*)

Due to the shuttle system, two strategies were necessary to introduce the transgenes, whereas i. and iii. used the same shuttle plasmid system (**Strategy 1**, left panel of **Figure 31**), while ii. required another (**Strategy 2**, right panel of **Figure 31**).

**Strategy 1**: The shuttle plasmids pShuttleX contained the viral genes *E4*, the left and right inverted terminal repeats (LITR, RITR), and the early genes *E1A* and *E1B*. In the plasmid map of pShuttleX in **Figure 31** are in red the two sites shown, where modifications were introduced, namely the *E1B19K* deletion and the site of transgenes insertion. The bacterial elements (origin and antibiotic resistance) were between LITR and RITR. HR1 and HR2 refer to the homologous regions to the viral backbone vector. The modifications were introduced via restriction enzyme digestion and re-ligation. The modified pShuttleX was then digested with PmeI, which linearized the plasmid. Linearization opens the plasmid in a way that the homologous regions were on either side of the free ends.

The vectors, which contain the entire viral genome and where the modifications have to be introduced, are called pVKs. The pVKs used in this study and from which one is shown in **Figure 31**/Strategy1 already contained modifications in other parts of the viral genome (deletion of *E3*: Δ*E3*, fiber5/3).

Both plasmids were electroporated into BJ5183 bacteria. The pShuttleX aligns to the pVK via the homologous regions and the bacterial enzymes catalyze the homologous recombination. This leads to an exchange of the pShuttle sequence with the according sequence of the pVK plasmid, including the antibiotic resistance genes. This allowed a subsequent selection for kanamycin-resistant clones. The DNA of the resulting colonies was isolated and genomes were analyzed by restriction enzyme digestion. Finally, the DNA of the recombined constructs were PacI digested, which removed all sequences with bacterial origin. The viral DNA was then transfected into A549 cells (see Methods **section 10.3.1**) resulting in infectious viral particles production within 1-2 weeks.

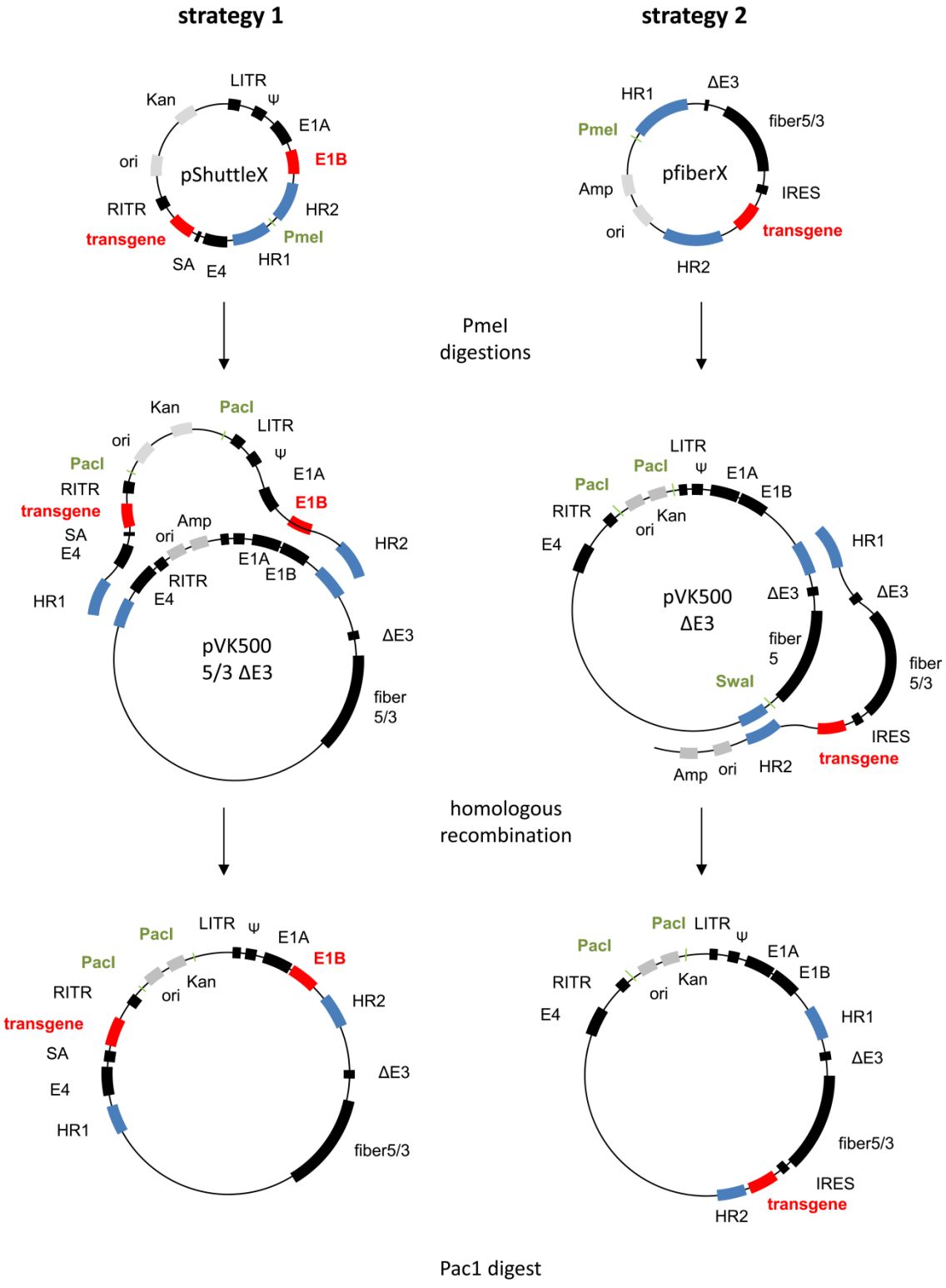


**Figure 31: Strategies of Virus Cloning.** Shuttle plasmids pShuttleX (strategy 1) or pfiberX (strategy 2) were modified by gene modification or transgene insertion. Via homologous recombination with the pVK plasmid, which contained the viral backbone, the modifications were introduced into the viral genome. LITR/RITR: left/right inverted terminal repeat, Ψ : packaging signal, *E1A, E1B:* immediate early genes, *E3* gene, *ΔE3:* deletion of *E3*, fiber5: HAdV-5 wild type fiber, fiber 5/3: HAdV-5 shaft/HAdV-3 knob fiber chimera, IRES: internal ribosomal entry site, *E4* gene, SA: splice acceptor site, HR1/HR2: homologous regions 1 and 2, ori: origin, Amp: ampicillin resistance gene, Kan: kanamycin resistance gene.

**Strategy 2**: Via this strategy, a transgene was inserted downstream of the fiber5/3. In order to allow transgene translation with the fiber, an internal ribosomal entry site (IRES) sequence was introduced as connector between the two genes. The shuttle plasmids pfiberX contained the viral genes *E3* (in this case Δ*E3*), the fiber5/3, the IRES sequence, and the transgene. The plasmid map of pfiberX in **Figure 31** shows in red the sites where a transgenes was inserted. The homologous region 1 and 2 flank the viral sequence. The bacterial elements (origin and antibiotic resistance) were between HR1 and HR2. The transgene was introduced via restriction enzyme digestion and re-ligation. The modified pfiber was then linearized by digestion with PmeI.
The homologous recombination procedure was analogous as described for Strategy 1. Here, linearization of the pVK vector with SwaI was essential, as the original pVK and the recombination product contained the same antibiotic resistance. The recombined constructs were PacI digested to remove bacterial sequences and transfected into A549 cells.

In the following chapters, the cloning of the individual viruses is explained, referring to either strategy 1 or 2.

### 7.8.2. Cloning of Ad-GFP

pGL3-BPSA-GFP was generated by replacing Luciferase of pGL3-BPSA-Luc (described in [93]) with *GFP* (from Clontech, Mountain View, CA). The BPSA-GFP-SV40polyA cassette was then introduced into the pShuttle plasmid pSΔ24 (described in [161]). Following **strategy 1** (**Figure 31**), the generated pSΔ24-GFP was recombined with pVK500 5/3 ΔE3 (generated in the Nettelbeck lab), resulting pVK500 5/3 Δ24 ΔE3 GFP. Subsequent PacI digestion resulted in the genome of Ad-GFP (**Figure 32**).

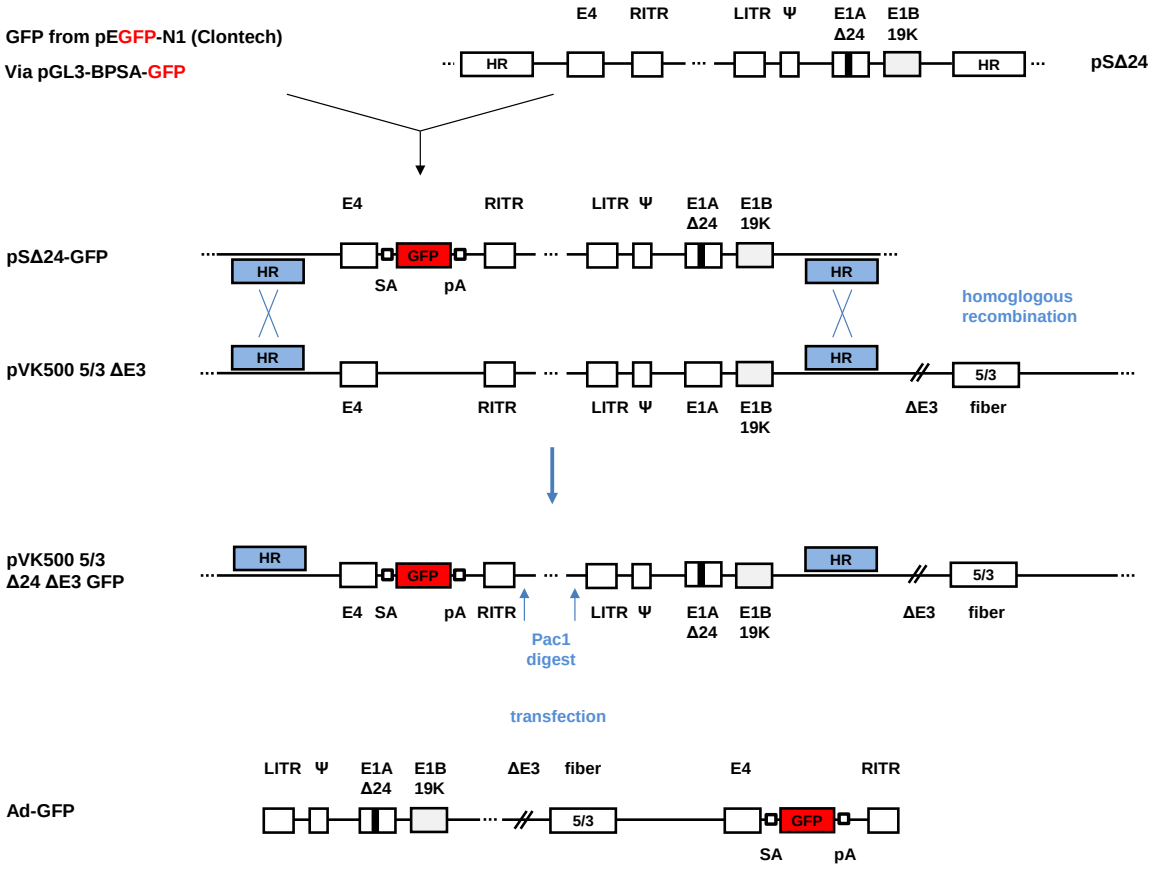


**Figure 32: Outlines of Cloning Intermediate Constructs for the Generation of Ad-GFP.** LITR/RITR: left/right inverted terminal repeat, Ψ: packaging signal, *E1A, E1B:* immediate early genes, *E1AΔ24*: deletion of pRb-binding region in *E1A* for cancer selective replication, *ΔE3:* deletion of *E3*, fiber 5/3: HAdV-5 shaft/HAdV-3 knob fiber chimera, *E4* gene, SA: splice acceptor site, *GFP*: gene encoding green fluorescent protein, pA: SV40polyA, HR: homologous region.

### 7.8.3. Cloning of Ad-Luc-GFP

Following **strategy 1**, pSΔ24-GFP, generated in **section 7.8.2**, was recombined with pVK500 5/3 ΔE3 IL [81], resulting in pVK500 5/3 Δ24 ΔE3 Luc GFP. Subsequent PacI digestion resulted in the genome of Ad-Luc-GFP (**Figure 33**).

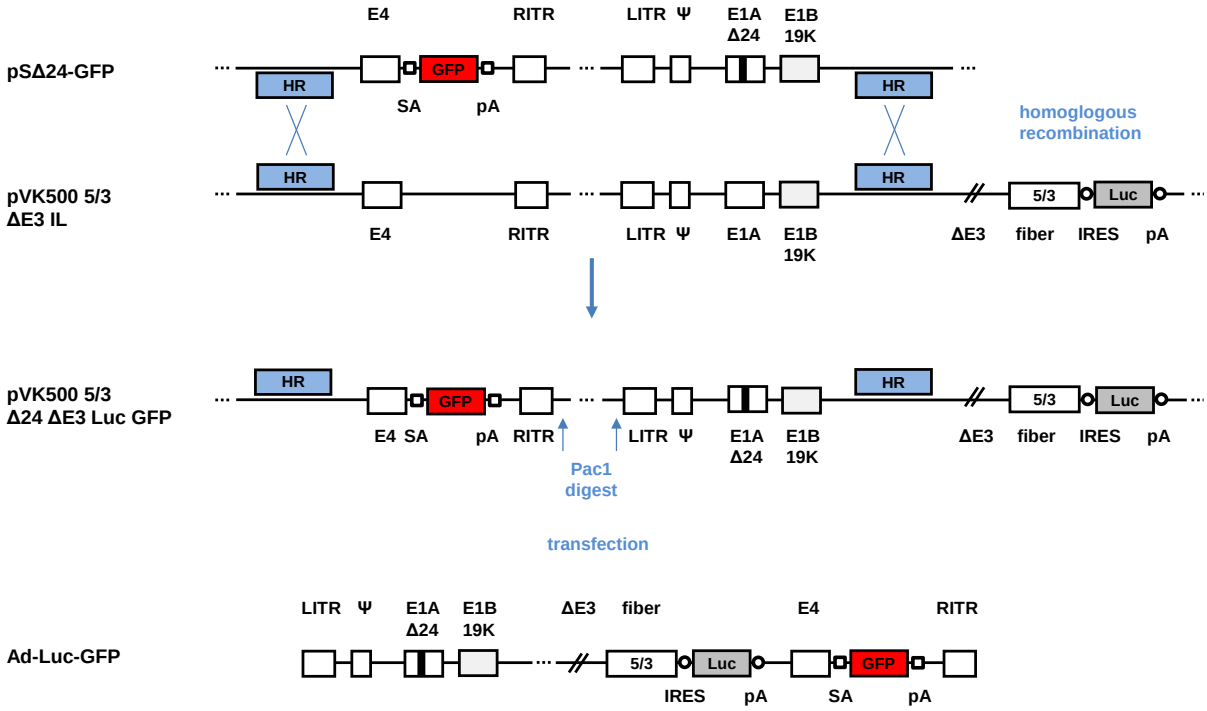


**Figure 33: Outlines of Cloning Intermediate Constructs for the Generation of Ad-Luc-GFP.** LITR/RITR: left/right inverted terminal repeat, *Ψ*: packaging signal, *E1A, E1B:* immediate early genes, *E1AΔ24*: deletion of pRb-binding region in *E1A* for cancer selective replication, *ΔE3:* deletion of *E3*, fiber 5/3: HAdV-5 shaft/HAdV-3 knob fiber chimera, IRES: internal ribosomal entry site, *Luc*: gene encoding firefly luciferase, *E4* gene, SA: splice acceptor site, *GFP*: gene encoding green fluorescent protein, pA: SV40polyA, HR: homologous region.

### 7.8.4. Cloning of Ad-Δ19K-Luc-GFP

From pSΔ24-E1B19K- (described in [81]), the *E1B19K* deletion was inserted into the pSΔ24-GFP (generated in **section 7.8.2**) via restriction enzyme digestion. The resulting vector was called pSΔ24-ΔE1B19K-GFP. Following **strategy 1**, pSΔ24-ΔE1B19K-GFP was recombined with pVK500 5/3 ΔE3 IL [81], resulting in pVK500 5/3 Δ24 ΔE1B19K ΔE3 Luc GFP. Subsequent PacI digestion resulted in the genome of Ad-Δ19K-Luc-GFP (**Figure 34**).

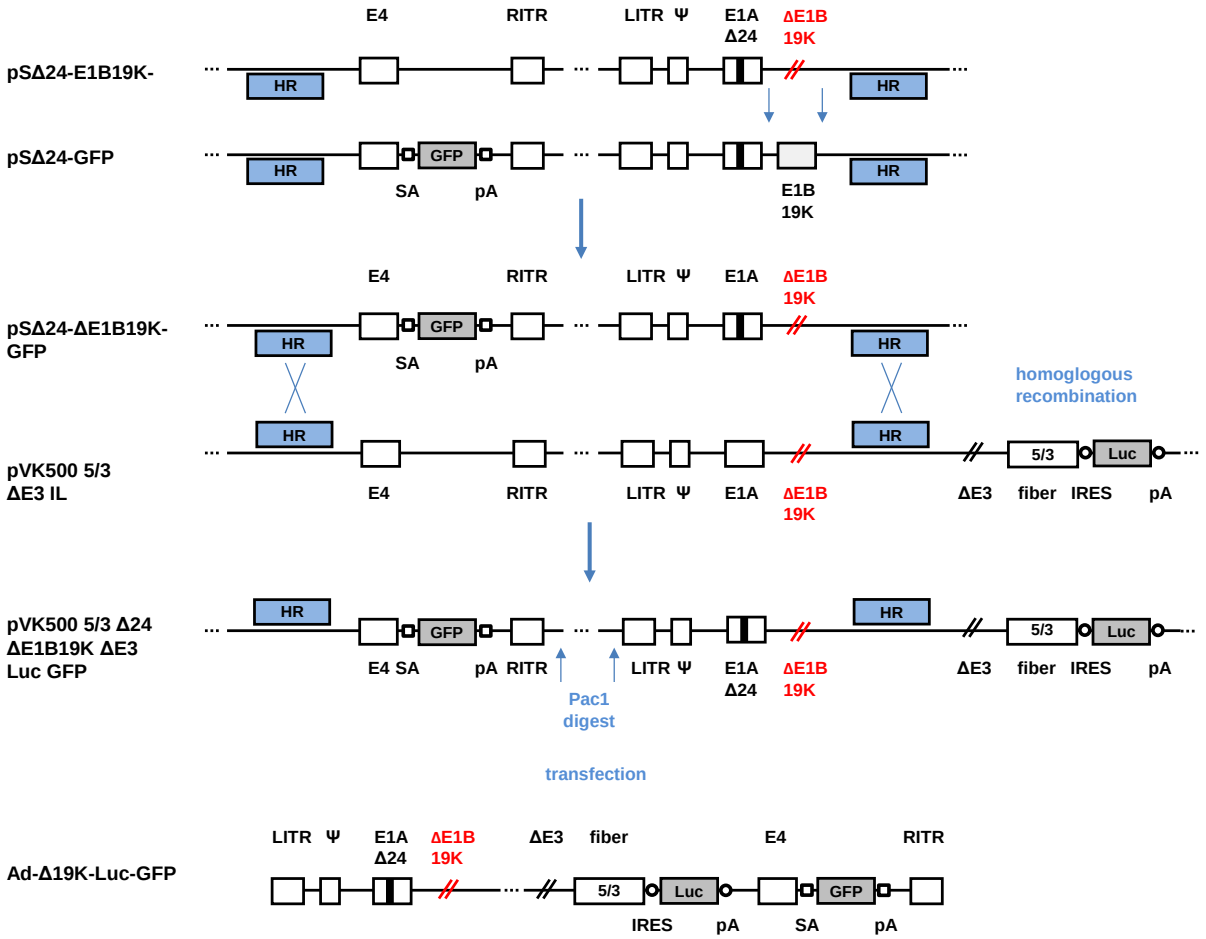


**Figure 34: Outlines of Cloning Intermediate Constructs for the Generation of Ad-Δ19K-Luc-GFP.** LITR/RITR: left/right inverted terminal repeat, Ψ: packaging signal, *E1A, E1B:* immediate early genes, *E1AΔ24*: deletion of pRb-binding region in E1A for cancer selective replication, Δ*E1B19K*: deletion of a 19 kDa protein coding region of *E1B*, *ΔE3:* deletion of *E3*, fiber 5/3: HAdV-5 shaft/HAdV-3 knob fiber chimera, IRES: internal ribosomal entry site, *Luc*: gene encoding firefly luciferase, *E4* gene, SA: splice acceptor site, *GFP*: gene encoding green fluorescent protein, pA: SV40polyA, HR: homologous region.

### 7.8.5. Cloning of Ad-TRAIL

pGL3-IRES-TRAIL was generated by replacing Luciferase of pGL3-IRES-Luc (described in [93]) with *TRAIL* (full-length *TRAIL* provided by AG Herr, University Heidelberg). The BPSA-TRAIL-SV40polyA cassette was then introduced into the shuttle plasmid pfiber5/3 ΔE3 IRES Luc (generated in the Nettelbeck lab). Following **strategy 2** (**Figure 31**), the generated pfiber5/3 ΔE3 IRES TRAIL was recombined with pVK500 Δ24 (generated in the Nettelbeck lab), resulting in pVK500 5/3 Δ24 ΔE3 TRAIL. Subsequent PacI digestion resulted in the genome of Ad-TRAIL (**Figure 35**).

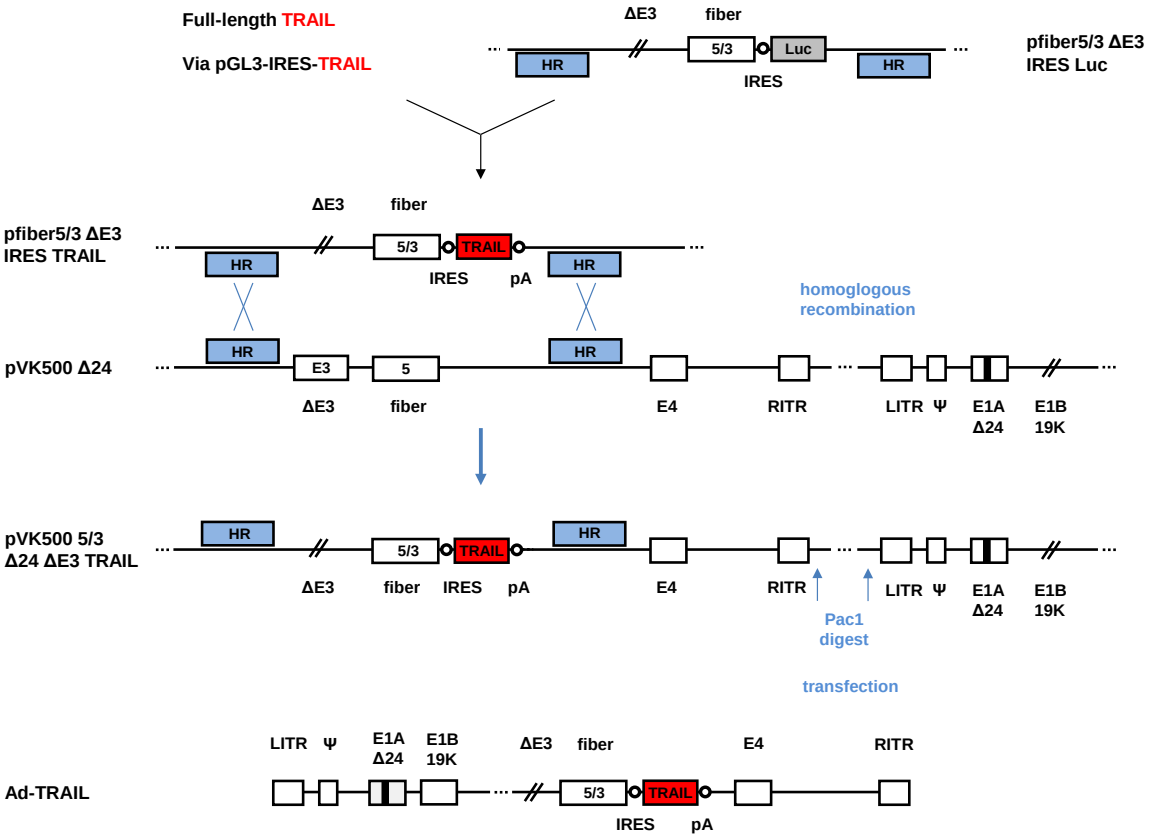


**Figure 35: Outlines of Cloning Intermediate Constructs for the Generation of Ad-TRAIL.** LITR/RITR: left/right inverted terminal repeat, Ψ: packaging signal, *E1AΔ24*: deletion of pRb-binding region in *E1A* for cancer selective replication, *E1B:* immediate early genes, *ΔE3:* deletion of *E3*, fiber5: HAdV-5 wild type fiber, fiber 5/3: HAdV-5 shaft/HAdV-3 knob fiber chimera, IRES: internal ribosomal entry site, *TRAIL*: gene encoding TNF-related apoptosis-inducing ligand, pA: SV40polyA, *E4* gene, HR: homologous region.

### 7.8.6. Cloning of Ad-TRAIL-GFP

Following s**trategy 1**, pSΔ24-GFP, generated in **section 7.8.2**, was recombined with pVK500 5/3 Δ24 ΔE3 IRES TRAIL (generated in **section 7.8.5**) resulting in pVK500 5/3 Δ24 ΔE3 TRAIL GFP. Subsequent PacI digestion resulted in the genome of Ad-TRAIL-GFP (**Figure 36**).

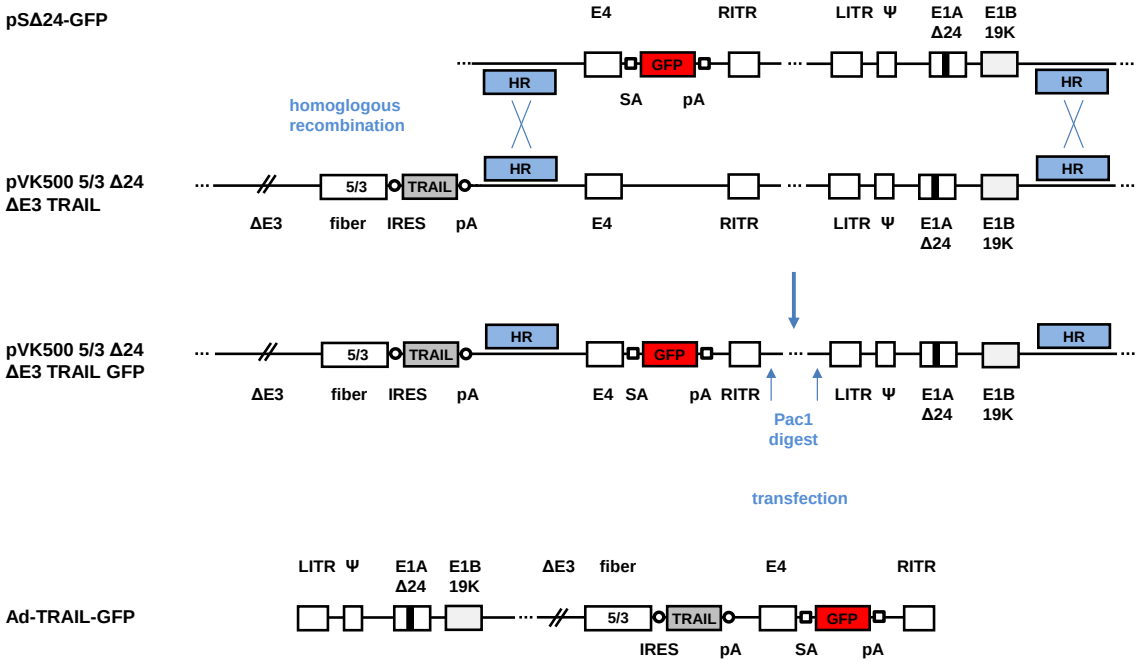


**Figure 36: Outlines of Cloning Intermediate Constructs for the Generation of Ad-TRAIL-GFP.** LITR/RITR: left/right inverted terminal repeat, Ψ: packaging signal, *E1AΔ24*: deletion of pRb-binding region in *E1A* for cancer selective replication, *E1B:* immediate early genes, *ΔE3:* deletion of *E3*, fiber 5/3: HAdV-5 shaft/HAdV-3 knob fiber chimera, IRES: internal ribosomal entry site, *TRAIL*: gene encoding TNF-related apoptosis-inducing ligand, *E4* gene, SA: splice acceptor site, *GFP*: gene encoding green fluorescent protein, pA: SV40polyA, HR: homologous region.

### 7.8.7. Cloning of Ad-FCU1-GFP

Following **strategy 1**, pSΔ24-GFP, generated in **section 7.8.2**, was recombined with pVK500 5/3 ΔE3 IRES FCU1 (generated in the Nettelbeck group), resulting in pVK500 5/3 Δ24 ΔE3 FCU1 GFP. Subsequent PacI digestion resulted in the genome of Ad-FCU1-GFP (**Figure 37**).

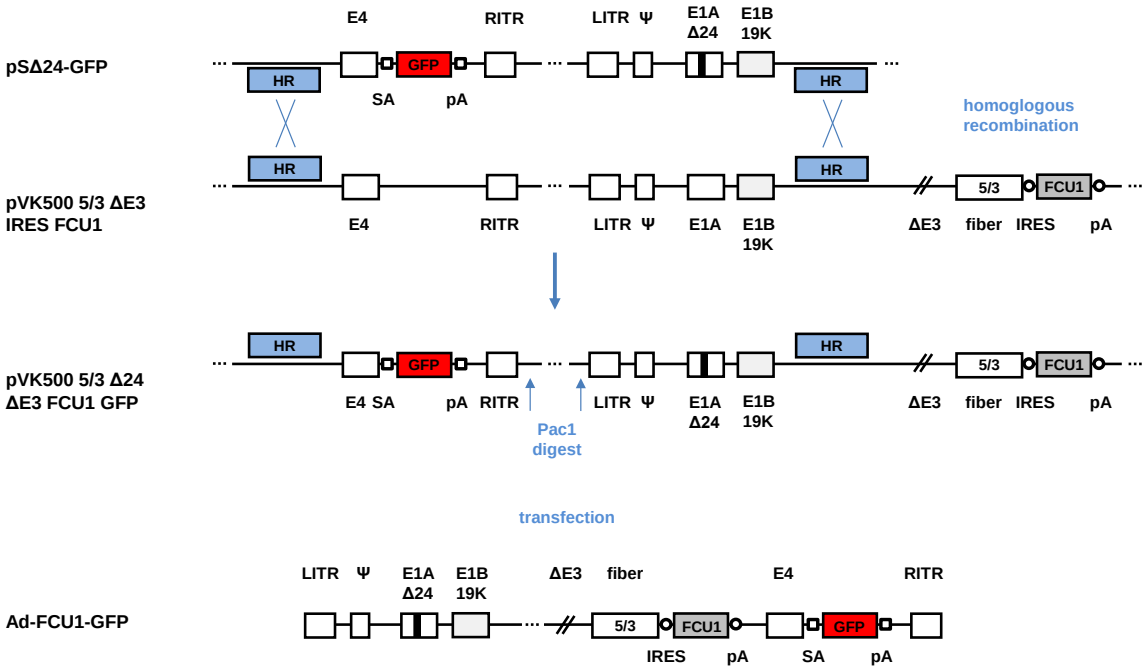


**Figure 37: Outlines of Cloning Intermediate Constructs for the Generation of Ad-FCU1-GFP.** LITR/RITR: left/right inverted terminal repeat, Ψ: packaging signal, *E1AΔ24*: deletion of pRb-binding region in *E1A* for cancer selective replication, *E1B:* immediate early genes, *ΔE3:* deletion of *E3*, fiber 5/3: HAdV-5 shaft/HAdV-3 knob fiber chimera, IRES: internal ribosomal entry site, *FCU1*: gene encoding prodrug converting enzyme with CD and UPRT activity, *E4* gene, SA: splice acceptor site, *GFP*: gene encoding green fluorescent protein, pA: SV40polyA, HR: homologous region.

# 8. Discussion

## 8.1. General Remarks

Several clinical trials have shown that oncolytic adenoviruses are very well suited for cancer therapy featuring great safety and only very little side effects. (reviewed in [117]). These trials further revealed that no dose limiting toxicity was observed [109, 111, 162], as predicted when these agents were first developed [163]. Instead, after intravenous virus application, the oncolytic adenovirus delivery to the tumor site was insufficient due to liver sequestration and neutralization [113, 164]. Further, Phase 1/2 studies, where the oncolytic adenoviruses were injected intra-tumorally, resulted in inefficient oncolysis [109, 110, 162, 165]. Therefore, strategies to improve adenovirus delivery and tumor cell killing have to be exploited.
Mesenchymal stem cells were exploited as carrier cells in this study, to deliver optimized oncolytic adenoviruses. Utilizing their shielding function and a natural tropism to tumors [128, 130] it was shown in previous studies that they are able to efficiently deliver oncolytic adenoviruses to tumors [125, 141, 166]. Furthermore it was shown that MSCs are productively infected by oncolytic adenoviruses and can serve as virus-propagating machinery while homing to the tumor [124, 167]. The system allows the circumvention of the named delivery problems, which however does not solve the need for improvement of the oncolytic efficiency. Enhancement of tumor cell killing can be achieved by modifications of the viral agents.
In this study, modified oncolytic adenoviruses were tested for improved delivery by MSCs to pancreatic adenocarcinoma. Modifications were identified which featured i) improved transduction as well as replication and release in MSCs, as well as ii) improved oncolytic properties for killing of human pancreatic adenocarcinoma cells. This was achieved by genetic modifications including capsid modification for optimizing transduction, modification of apoptosis-regulating viral genes for optimizing viral replication and release kinetics, and therapeutic transgene insertion for bystander killing. The latter two had not been tested in in the context of a adenovirus carrier system before. The modified viruses have the potential to improve MSC-mediated virotherapy for pancreatic cancer.

## 8.2. Transduction of MSCs and Tumor Cells With Capsid Variants

In order to improve transduction, replication-deficient vectors with capsid variants Ad5, Ad5/3, and Ad5RGD were tested on MSCs as well as established and low-passage pancreatic adenocarcinoma cells. All viruses carried a CMV-Luciferase cassette and transduction efficiency was determined by comparing luciferase activities.

In this study, transduction experiments in MSCs with Ad5 viral vectors showed comparably low transduction compared to Ad5/3 and Ad5RGD (**Figure 12**). This was in line with previous studies reporting that the primary receptor for HAdV-5, CAR, was poorly expressed on MSCs [140, 148, 151, 168]. Further, in three out of four MSCs isolated from different donors, Ad5/3 was superior to Ad5RGD. Only in one case (Donor 2), Ad5/3 and Ad5RGD had comparable transduction rates. Previous reports, which compared the transducibility of MSCs with the three capsid variants, did not result in consistent observations. Though all agreed that either Ad5/3 or Ad5RGD generally improved transduction, some found Ad5RGD [124, 149], and others Ad5/3 [125] superior. This variability has

been analyzed and was shown to be dependent on MSC donor [124] and the applied viral dose [136]. With that background, it was remarkable that the identification of Ad5/3 as the best transducing capsid variant was so congruent between all 4 analyzed MSC donors. Perhaps, factors as the culture conditions (e.g. culture medium) or donor selection (e.g. age of the donors) have also influence on transduction with different capsid variants [146, 169]. However, as MSC origin and handling was often not described in detail in the publications, it is not possible to draw conclusions about the impact of these parameters.

The number of transduced MSCs was visualized through infection with a fiber5/3, GFP-expressing oncolytic adenovirus and the observation of green-fluorescent cells 48 hours post-infection (**Figure 19**). MSCs from different donors showed a high variability in the viral dose necessary for complete transduction. For Donor 3 infection with 2,500 $TCID_{50}$/cell was sufficient (see Results **section 7.5**), while for Donor 2 infection with 10,000 $TCID_{50}$/cell was not enough to transduce all cells. However, complete transduction was aimed for to obtain maximum delivery rates. Therefore, in future experiments with untested MSCs, it remains necessary to pre-test the optimal transduction dose and perhaps pre-select for better transducible MSCs.

In order to reduce the amount of viral particles needed for complete transduction, Polybrene was tested as transduction helper (**Figure 19**). The positively charged Polybrene serves as bridge between the negatively charged cell surface and the adenovirus particle and therefore mediates improved transduction [170]. In pre-experiments, 8 µg/ml was identified as the optimal Polybrene concentration (from the range from 2 to 16 µg/ml Polybrene) for adenovirus transduction of the MSCs used in this study (data not shown). With 16 ng/ml Polybrene, no further improvement of transduction was observed compared to 8 ng/ml Polybrene. The use of Polybrene allowed to reduce the amount of viral particles about 10-fold to achieve similar transduction rates compared to transduction without Polybrene. The outcome was in line with previous studies, which reported a dose-dependent adenovirus transduction enhancement between 10- to 20-fold in different epithelial and endothelial established and primary cells [155, 170, 171] with the optimal dose between 4-8 µg/ml Polybrene [155, 156, 170, 171]. Similar results were also obtained in a recent study from Zhao et al. [156], which tested the use of Polybrene for the transfer of an adenovirus vector into mouse pro-osteoblastic progenitor cells. Here, they saw a 10-fold improved transduction with 4.0 µg/ml Polybrene. Further, it was reported that Polybrene at higher doses interfered with MSC proliferation [171, 172]. However, the question whether virus replication and release might be affected by the use of Polybrene had never been addressed before. During the current study, analysis of replication and release kinetics of the virus after transduction with Polybrene gave indications that this possibility can be ruled out (**Figure 20**) and Polybrene as a feasible transduction helper was validated.

Clinical or *in vivo* studies with Polybrene as transduction helper for delivery of oncolytic adenovirus by MSCs have not been performed so far. However, the feature of Polybrene, to significantly reduce the amount of virus particles needed for transduction, implies great potential for clinical applications. This can be illustrated by analyzing the set-up of a performed clinical delivery study. Garcia-Castro et al. [147] reports about an exploratory trial testing adenovirus delivery by MSCs. The number of MSCs used in this study was in line with those used for clinical trials of tissue repair [173-175] and were between $10^8$ and $10^9$ MSCs per patient and injection. The study used for infection 2,000 pfu/MSCs, which is also in line with the observations in the MSCs in **Figure 19** in order to reach sufficient transduction. Assuming that Polybrene can reduce the amount of needed virus by about 10-fold, the amount could be reduced from about $1x10^{12}$ to about $1x10^{11}$ for a single injection. This number is in contrast to up to $10^{13}$ viral particles which were used during dose escalation of i.v. administered

adenovirus [111]. Therefore, by using Polybrene the amount of viral particles is highly feasible and handling becomes more convenient.

Transduction experiments in established pancreatic adenocarcinoma cell lines and low-passage pancreatic adenocarcinoma cultures resulted in best transduction with the Ad5/3 adenoviral vector compared to Ad5 and Ad5RGD (**Figure 13**). This is in accordance to previous reports that adenoviral vectors with modified fiber5/3 [66] and fiber5RGD [67] improved transduction of various cancer cell lines [66, 68-70]. The primary receptor for Ad5, CAR, is weakly expressed in established pancreatic adenocarcinoma cell lines [64, 65]. Clinical trials using oncolytic viruses with HAdV-5 capsid showed the need for improvement of the viral vector [111], therefore, alternative capsid variants for improved infection present one option for improvement of the viral agent. Oncolytic viruses with fiber5/3 capsid modifications were tested in in clinical studies for i.t. and i.p. injections [165, 176, 177]. In these trials, no severe side effects were observed and the virus was well tolerated.
To visualize infection efficiency of low-passage pancreatic tumor cultures, the cells were infected with the fiber5/3 and GFP-expressing oncolytic virus Ad-GFP (**Figure 29**). The fluorescent pictures showed that the population was not completely infectable with as much as 1,000 $TCID_{50}$/cell. In contrast, 10 $TCID_{50}$/cell were sufficient to achieve full transduction of established pancreatic cancer cell lines (data not shown). This difference in infectibility of established and low-passage cells had been shown for Ad5 [150] and Ad5/3 [178] capsid variants before for malignant glioma.
Furthermore, as already described in Results **section 7.7**, the investigated low-passage pancreatic cancer cultures JoPaca-1 and PacaDD-159 did not contain one homogenous population of cells. Images in **Figure 29** also suggest that the different cell populations were not equally well infectable. The observed infection in a patch-like pattern seen may indicate that only one subpopulation of cells, which had grown as a colony on the plate, was infected. Assuming that this hypothesis is valid, it is likely that a subset of cells would remain non-infected in an *in vivo* setting and complete tumor targeting would not have been achieved. The 5/3 capsid variant was the most efficient of the tested capsid variants; however, in order to guarantee complete tumor eradication further strategies which perform bystander killing have to be exploited to target the non-infectable tumor cells.
Based on the outcome of the transduction experiments in MSCs and pancreatic cancer cell cultures and the previous reports in the literature, the fiber5/3 background was chosen as modification for improved MSCs carrier cell-mediated delivery as well as improved subsequent oncolysis.

## 8.3. Modification of the Viral Genome – Δ*E1B19K*

As explained above, oncolytic adenoviruses need to be improved in order to achieve efficient tumor cell killing. Beside capsid modifications for improved transduction, adenoviral genes can be modified to obtain improved viral replication and release behavior. Known modifications that improve viral life cycle kinetics in tumor cells are the deletion of the early gene *E1B19K* [76-78, 81], the truncation of the i-leader [179], the truncation of the *E3B* [180], and overexpression of the ADP protein [59]. The mechanisms of interference are different and range from interference with apoptosis pathways (E1B19K, E3B), to earlier release (i-leader, [181]), and increased efficiency of host cell lysis (ADP). The *E1B19K* deletion was chosen as modification for this project. In contrast to the other listed modifications, which just alter viral life cycle kinetics, previous studies with *E1B19K*-deleted adenoviruses in tumor cells have shown that the amount of total produced viral progeny particle [79] as well as the amount of viral particles released from the host cell was significantly increased [79,

81]. The anti-apoptotic activity of the E1B19K protein and the pro-apoptotic activity of E1A [57, 58], are main mediators to balance host cell maintenance. This balance between pro- and anti-apoptotic factors is critical. On the one hand the virus needs to spread efficiently while on the other hand completion of the virus life cycle and therefore viable virus progeny production needs to be ensured. Other virus species have evolved analogous mechanisms to control their virus life cycles, as Epstein Barr virus or African swine fever virus [182, 183]. The deletion of *E1B19K* and therefore its anti-apoptotic function leads to a more pro-apoptotic phenotype of the virus [77, 78]. This shows in improved viral life cycle kinetics in tumor cells as described above. In terms of more efficient delivery of modified oncolytic viruses by MSCs, this modification was the most promising strategy. However, there was no pre-existing data about replication and release behavior of an *E1B19K*-deleted adenovirus in MSCs.

Experiments in MSCs from three different donors revealed that replication and release was significantly increased (**Figure 15**). At day 8 post-infection, Ad-Δ19K-Luc showed a 4 to 17-fold increase in total virus particle production (virus in cells and supernatant) and a 14 to 72-fold increase in released viral particles (virus in supernatant) compared to the control virus Ad-Luc. Further, the increase in release (up to 72-fold) exceeded the increase in total virus particle production (up to 17-fold) by far, which indicates that enhancement of virus replication and release were two complementing mechanisms.

The virus Ad-Δ19K-Luc was analyzed before in a study presented by Rohmer et al. [81]. There, improved viral kinetics were shown in the lung carcinoma cell line A549. Infection with Ad-Δ19K-Luc resulted in an increased viral release of 14.2-fold after 2 days and 243.6-fold after 4 days compared to Ad-Luc. However, the produced amount of total infectious viral particle was not altered compared to Ad-Luc. Increased induction of apoptosis was shown responsible for enhanced virus release. In other studies using a different virus, the viral burst of an *E1B19K*-deleted Ad5 in pancreas and prostate cancer cell lines was investigated. Here again, no difference in viral particle production was observed compared to an Ad5 wild type virus 3 days post-infection, although cancer cell killing was improved [76, 80]. Summarizing the results of the described studies, the *E1B19K*-deleted viruses resulted in increased cell killing without altering the amount of total virus particle in cancer cells between day 2 to 4 post-infection. This is in contrast to the burst assay in MSCs shown in **Figure 15**. Here, an increase in total virus infectious particle production compared to Ad-Luc was observed. In comparable time spans (2-4 days), MSCs infected with Ad-Δ19K-Luc resulted in an increase of infectious viral particles of 2-fold at day 2 post-infection and 5-fold at day 4 post-infection (numbers are averages of experiments in the three MSC donors). The mechanism by which the viruses were mediating increased replication and release in MSCs, e.g. increased induction of apoptosis as described in Rohmer et al. [81], remained to be elucidated.

The improved replication and release kinetics in MSCs were further remarkable, as it was reported that untransformed somatic cells did not show increased sensitivity to *E1B19K*-deleted viruses [76, 78, 80, 148]. On the contrary, the studies even suggested that *E1B19K*-deleted adenoviruses showed an impaired phenotype and therefore could contribute to tumor-specificity of virus replication in untransformed cells [76, 78, 80]. Therefore, the mechanism by which *E1B19K*-deleted adenovirus led to improved viral kinetics in MSCs must be one that is differently regulated in untransfomed somatic cells and MSCs, but remains to be elucidated.

The time point, where most viruses had been released into the supernatant, varied between day 3 to 4, depending on the donor. This time presents a key information for the system, as this needs to correlate with the homing time of MSCs to reach the tumor. The maintenance of migration ability of virus-infected MSCs was later tested in a migration experiment. However, the observations suggest

that the Δ*E1B19K* modification is very efficiently improving viral replication and release in MSCs and is therefore benefitting the aim to optimize MSC-mediated oncolytic adenovirus delivery.

Ad-Δ19K-Luc-GFP was tested for improved oncolytic behavior compared to Ad-Luc-GFP in established and low-passage pancreatic adenocarcinoma cell lines and cultures. From the 4 tested established pancreatic cell lines, in three no oncolytic benefit was seen during infection with Ad-Δ19K-Luc-GFP compared to Ad-Luc-GFP. On the contrary, the oncolytic potential was even decreased (**Figure 25**). Only in Panc-1, the Δ*E1B19K* virus caused an approximately 10-fold increase in killing. Following infection of the low-passage pancreatic cancer cell culture JoPaca-1, Ad-Δ19K-Luc-GFP and Ad-Luc-GFP showed similar oncolytic behavior, whereas for PacaDD-159 killing was about 10-fold improved with Ad-Δ19K-Luc-GFP (**Figure 30**).

Therefore, it had to be concluded that there was a marked cell line variability for oncolytic improvement by Ad-Δ19K-Luc-GFP. Similar observations were already reported before, e.g. in Öberg et al [80], where the cell killing efficiency of an *E1B19K*-deleted HAdV-5 in 7 pancreatic and prostate cancer cell lines was determined by $EC_{50}$ assay. Three of the cell lines showed worse, four improved, and one unaltered oncolytic behavior compared to the control virus. The authors proposed that this cell line dependency was connected to intact p53 or pRb pathways. If these were intact, the deletion of an anti-apoptotic gene and enhancement of the action of E1A [76] could alter the virus life cycle in an adverse way and cause reduced production of viral particles. This is identical to the earlier explained possible mechanism, how the Δ*E1B19K* deletion led to attenuation of the virus in untransformed cells (also see Introduction **section 5.5.3**). However, this explanation was not applicable for the observations in this study. Enhanced replication and release was observed in MSCs, which are untransformed cells with intact p53 and pRb pathways. Furthermore, for the analyzed established pancreatic cell lines it is known that they all have different mutations in p53 [184], while all were reported to have wild type pRb protein [184, 185]. However, whether other proteins in the pRb pathways were mutated and thus pRb signaling was inactivated, remains unknown. Other studies reported the activation of apoptosis pathways by caspase-3 activation analysis and Annexin-V staining in infected cells, which were sensitive to Δ*E1B19K*-mediated improved oncolysis [76, 79, 81]. Therefore, it seems that the complex alterations of apoptosis pathways in cancer cells influence the sensitivity to the Δ*E1B19K* mutant oncolytic adenovirus.

While infection of MiaPaCa-2 monolayers with Ad-Δ19K-Luc-GFP did not result in improved killing, infection of MiaPaCa-2 spheroids resulted in increased LDH release, which indicates increased cell death (**Figure 28**). This suggests that physiological relevant results about the benefit of the virus for cancer cell killing can only be obtained if models are exploited which resemble the 3D-tumor structure and that monolayer models might be insufficient (further explained in **section 8.6**).

Being aware of the cell line-dependent sensitivity to Ad-Δ19K-Luc-GFP it might be worth thinking about a pre-screening system for tumor cells to define the susceptibility to this virus modification prior to treatment, e.g. in test infections of biopsies. Further, the delivery system aims for a combination of optimized viral delivery by MSCs and optimized oncolysis. As this virus showed more efficient replication and release kinetics in MSCs compared to the other viruses, the increased amount of delivered viral particles could result in an overall superiority, even if tumor cell lysis is not improved. Further experiments, especially in animal models, are necessary to evaluate the overall benefit and if the cell line dependent susceptibility proves to be relevant *in vivo*.

In order to further improve tumor treatment, some studies investigated if the combination of Δ*E1B19K* adenoviruses with chemotherapeutics. Leitner et al. [76] showed that a Δ*E1B19K* adenovirus in combination with gemcitabine could further potentiate tumor cell killing. Further, Cherubini et al [82] reported that the combination of an *E1B19K* deleted adenovirus with a

chemotherapeutic agent could sensitize previously chemotherapy-resistant cancer cell lines to treatment.

## 8.4. Modifications Through Transgene Insertions

An alternative strategy to improve tumor cell killing, besides the modification of viral genes, is the insertion of transgenes into the viral genome. Arming strategies have been summarized in several reviews [87, 99]. In this project, the TRAIL protein was investigated. Expression of TRAIL enhanced tumor cell killing and delivery in TRAIL-sensitive cancer cells and MSCs, respectively.
Further, by utilizing a sheddable, diffusable TRAIL bystander killing was achieved, which mediated killing of non-infected tumor cells. Another strategy of bystander killing was exploited by the generation of a virus that expressed the prodrug-converting enzyme FCU1, for 5-FC to 5-FU conversion.

### 8.4.1. The Modified TRAIL-Expressing Oncolytic Adenoviruses

The strong stromal reaction, which is present in pancreatic tumors [84], is a diffusion barrier for the oncolytic adenoviruses [86, 186]. To overcome this barrier, the gene for the secretable, diffusible TRAIL ligand was inserted into the late viral unit. After shedding, this TRAIL protein would be able to diffuse and reach parts of the tumor, which are not accessible for the virus, inducing bystander killing [187]. TRAIL is a broadly used biotherapeutic, which was shown to kill a wide range of cancer cells without affecting normal cells [188]. However, the half life of a homotrimeric, soluble TRAIL in the serum of non-human primates was determined to be 30 minutes and therefore very short [189]. In order to decelerate degradation kinetics, TRAIL was modified, e.g. by oligomerization for size increase, which resulted in a prolonged half life [188]. In this study, the gene encoding a full-length, homotrimeric, sheddable TRAIL was used. The combination of an optimized TRAIL variant and the expression of TRAIL by an oncolytic adenovirus directly at the tumor site, aimed for an optimized TRAIL effect.

The acquired data shows that MSCs of different donors infected with TRAIL-expressing Adenovirus, Ad-TRAIL, showed up to a 5-fold increase in infectious virus particle production compared to the control virus Ad-Luc at day 8 post-infection (**Figure 15**). Further, the amount of released virus was much enhanced and up to 17-fold increased compared to the control virus. For Ad-TRAIL infected cells the amount of released infectious viral particle started to be greater than the amount of cell-bound viral particles between day 5 to 8, while for the Ad-Δ19K-Luc this was between day 3 to 4. The difference could be explained with the fact that Δ*E1B19K* is a deletion in an immediate early protein, which causes enhanced viral replication from the start, whereas TRAIL is expressed late, and therefore a TRAIL-induced effect can only emerge towards the end of the virus life cycle. The observed enhanced kinetics compared to Ad-Luc were not as pronounced as the effect seen with Ad-Δ19K-Luc. Ad-Δ19K-Luc resulted in 2- to 4-fold (depending on the donor) higher infectious produced viral particle titers than Ad-TRAIL at day 8 post-infection.
The observed enhancement of replication and release kinetics with Ad-TRAIL compared to Ad-Luc were especially remarkable, as MSCs have been reported to be TRAIL-resistant [190, 191] like other untransformed cells [192]. Studies showed that in normal, untransformed cells the induction of only the extrinsic apoptosis pathway by TRAIL is often not sufficient to induce apoptosis [89]. Even though it was reported that the TRAIL receptor TRAIL-R2 as well as the decoy receptor TRAIL-R4 are

expressed on MSCs (some donor dependencies observed), neither recombinant nor adenoviral expressed TRAIL could induce cytotoxicity in these studies [191]. However, the results of the burst assay (**Figure 15**) suggest that MSCs from all three donors showed TRAIL-sensitivity resulting in enhanced Ad-TRAIL replication and release. The enhancement mechanism of Ad-TRAIL kinetics in MSCs remains to be elucidated. Preliminary experiments (data not shown) suggested increased PARP cleavage following infection with Ad-TRAIL-GFP compared to Ad-Luc-GFP. This could indicate increased induction of apoptosis by TRAIL and would contradict the previous reports about TRAIL-insensitive MSCs. However, none of the described previous studies used a TRAIL-expressing oncolytic adenovirus, but TRAIL protein [190] or replication-deficient, TRAIL-expressing adenoviral vectors [191]. Therefore, the observed difference could be due to the different set-ups. The effect of TRAIL-mediated increase in production of infectious viral particles was shown before in cancer cell lines [193-196]. These studies further showed by propidium iodide staining or Caspase-3/8 cleavage assays that the effect was mediated through increased induction of apoptosis. Further, Dong et al. [193] suggested that the increase of viral progeny production could be explained with the induction of alternative signaling pathways like Akt, NFκB, or JNK which are connected to pro-proliferative activity. Further studies need to clarify whether one of these mechanisms provides the explanation for the TRAIL-sensitivity of MSCs used in this study.

Of the analyzed four established and two low-passage pancreatic cancer cell lines, three established and one low-passage cell line showed increased sensitivity to Ad-TRAIL-GFP compared to the control virus Ad-Luc-GFP. The non-TRAIL-sensitive cell lines showed a comparable oncolytic behavior than the control virus and no reduced cytotoxicity as described for Ad-Δ19K-Luc-GFP was observed (**Figure 25**).

Many publications described that established pancreatic cell lines showed different sensitivities to TRAIL [197, 198]. Even when comparing different publications using the same cell line, the outcome about the TRAIL sensitivity of this cell line varied greatly [197-199]. This indicates that changes in TRAIL sensitivity occur in long-term cell culture as well. Differences in TRAIL sensitivity have also been shown in patient tumors (reviewed in [89]). However, it has to be noticed that TRAIL resistance is often acquired during cancer development or treatment [200]. The mechanisms by which TRAIL induces apoptosis are very complex. It has been reported that there are p53-dependent and -independent mechanisms [89]. Neither the genetic status of p53 nor the expression of the death receptors TRAIL-R1 and TRAIL-R2 led to reliable predictions about TRAIL sensitivity [89]. It has been reported for primary pancreatic adenocarcinoma tissue that TRAIL sensitivity is connected to upregulated NFκB signaling levels (Khanbolooki, Nawrocki et al. 2006) and about 70% of pancreatic tumors show upregulated levels of NFκB signaling [201]. Therefore, a range in TRAIL sensitivity in the experiments was expected. However, the results of this study gave strong indications that the TRAIL delivery in therapeutic relevant concentrations by an oncolytic adenovirus is feasible and can improve lysis of TRAIL-sensitive cancer cell lines. In MiaPaCa-2 spheroids the LDH release was significantly increased compared to Ad-Luc infected spheroids (**Figure 28**). This indicated that the killing effect of TRAIL did lead to improved bystander tumor cell killing. *In vivo* experiments with the TRAIL-expressing oncolytic adenovirus have to be performed in order to analyze tumor killing in a physiological environment. Further, *in vivo* experiments need to be performed to analyze the features of TRAIL to overcome the tumor stroma as diffusion barrier for the virus, which was not analyzed in the course of this study.

Considering that some tumors will be resistant to TRAIL, it was shown that therapeutic efficiency by TRAIL can still be achieved in some cases by the addition of sensitizers, which can reverse resistance.

Numerous substances have been tested, such as the NFκB-inhibitor sulforaphane [202], the proteasome-inhibitor bortezomib [203], the Akt-inhibitor Triciribine [204], or the quercetin derivative LY303511 [205], just to name a few.

### 8.4.2. The Modified FCU1-Expressing Oncolytic Adenovirus

Treatment with 5-FU is one of the standard chemotherapy agents used for treating pancreatic ductal adenocarcinoma [14]. However, the treatment often does not achieve a sufficient therapeutic effect [106], because of resistance to 5-FU [206, 207]. The resistance can be due to the lack of salvage enzymes for 5-FU, which needs to be further metabolized to its active derivatives 5-dFMP and 5-dFUMP [103]. Further, therapeutic active concentrations of 5-FU are often not reached using systemic application routes. Following continuous i.v. infusion of 5-FU, the plasma levels are around 0.5 to 0.3 µM as reported in Shi et al. [207] and references therein. This concentration is lower than the $EC_{50}$ values for most pancreatic cancer cells [105, 207, 208] and therefore leads to an intrinsic resistance against 5-FU in *in vivo* settings. The main issue here is the short half life of 5-FU in the blood of only about 10 minutes [209, 210]. Further, high doses of bolus or continuous i.v. injected 5-FU led to dose-limiting toxicity, e.g. stomatitis, ataxia, and cardiac toxicity [211].
These *in vivo* limitations have to be considered when analyzing 5-FU sensitivity in cell culture. For established pancreatic tumor cell lines, the $EC_{50}$ values in the literature vary greatly comparing different publications. For example, in case of MiaPaCa-2, they reach from 15.38 µM [105] to 4.63 µM [207] in analogous experiments measuring $TCID_{50}$ 3 days after 5-FU application. For the MiaPaCa-2 cell line used in this study an $EC_{50}$ of about 0.05 µM was determined after 5 days incubation (**Figure 25**, 7th lane). Here, the comparably high 5-FU sensitivity is due to the longer incubation time and was therefore not comparable to the mentioned values from the literature. Compared to the $EC_{50}$ values in established pancreatic cancer cell lines, the values of low-passage pancreatic adenocarcinoma cultures were about 10-fold higher (**Figure 30**, 7th lane). The values were estimated with 1 and 0.5 µM for JoPaca-1 and PacaDD-159, respectively. Therefore, the low-passage pancreatic cell lines from this study would already be intrinsically resistant to 5-FU in an *in vivo* setting when applying 5-FU systemically.

Resistance to 5-FU can be overcome with two strategies: i. expression of a salvage enzyme to potentiate the effect of 5-FU and ii. the delivery of 5-FU to the tumor site avoiding lengthy system circulations of 5-FU. Further, toxic side effects caused by high concentrations of systemically applied 5-FU need to be avoided [211]. These points were approached by the development of the FCU1/5-FC prodrug activation system [106]. FCU1, a combination enzyme of CD (catalyzes conversion of 5-FC to 5-FU) and the 5-FU salvage enzyme UPRT, was first developed as a transgene for adenoviral vectors [106]. The idea was that an FCU1-encoding virus is injected intra-tumorally or targeted to the tumor site after systemic injection, transduces the tumor cells and locally expresses FCU1. The prodrug 5-FC is then applied systemically and becomes at the tumor site, where FCU1 is expressed, converted into 5-FU and further to its active metabolites. 5-FC has compared to 5-FU a prolonged half life of 3-4 hours [212]. 5-FC was reported to have relatively minor side effects, however, hepatotoxicity can occur through an unknown mechanism for concentrations >100 mg/l [212]. Through this strategy, higher concentrations of 5-FU can be reached at the tumor site compared to systemic 5-FU administration and therefore the therapeutic efficiency is increased. Compared to other prodrug systems as HSV-TK/Ganciclovir [213, 214], where direct cell-cell-contacts are necessary to mediate bystander killing, the membrane-diffusible 5-FU is better suited for tumors with strong stromal

reaction, where tumor parts might be separated by wide stretches of connective tissue, as it is the case in pancreatic tumors [100, 106].
In the delivery system in this project, the specific transfer of oncolytic adenoviruses by MSCs to the tumor site ensures the expression of FCU1 in proximity of the tumor. The systemic application of the prodrug 5-FC can then be timed in a way, that the conversion is initiated after the virus has been delivered to the tumor site. In this way, the toxic compound 5-FU is not present in the system during MSC infection and homing. Consequently, there is also no interference of 5-FU with virus replications and release in MSCs. Therefore, analysis of replication and release of Ad-FCU1-GFP in MSCs was not included in the studies, as it is expected to behave like the control virus Ad-Luc-GFP.
In *in vitro* cytotoxicity experiments in established (**Figure 25**) and low-passage (**Figure 30**) pancreatic cancer cells, the conversion of 5-FC by the FCU1 expressing virus Ad-FCU1-GFP led to improved lysis in three out of the four investigated established cell lines. In case of the low-passage PacaDD-159 culture, an improved killing was seen, in JoPaca-1 not. This indicates that the conversion of 5-FC by FCU1 was feasible in therapeutically relevant amounts and led to improved tumor cell killing in a subset of the tested cell lines and cultures. In case of BxPc-3 and AsPc-1, infection with as little as 0.1 $TCID_{50}$/cell was sufficient to express FCU1 in relevant amounts to convert 5-FC into 5-FU and cause a bystander killing effect.
Similar observations have been previously described in experiments with the first adenovirus expressing FCU1 (replication-deficient, described in Erbs et al. [106]). The authors showed that a relative small amount of initially infected cells (10-20%) are sufficient to eventually observe cytotoxicity in the entire tumor cell population. Dias et al. [107] was the first study, which used an oncolytic FCU1-expressing adenovirus. Here, the amount of FCU1 was greatly increased compared to FCU1-expression by a replication-deficient adenoviral vector. However, it was noticed that high levels of 5-FU and its toxic products inhibited virus replication. Experiments analyzing inhibition of viral replication by 5-FU have not been performed in the course of the present study, but have to be kept in mind in order to assure efficient virus replication and oncolysis of the tumor cells.
As already mentioned, the enzyme FCU1 does not only have CD activity to convert 5-FC into 5-FU, but also UPRT activity to convert 5-FU into its active metabolites. One study revealed that the sensitivity of pancreatic cancer cell lines to 5-FU can be greatly increased by co-treatment with a replication-deficient, UPRT-expressing adenovirus [105]. The increase in 5-FU sensitivity was 7.1-fold in MiaPaCa-2, and 20-fold in BxPc-3, proving the suitability of this salvage enzyme. Further, they showed significantly reduced tumor growth of pancreatic tumors in mice after treatment with the UPRT-expressing adenovirus and 5-FU compared to 5-FU alone. In the experiments during this thesis, the effects of the CD and UPRT activity were not distinguished from each other; however, both enzyme activities can be expected to have contributed to the improved killing by bystander effects.
No FCU1-expressing adenovirus has entered a clinical trial yet. However, in one clinical trial the effect of the *E1B55K*-deleted oncolytic virus ONYX-015 alone or in combination with gemcitabine or 5-FU was tested in SCHNC (squamous cell head and neck cancer) [110]. The combination treatment resulted in superior outcome compared to chemotherapy treatment alone, which proved the potential of this combination.

Overall, experiments with the modified viruses gave indications of improved killing of a subgroup of pancreatic cancer cells. It would be helpful to established pre-treatment personal screenings to analyze resistance and susceptibility prior to treatment start [215, 216]. This could be possible through test-treatment of tumor biopsies *ex vivo* prior to treatment [215] or the identifications of

markers, e.g. of 5-FU metabolizing enzymes in tumor biopsies for the prediction of chemosensitivity [216].
In order to further improve the viral agent, it could also be feasible to combine the analyzed modifications, namely to combine the *E1B19K* deletion, TRAIL insertion, or the expression of FCU1. Replication and release experiments in MSCs, homing, and cytotoxicity experiments would clarify, if an additional therapeutic effect could be achieved.

## 8.5. Migration of Virus-Infected MSCs

In order to verify delivery feasibility, it was important to show that infection of MSCs with the control virus or one of the modified viruses did not interfere with migration behavior of MSCs. Especially the observed improved release kinetics of Ad-Δ19K-Luc and Ad-TRAIL from MSCs needed to be compatible with the time the MSCs needed to reach the tumor site. Premature virus release, before the MSCs have reached the tumor, as well as inhibition of the migratory abilities of MSCs would make the delivery system useless.
The maintenance of migration capacity of MSCs was shown *in vitro* in a transwell migration assay (**Figure 24**). The number of migrated cells of infected MSCs was compared to the number of cells of non-infected MSCs and showed the retaining of migration behavior for all virus variants. The chosen migration time of 40 hours corresponded to the time reported in the literature, for MSCs to home to tumors in an *in vivo* setting [142-144]. These studies tested the delivery of oncolytic adenovirus-infected MSCs to different tumors and via different application routes in mice. Yong et al. [144] described the delivery of the virus (*E1AΔ24*, fiber5RGD) to intracranial glioma following carotid artery injection. Within one hour, the GFP-expressing virus-loaded MSCs were located to the tumor vessels, until day 2 they found GFP clusters in the tumor, and dispersion of the GFP signal was seen at day 3. In Xia et al. [143] following i.v. injection of virus-loaded MSCs, the MSCs were localized at the tumor periphery (breast cancer tumors in the mammary fat pad) 24 hours post-injection, and in the tumor parenchyma 72 hours post-injection. Komarova et al. [142] described the delivery of an adenoviral vector, which expressed luciferase as well as a tumor-targeting receptor. Homing was monitored following i.p. injection of transduced MSCs into mice with i.p. ovarian cancer xenografts. Here, the tumors were the major target and luciferase intensity had its maximum after 24 hours post-infection, allowing the conclusion that the virus-loaded MSCs had reached the tumor site after this time. From these studies can be concluded that the virus reached the tumor most likely within 2 days. Therefore, the virus release kinetic from MSCs (**Figure 15**), which revealed that the majority of viral particles were found in the supernatant 3-4 and 4- 8 days post-infection for Ad-Δ19K-Luc and Ad-TRAIL, respectively, are in accordance with the time MSCs need to migrate to the tumor site.
Furthermore, the performed migration assay showed that migration behavior was not altered by the virus genome modifications. Other studies have investigated MSCs as delivery cells for adenoviruses and have performed similar experiments. Sonabend et al. [125] reported that MSCs infected with a replication competent oncolytic adenoviruses (tissue-specific CXCR4-promoter driven *E1A*) showed unaltered migration for 19 hours towards 10% FBS. Further, Treacy et al. [145] mentioned that the migration is not altered when MSCs are infected with a replication-deficient adenovirus expressing GFP. Oncolytic adenoviruses with modifications that enhance the viral replications and release kinetics have not been tested in terms of delivery by MSCs before.
Worth mentioning is a study performed by Secchiero et al. [191], which analyzed migration of MSCs towards different stimuli. They found that migration of MSCs can be promoted by TRAIL-containing

medium in a transwell assay. They determined 100 pg/ml as the optimal TRAIL concentration. No improved migration with the Ad-TRAIL-GFP virus in the performed transwell migration assay was observed in **Figure 24**. This could be due to the difference of a steady medium gradient versus intrinsic TRAIL expression late in the viral life cycle, whose onset is not early enough to affect migration. However, it might be interesting to see in an *in vivo* setting if differences can be observed in terms of homing of Ad-TRAIL-GFP-infected MSCs or in tumor engraftment efficiency.
From the obtained data it can be concluded that virus-infected MSCs maintained their migration independent from the genetic alterations they were carrying. It now remains to be elucidated if the tumor homing capacity can also be preserved in an *in vivo* situation, which has not been done in the course of this study. All of the viruses carry GFP, which intended to simplify monitoring and to allow the identification of virus-infected cells within tissues in further studies.
For *in vivo* delivery studies, considerations have to be taken in terms of the application route. All the examples given above avoid systemic application that involves the pulmonary circulation. As MSCs are very big cells with a diameter of about 20 µm, it has been reported that they are prone to be trapped in capillary systems, which have a smaller diameter [217-219]. Therefore, the most reasonable and shortest application route should be chosen in order to avoid unspecific loss of MSCs. In terms of treatment of pancreatic cancer, this route could be i.p. or into suitable blood vessels in proximity to the tumor site.

## 8.6. Modified Virus Infection of Spheroids

The infection of MiaPaCa-2 spheroids with the modified oncolytic viruses resulted in altered spheroid shape and size and higher LDH release in case of the Ad-Δ19K-Luc-GFP and Ad-TRAIL-GFP-infected spheroids compared to Ad-Luc-GFP-infected spheroid controls.
For the spheroid experiments, 5,000 MiaPaCa-2 cells were seeded, which formed spheroids with a diameter of about 1.5 mm. In case of the uninfected spheroids, the size increased to a diameter of about 2.4 mm within 8 days, indicating that cell proliferation was continuing during the time the spheroids were monitored. Spheroid model studies reported that spheroids of that size have a layered structure, composed of a necrotic core, a middle layer of quiescent cells, and a proliferating outside layer [158]. In diffusion studies it was shown that the limit of molecules (especially oxygen) is about 150-200 µm [220], which leads to nutrients depletion as well as accumulation of toxic residues in the core of the spheroid [221]. This situation closely resembles the avascular stages of early tumors [222]. Beside the tumor-mimicking 3D architecture they were also shown to have more physiological cell-cell-contacts than monolayer cultures as well as altered intercellular signaling, which were both shown to influence responses to drugs (reviewed in [158]). Further, several primary tumor cells cultured as spheroids showed increased chemotherapeutic resistance, invasiveness, and migration potential, indicating an enrichment in cancer stem cells [157, 223]. The same was observed in pancreatic tumor cell line spheroids [157]. Therefore, this model was very well suited to mimic viral spread of the oncolytic viruses in an *in vivo* situation and further gave an indication if cancer stem cell-targeting can be achieved. Because of the described differences between spheroid and monolayer cultures, it was not necessarily expected that oncolytic viruses behave the same in monolayers and spheroid preparations of the same cell line. This proved true for Ad-Δ19K-Luc-GFP. The virus did not improve oncolysis in MiaPaCa-2 monolayers (**Figure 25**), but showed an effect in MiaPaCa-2 spheroids (**Figure 26**). Importantly, the differences observed between spheroid and

monolayer infection showed that further *in vivo* experiments need to clarify if the reduced oncolysis of Δ*E1B19K* deleted viruses seen in monolayers is a physiologic relevant issue.

Images in **Figure 26** show the progression of spheroid infection via GFP monitoring. It was observed that the virus infection started at the rim and slowly progressed to the inside, but spared the core area, which might be explained with an already necrotic core. By visually assessing the spheroid development over 8 days during virus infection, the following observations were made in comparison to the uninfected control: i. a smaller spheroid size of Ad-TRAIL-GFP-infected spheroids; ii. the disintegration of the spheroids following infection with Ad-Δ19K-Luc-GFP and Ad-TRAIL-GFP, which was most apparent in the diffuse rim areas; iii none of these effects were observed for spheroids infected with Ad-Luc-GFP and Ad-FCU1-GFP. The reduction in size following virus infection with Ad-TRAIL-GFP-infected spheroids (**Figure 27**) was described before by Lam et al. [224] and was there attributed to viral replication and induced oncolysis. Oncolysis could also be suspected to cause the diffuse rim areas. Observations of disintegration were reported before for primary tumor spheroids treated with chemotherapeutics [202], as well as for treatment with oncolytic viruses [225]. The hypothesis that Ad-Δ19K-Luc-GFP and Ad-TRAIL-GFP infection led to increased spheroid lysis compared to the control virus Ad-Luc-GFP was further proven in an LDH assay (**Figure 28**). The observations indicate improved viral lysis due to the *E1B19K*-deletion for Ad-Δ19K-Luc-GFP and bystander killing through TRAIL-expression by Ad-TRAIL-GFP.

An observation that was made during the LDH assay was a pronounced difference between the spheroid preparations (**Figure 28**). In case of spheroid preparation 1, the background LDH levels and therefore the percentage of dead cells were already high, which indicated advanced necrosis of spheroid cells independent of infection. The second preparation had much lower background LDH levels. It had been reported that size uniformity and a high level of equal conditioning of spheroids is very important, but also very difficult to accomplish [158]. Both greatly affects spheroid structure and therefore drug penetration [158]. Though there were no intentional differences in handling between the preparations, the difference in the spheroid viability occurred, confirming the importance of completely identical culture conditions of spheroids. Although the background levels of dead cells were different between the preparations, the absolute differences of the percentage of dead cells between mock and e.g. Ad-Δ19K-Luc-GFP were similar (experiment 1: 18%, experiment 2: 23%). This proves that improved LDH release was due to virus effects and not a to the different spheroid preparations qualities.

The observation that spheroid infection with Ad-Δ19K-Luc-GFP and Ad-TRAIL-GFP led to much higher LDH release and more pronounced physiological changes than infection with Ad-Luc-GFP and Ad-FCU1-GFP, allowed the conclusion that viral gene modification and arming are necessary strategies to achieve efficient oncolysis [100]. Taken in account that MiaPaCa-2 are considered to have stem cell-like features and further, cancer stem cells become enriched when cell lines are grown as spheroids, this would also allow to assume that the two viruses can target the tumor stem cell population. However, experiments *in vivo* have to finally clarify the physiologic oncolytic potential.

## 8.7. Ideas for Further Optimization

### 8.7.1. Improving Migration

Knowing the mediators of MSC migration to tumors, it is reasonable to consider improvement of tumor homing and therefore delivery of oncolytic viruses by MSCs. MSCs are known to express a variety of growth hormones, chemokines, cytokines, and innate immune receptors [128]. They sense

the corresponding ligands, which are released by tumors and tumor microenvironments, and induce migration of MSCs along these gradients.
One option could be the pre-treatment of *ex vivo* cultured MSCs with growth-factors prior to virus infection and systemic application. It was shown in several publications, that pre-incubation with different cytokines and growth factors, like IGF-1, EGF, SDF-1, or TNF-α, significantly enhanced migration *in vitro* [226, 227]. After MSCs were exposed to these stimuli, the corresponding receptors were up-regulated and further promoted migration [228].
An increase in released stimulating growth factors and cytokines was achieved by prior irradiation of the tumor, which then improved MSC migration *in vitro* [229] and in mouse models [229-231]. Alternatively, MSCs can be genetically modified in order to overexpress certain chemokine or growth factor receptors to make them more sensitive [128].

### 8.7.2. Improving Safety

The homing properties of MSCs were widely investigated [128]. What is not so well understood is the role of MSCs once they have engrafted in the tumor stroma. In their normal physiological role of tissue repair, they start to differentiate and produce stimulating factor, like growth factors and cytokines [232], once they located to wounded tissue.
In terms of engraftment into tumor stroma, these effects can be different. The factors, which are produced by MSCs (e.g. growth factors) have been connected to cancer progression. The differentiation to endothelial-like, fibroblast-like, or perivascular-like cells, which actively form blood vessels, suggests that they are precursor population of tumor-associated fibroblasts, endothelial cells, and pericytes [233].
Some studies claimed to have shown that MSCs can also be pro-tumorigenic because of their pro-angiogenic, immune-suppressive and tumor promoting properties [130, 232]. This has been shown in several mouse models studies. Subcutaneous co-injection of murine MSCs with murine melanoma cells resulted in enhanced tumor growth compared to injection of tumor cells alone [234]. In another study, human MSCs were co-injected with human breast cancer cells subcutaneously into immunocompromised mice. There, MSCs promoted metastasizing without affecting primary tumor size [235]. MSCs were even suspected to have tumor-initiating potential [236].
Other studies presented data that strongly supported the hypothesis that MSCs have solely anti-tumorigenic outcome. MSCs were tested in a mouse model using s.c. or i.p. injection alone or in co-injection with human ovarian tumor cells. Here, neither tumor-initiation, nor tumor-promotion, nor adverse side effects (e.g. ascites, weight loss) caused by MSCs were observed [237]. Similar outcomes were also shown for several other tumor entities (reviewed in [232]). Kidd et al. [232] suggested that the pro-tumorigenic effect of MSCs was an artefact, as all studies, which have seen tumor or metastasis promotion, used a large excess of MSCs in relation to the tumor mass, which does not represent a physiological situation. All studies that have used lower amounts of MSCs did not see a tumor-promoting effect. However, the effect is not fully explained.
Studies that tested MSCs as carrier cells for oncolytic adenoviruses never reported tumor increase or initiation in MSC-only controls or adenovirus-infected MSCs, though they did no experiments to explicitly rule out pro-tumorigenic behavior of the MSCs [124, 126, 141, 143, 144]. It is expected that MSCs infected with oncolytic adenoviruses will not survive longer than the end of the first viral life cycle. However, due to incomplete transduction, some non-infected MSCs might be systemically applied as well. This was also considered in a an exploratory clinical trial described in Garcia-Castro et al. [147], where oncolytic adenovirus-delivery by MSCs was investigated in children with

neuroblastoma. Here, MSCs were γ-irradiation with 30 Gy prior to infection and i.v. administration. Importantly, the study reported that irradiation of MSCs had no effect on infectibility with the virus, virus-replication in MSCs, or migration behavior of infected MSCs [147]. Therefore, irradiation of MSCs is a valid precaution method to contribute to improved safety while leaving the efficiency of the system unaltered.

## 8.8. Conclusion and Outlook

Summarizing this thesis, modifications of oncolytic adenoviruses, which were originally developed to improve killing of tumor cells, can efficiently increase virus replication and release from MSC carriers. The deletion of the *E1B19K* gene and the expression of the human TRAIL protein by an oncolytic adenovirus showed improved kinetics in MSCs of different donors, as well as improved killing in a subset of pancreatic cancer cell lines and low-passage pancreatic cultures. Further it was shown that tumor cell killing was improved by an oncolytic virus engineered to express the prodrug converting enzyme FCU1 after 5-FC addition.

Experiments in a transwell migration assay gave a first indication that infection of MSCs with the modified viruses did not alter MSC migration behavior for 2 days post-infection, the time reported in the literature MSCs need for tumor homing *in vivo*. Therefore, the reported oncolytic adenoviruses Ad-Δ19K-Luc-GFP, Ad-TRAIL-GFP, and Ad-FCU1-GFP have the potential to improve MSCs carrier cell-mediated virotherapy of pancreatic cancer. *In vivo* homing studies of MSCs loaded with the modified viruses to pancreatic ductal adenocarcinoma xenografts need to be performed in animals to verify the efficiency of the MSC delivery system.

# 9. Materials

## 9.1. Cell Culture

| Name | Supplier |
|---|---|
| 1,5-Dimethyl-1,5-diazaundecamethylene polymethobromide, hexadimethrine bromide (Polybrene) | Sigma-Aldrich, Taufkirchen |
| 2-mercaptoethanol | Sigma-Aldrich, Taufkirchen |
| 5-Fluorocytosine (5-FC) | Sigma-Aldrich, Taufkirchen |
| 5-Fluorouracile (5-FU) | Sigma-Aldrich, Taufkirchen |
| Adenosine 5'-monophosphate disodium salt (AMP) | Sigma-Aldrich, Taufkirchen |
| Adenosine 5'-triphosphate disodium salt hydrate (ATP) | Sigma-Aldrich, Taufkirchen |
| Agarose | Invitrogen, Karlsruhe |
| Ammonium persulfate (APS) | Sigma-Aldrich, Taufkirchen |
| Ampicillin (Amp) | Carl Roth, Karlsruhe |
| Arabinosyl cytosine (AraC) | Sigma-Aldrich, Taufkirchen |
| Bactotryptone | Carl Roth, Karlsruhe |
| Bio-Rad DC Protein Assay | Bio-Rad, Munich |
| Bromophenol blue | AppliChem, Darmstadt |
| Caesium chloride (CsCl) | AppliChem, Darmstadt |
| Cell lysis buffer | Promega, Madison, WI |
| Crystal violet | Carl Roth, Karlsruhe |
| CytoSelect™ 24-Well Cell Migration Assay | Cell Biolabs, San Diego, CA |
| Detection Reagent 1 & 2 | Thermo Fisher Scientific, Schwerte |
| Dimethyl sulfoxide (DMSO) | Sigma-Aldrich, Taufkirchen |
| Disposable PD-10 Desalting Columns | GE Healthcare, Little Chalfont, UK |
| Dithiothreitol (DTT) | AppliChem, Darmstadt |
| Dulbecco's modified Eagles medium (DMEM GlutaMAX™) | Gibco, Life Technologies, Darmstadt |
| Ethanol absolute (EtOH) | VWR International, Bruchsal |
| Ethidium bromide | AppliChem, Darmstadt |
| Ethylendiaminetetraacetic acid (EDTA) | Sigma-Aldrich, Taufkirchen |
| Ethylene glycol tetraacetic acid (EGTA) | Sigma-Aldrich, Taufkirchen |
| Fetal bovine serum (FBS) | PAA, Pasching |
| Formaldehyde, 37 % | Merck, Darmstadt |
| GeneRuler™ 1 kb DNA ladder | Fermentas, St. Leon-Rot |
| Gentamycin | Invitrogen, Karlsruhe |
| Glucose | AppliChem, Darmstadt |
| Glycerol | Carl Roth, Karlsruhe |
| HEPES | Gibco, Life Technolgies, Darmstadt |
| Hoechst 33258 | Invitrogen, Karlsruhe |

| Name | Supplier |
|---|---|
| IGEPAL NP-40 | Sigma-Aldrich, Taufkirchen |
| Isocove's modified Dulbecco's medium (IMDM) | Gibco, Life Technologies, Darmstadt |
| Isopropanol | VWR International, Bruchsal |
| Kanamycin (Kan) | Sigma-Aldrich, Taufkirchen |
| KSF medium (Keratinocyte SF medium) | Gibco, Life Technologies, Darmstadt |
| LB agar „Luria Miller" | Carl Roth, Karlsruhe |
| Lipofectamine Reagent | Invitrogen, Karlsruhe |
| Lithium chloride (LiCl) | Carl Roth, Karlsruhe |
| Luciferin | PJK GmbH, Kleinblittersdorf |
| Luria Bertani medium "Lennox" (LB) | Carl Roth, Karlsruhe |
| Magnesium chloride ($MgCl_2$) | Carl Roth, Karlsruhe |
| Magnesium sulfate ($MgSO_4$) | Carl Roth, Karluhe |
| Methanol | VWR International, Bruchsal |
| Modified Eagle's minimum essential medium (OptiMEM) | Gibco, Life Technologies, Darmstadt |
| N,N,N',N'-tetra-methylethylenediamine (TEMED) | Sigma-Aldrich, Taufkirchen |
| Nonhematopoietic stem cell expansion medium (NH medium) | Miltenyi Biotec, Bergisch Gladbach |
| PageRuler$^{TM}$ Prestained Protein Ladder | Fermentas, St. Leon-Rot |
| Penicillin | Invitrogen, Karlsruhe |
| Penicillin/Streptomycin | Gibco, Life Technolgies, Darmstadt |
| Phenylmethylsulfonyl fluoride (PMSF) | AppliChem, Darmstadt |
| Phosphate buffered saline (PBS) | Gibco, Life Technolgies, Darmstadt |
| PKH26 Red Fluorescent Cell Linker Kit | Sigma-Aldrich, Taufkirchen |
| Potassium chloride (KCl) | Sigma-Aldrich, Taufkirchen |
| Roswell Park Memorial Institute medium (RPMI-1640) | Gibco, Life Technologies, Darmstadt |
| Rotiophorese Gel 30 | Carl Roth, Karlsruhe |
| Skim milk powder | Carl Roth, Karlsruhe |
| Sodium acetate | Sigma-Aldrich, Taufkirchen |
| Sodium chloride (NaCl) | Carl Roth, Karlsruhe |
| Sodium deoxycholate | BD Biosciences, Heidelberg |
| Sodium dodecyl sulfate (SDS) | Sigma-Aldrich, Taufkirchen |
| Sodium fluoride | Sigma-Aldrich, Taufkirchen |
| Sodium orthovanadate | Sigma-Aldrich, Taufkirchen |
| Super Killer TRAIL | Axxora, Farmingdale, NY |
| Triton X-100 | Carl Roth, Karlsruhe |
| Trizma base (tris) | Sigma-Aldrich, Taufkirchen |
| Trizma hydrochloride (tris-HCl) | Sigma-Aldrich, Taufkirchen |
| Trypan Blue Solution | Sigma-Aldrich, Taufkirchen |
| Trypsin-EDTA, 0.05 % | Gibco, Life Technolgies, Darmstadt |
| Tween 20 | Sigma-Aldrich, Taufkirchen |
| Yeast extract | Carl Roth, Karlsruhe |

## 9.2. Buffers

### 9.2.1. Nucleic Acid and Agarose Gel

| Name | Ingredients |
|---|---|
| 50x TAE buffer | 2 M tris<br>1M sodium acetate<br>62.5 mM EDTA<br>pH 8.5 |
| 10x DNA loading buffer | 0.1 % (w/v) bromophenol blue<br>50 % (v/v) glycerol<br>0.1 M EDTA<br>0.2 pH 8.0 |
| Agarose gel solution | 1 x TAE buffer<br>1-2 % (w/v) agarose<br>1 µg/ml ethidium bromide |

### 9.2.2. Acrylamide Gel

| Name | Ingredients |
|---|---|
| 4x protein loading dye | 200 mM tris-HCl<br>400 mM dithiothreitol<br>8 % (w/v) SDS<br>0.4 % (w/v) bromophenol blue<br>40 % glycerol<br>10 % (w/v) 2-mercaptoethanol<br>pH 6.8 |
| RIPA buffer | 10 mM tris-HCl<br>150 mM NaCl<br>1 % (v/v) IGEPAL NP-40<br>1 % (w/v) sodium deoxycholate<br>0.1 % (w/v) SDS<br>1 mM PMSF<br>20 mM sodium fluoride<br>2 mM sodium orthovanadate<br>pH 7.5 |
| 4x seperating buffer | 1.5 mM tris-HCl<br>0.04 % (w/v) SDS<br>pH 8.8 |
| 4x stacking buffer | 0.5 M tris-HCl<br>0.4 % (w/v) SDS<br>pH 6.8 |

| Name | Ingredients |
|---|---|
| 12.5% seperating gel | 3 ml bi-distilled water<br>2.25 µl 4 x seperating buffer<br>3.75 Rotiophorese Gel 30<br>60 µl 10 % (w/v) APS<br>12.5 µl TEMED |
| 4% stacking gel | 5.15 ml bi-distilled water<br>2.1 ml 4 x stacking buffer<br>1.1 ml Rotiophorese Gel 30<br>60 µl 10 % (w/v) APS<br>17.5 µl TEMED |
| 10x running buffer | 2 M glycine<br>250 mM tris<br>1 % (w/v) SDS |

### 9.2.3. Western Blot

| Name | Ingredients |
|---|---|
| 10x TBS | 250 mM tris-HCl<br>1.5 M NaCl<br>pH 7.4 |
| 1x transfer buffer | 25 mM tris<br>192 mM glycerol<br>20% (v/v) methanol |
| Western blot blocking solution | 1x TBS<br>0.3 % (v/v) Tween 20<br>5 % skim milk powder |
| Western blot washing buffer | 1x TBS<br>0.3 % (v/v) Tween 20 |

## 9.3. Virus Purification and Viral Particle Determination

| Name | Ingredients |
|---|---|
| Caesium chloride solution (1.27 g/cm$^3$) | 500 ml bi-distilled water<br>227.2 g caesium chloride<br>pH 7.8 |
| Caesium chloride solution (1.41 g/cm$^3$) | 500 ml bi-distilled water<br>304.6 g caesium chloride<br>pH 7.8 |
| TE buffer | 0.1 % SDS<br>1mM EDTA<br>10 mM tris-HCl<br>pH 7.4 |
| Virus lysis buffer | 100 µM TE-buffer<br>0.5 % (w/v) SDS |

## 9.4. Others

| Name | Ingredients |
|---|---|
| Crystal violet staining solution | 70 % (v/v) ethanol<br>2 % (w/v) crystal violet |
| Hoechst 33258 staining solution | 1:2000 in PBS |
| Triton X-100 permeabilization solution | 0.5 % (v/v) in bi-distilled water |
| Formaldehyde fixation solution | 4 % (v/v) in bi-distilled water |
| Luciferase assay substrate | 1 M tris-HCl (pH 7.8)<br>0.25 M EGTA (pH 8.3)<br>200 mM ATP<br>100 mM DTT<br>1 M $MgSO_4$<br>200 mM AMP<br>10 mM luciferin |

## 9.5. Bacterial Strains

| Name | Description |
|---|---|
| Escherichia coli BJ5183 | Genotype: endA1, sbcBC, recBC, galK, met, thi-1, bioT, hsdR (Stratagene, Amsterdam). |
| Escherichia coli XL-1 blue | Genotype: recA1 endA1 gyrA96 thi-1 hsdR17 supE44 relA1 lac [F´ proAB lacIqZΔM15 Tn10 (Tetr)] |

## 9.6. Cell Lines

| Name | Description | Culture Medium | Source |
|---|---|---|---|
| HEK 293 | Human embryonic kidney cells | DMEM/5% | G. Fey (Erlangen, Germany) |
| A549 | Human lung adenocarcinoma epithelial cell line | DMEM/5% | ATCC (Manassas, USA) |
| C8161 | Human melanoma cell line | DMEM/5% | [238] |
| MiaPaCa-2 | Human pancreatic adenocarcinoma cell line | DMEM/5% | AG Herr, University Heidelberg |
| BxPc-3 | Human pancreatic adenocarcinoma cell line | DMEM/5% | AG Herr, University Heidelberg |
| Panc-1 | Human pancreatic adenocarcinoma cell line | RPMI/5% | C. Cziepluch, DKFZ Heidelberg |
| AsPc-1 | Human pancreatic adenocarcinoma cell line | RPMI/5% | C. Cziepluch, DKFZ Heidelberg |

| Name | Description | Culture Medium | Source |
|---|---|---|---|
| JoPaca-1 | Low-passage human ductal adenocarcinoma cell line | IMDM/10% | J. Hoheisel, DFKZ Heidelberg |
| PaCaDD-159 | Low-passage human ductal adenocarcinoma cell line | PacaDD medium | C. Pilarsky, TU Dresden |
| MSC different donors | Primary cells | NH medium | University Hospital Heidelberg |

## 9.7. Media

| Name | Ingredients |
|---|---|
| LB medium | 25 g/l LB powder dissolved in bi-distilled water, sterile<br>Containing either 1 mg/ml ampicillin or 50 µg/ml kanamycin |
| LB agar | 15 g/l LB agar „Luria Miller“ dissolved<br>in LB medium containing antibiotics |
| SOC medium | 2% bactotryptone pH 7.0<br>0.5% yeast extract<br>10mM NaCl<br>2.5mM KCl<br>10mM $MgSO_4$<br>10mM $MgCl_2$<br>20mM glucose |
| DMEM/2% | DMEM GlutaMAX™ (already supplemented with 4500 mg/L glucose, 25mM HEPES, sodium bicarbonate, and L-Ala-L-Gln)<br>2% FBS<br>100 U/ml penicillin<br>100 µg/ml streptomycin |
| DMEM/5% | DMEM GlutaMAX™<br>10% FBS<br>100 U/ml penicillin<br>100 µg/ml streptomycin |
| RPMI/2% | RPMI-1640 medium (already supplemented with L-glutamine and sodium bicarbonate)<br>2% FBS<br>100 U/ml penicillin<br>100 µg/ml streptomycin |

| Name | Ingredients |
|---|---|
| RPMI/5% | RPMI-1640 medium<br>5% FBS<br>100 U/ml penicillin<br>100 µg/ml streptomycin |
| IMDM/2% | IMDM medium (already supplemented with L-glutamine)<br>2% FBS<br>100 U/ml penicillin<br>100 µg/ml streptomycin |
| IMDM/10% | IMDM medium (already supplemented with L-glutamine)<br>10% FBS<br>100 U/ml penicillin<br>100 µg/ml streptomycin |
| PacaDD medium | Ration 2:1 of DMEM GlutaMAX™ supplemented with 20% FBS and KSF medium<br>100 U/ml penicillin<br>2.5 mg/ml gentamycin |

## 9.8. Plasmids

| Name | Description | Origin |
|---|---|---|
| pGL3-BPSA-Luc | pGL3-basic containing the human beta globin splice acceptor sequence (BPSA), the firefly luciferase gene (*Luc*), and a polyA sequence | Quirin et al. [93] |
| pSΔ24 | adenovirus transfer vector which contains a mutant *E1A* gene with a 24 bp deletion of nucleotides 923 – 946 corresponding to amino acids LTCHEAGF of *E1A* to prevent binding and inactivation of pRB | Suzuki et al., 2002 [161] |
| pSΔ24-GFP | adenovirus transfer vector which contains a mutant *E1A* gene with a 24 bp deletion, and a *GFP* gene introduced via an splice acceptor site downstream of the *E4* gene | See section 7.8.2 |
| pSΔ24-E1B19K- | adenovirus transfer vector which contains a mutant *E1A* gene with a 24 bp deletion, the *E1B19K* deletion was derived by PCR with oligonucleotides 19K-5' (5'-CGA GGA CTT GCT TAA CGA GC-3') and 19K-3' (5'-GGA CGG AAG ACA ACA GTA GC-3') from Ad337 | Rohmer et al. [81] |

| Name | Description | Origin |
|---|---|---|
| pSΔ24-ΔE1B19K-GFP | adenovirus transfer vector which contains a mutant *E1A* gene with a 24 bp deletion, the deletion of *E1B19K*, and the *GFP* gene introduced downstream of *E4* via a splice acceptor site | See section 7.8.4 |
| pGL3-IRES-Luc | pGL3-basic containing an internal ribosomal entry site, the firefly luciferase gene (*Luc*), and a polyA sequence | [93] |
| pGL3-IRES-TRAIL | pGL3-basic containing an internal ribosomal entry site, the full-length *TRAIL* gene, and a polyA sequence | See section 7.8.5 |
| pfiber5/3 ΔE3 IRES Luc | adenovirus transfer vector containing a chimeric 5/3 fiber, the full-length firefly luciferase gene (*Luc*) inserted via an internal ribosomal entry site downstream of the fiber, and the deletion of the *E3* gene | Generated in the Nettelbeck lab |
| pfiber5/3 ΔE3 IRES TRAIL | adenovirus transfer vector containing a chimeric 5/3 fiber, the full-length *TRAIL* gene inserted via an internal ribosomal entry site downstream of the fiber, and the deletion of the *E3* gene | See section 7.8.5 |
| pVK500 5/3 ΔE3 IL | plasmid containing the HAdV-5 genome with a chimeric 5/3 fiber, the deleted *E3* region and the firefly luciferase gene (*Luc*) inserted via an internal ribosomal entry site downstream of the fiber | [81] |
| pVK500 5/3 ΔE3 | plasmid containing the HAdV-5 genome with a chimeric 5/3 fiber and a deleted *E3* region | Generated in the Nettelbeck lab |
| pVK500 Δ24 | plasmid containing the HAdV-5 genome with partial deletion of the fiber gene, a 24 bp deletion in the *E1A* region | Generated in the Nettelbeck lab |
| pVK500 5/3 Δ24 IRES FCU1 | plasmid containing the HAdV-5 genome with a chimeric 5/3 fiber, with partial deletion of the fiber gene, a 24 bp deletion in the *E1A* region, and inserted *FCU1* via an internal ribosomal entry site | Generated in the Nettelbeck lab |

## 9.9. Viruses

| Name | Description | Origin |
|---|---|---|
| Ad5 | Replication-deficient hAdV-5, Δ*E1*, Δ*E3*, luciferase gene under CMV promoter control | [67] |
| Ad5/3 | Replication-deficient hAdV-5, Δ*E1*, Δ*E3*, modified fiber hAdV-5 fiber and hAdV-3 knob, luciferase gene under CMV promoter control | [67] |
| Ad5RGD | Replication-deficient hAdV-5, Δ*E1*, Δ*E3*, modified fiber RGD peptide introduced into HI-loop, luciferase gene under CMV promoter control | (Dmitriev, Krasnykh et al. 1998) |
| Ad-GFP | hAdV-5/3, 24 aa deletion in *E1A*, Δ*E3*, *GFP* downstream of *E4* via splice acceptor site | See section 7.8.2 |
| Ad-Luc | hAdV-5/3, 24 aa deletion in *E1A*, Δ*E3*, firefly luciferase gene (*Luc*) downstream of the fiber gene via internal ribosomal entry site | [81] |
| Ad-Δ19K-Luc | hAdV-5/3, 24 aa deletion in *E1A*, Δ*E3*, Δ*E1B19K*, firefly luciferase gene (*Luc*) downstream of the fiber gene via internal ribosomal entry site | [81] |
| Ad-TRAIL | hAdV-5/3, 24 aa deletion in *E1A*, Δ*E3*, human *TRAIL* gene downstream of the fiber gene via internal ribosomal entry site | See section 7.8.5 |
| Ad-Luc-GFP | hAdV-5/3, 24 aa deletion in *E1A*, Δ*E3*, firefly luciferase gene (*Luc*) downstream of the fiber gene via internal ribosomal entry site, GFP downstream of *E4* via splice acceptor site | See section 7.8.3 |
| Ad-Δ19K-Luc-GFP | hAdV-5/3, 24 aa deletion in *E1A*, Δ*E3*, Δ*E1B19K*, firefly luciferase gene (*Luc*) downstream of the fiber gene via internal ribosomal entry site, *GFP* downstream of *E4* via splice acceptor site | See section 7.8.4 |
| Ad-TRAIL-GFP | hAdV-5/3, 24 aa deletion in *E1A*, Δ*E3*, human *TRAIL* gene downstream of the fiber gene via internal ribosomal entry site, *GFP* downstream of *E4* via splice acceptor site | See section 7.8.6 |
| Ad-FCU1-GFP | hAdV-5/3, 24 aa deletion in *E1A*, Δ*E3*, *FCU1* gene downstream of the fiber gene via internal ribosomal entry site, *GFP* downstream of *E4* via splice acceptor site | See section 7.8.7 |
| Ad-CMV-GFP | Replication-deficient hAdV-5/3, Δ*E1*, Δ*E3*, *GFP* under CMV promoter control | provided by Igor Dmitriev and David Curiel |
| Ad-CMV-FCU1 | Replication-deficient hAdV-5, Δ*E1*, Δ*E3*, *FCU1* under CMV promoter control | Provided by Phillippe Erbs |

## 9.10. Antibodies

| Name | Description | Dilution | Supplier |
|---|---|---|---|
| Adenovirus fiber monomer and trimer | Mouse monoclonal [4D2] | 1:500 | Abcam, Cambridge, UK (ab3233) |
| Adenovirus Type 5 hexon | Rabbit polyclonal | 1:500 | Abcam, Cambridge, UK (ab24240) |
| TRAIL | Rabbit, polyclonal | 1:500 | Invitrogen, Karlsruhe |
| Anti-yCD | Sheep, polyclonal | 1:200 | AbD Serotec, Düsseldorf |
| Anti-EGFP | Mouse $IgG_1$, monoclonal (clones 7.1 and 13.1) | 1:10,000 | Roche, Mannheim |
| Anti-β-actin | Mouse $IgG_{2a}$, monoclonal (clone AC-74) | 1:50,000 | Sigma-Aldrich, Taufkirchen |
| Anti-mouse-HRP | Goat, polyclonal | 1:2,000 | Cell Signaling Technologies, Danvers, MA |
| anti-sheep-HRP | Rabbit, polyclonal | 1:8,000 | Thermo Fisher Scientific, Life Technologies, Schwerte |
| Anti-rabbit-HRP | Goat, polyclonal | 1:2,000 | Cell Signaling Technologies, Danvers, MA |

## 9.11. PCR Primers

| Name | Sequence (5'-3') |
|---|---|
| Delta 24 | aaagccagcctcgtggcaggtaag |
| SeqITR | cgggaaaactgaataagaggaagtga |
| E3-rev | ggcaaggaggtgctgctgaataaac |
| E3-for | ctgctagttgagcgggacaggggac |
| 3knob | ttaatgtagaactatactttgatgc |
| 5knob | aggcagtttggctccaatatctgg |
| Seq Mfe Fiber | tgtataagctatgtggtggtgggg |
| GFP-N1 f2 | cgccaccatggtgagcaag |
| 3' pShuttle rv | cggatccttatcgattttaccac |
| hTRAIL fw | gatcccatggctatgatggaggtcc |
| hTRAIL rv2 | gcatctagatcattagccaactaaaaagg |
| E1B-rev | gcggacggaagacaacagtag |

## 9.12. Sequencing Primers

| Name | Sequence (5'-3') |
|---|---|
| E1B-rev | gcggacggaagacaacagtag |
| 3knob | ttaatgtagaactatactttgatgc |
| 3' pShuttle rv | cggatccttatcgattttaccac |
| Seq Mfe Fiber | tgtataagctatgtggtggtgggg |
| 3'E4_fw | gagctatgctaaccagcgtagcc |
| E4p_rev | attgaagccaatatgataatgaggg |
| midGFP_fw | tacaactacaacagccacaacg |
| 5'GFP_fw | cccggtgaacagctcctcgccc |
| 5´RITR_rev | gaacctgaaacataaaatgaatgc |

# 10. Methods

## 10.1. DNA Methods

### 10.1.1. Polymerase Chain Reaction (PCR)

Amplification for test PCRs were done with Taq-Polymerase (Invitrogen, Life Technologies, Darmstadt). In order to amplify fragments for cloning (GFP and TRAIL) the Precisor High-Fidelity-Polymerase was used (BioCat, Heidelberg). The reagents were taken from the Taq Polymerase Kit (Invitrogen, Life Technologies, Darmstadt). dNTPs were obtained from Bioron, Ludwigshafen. The reaction mixes were set up according to the manufacturer's manual as summarized below.

| | Taq | PRECISOR |
|---|---|---|
| 10 x PCR buffer | 1x | 1x |
| 50 mM $MgSO_4$-solution | 1.5 mM | - |
| 10 mM dNTPs | 200 µM | 400 µM |
| DMSO | - | 3.5% |
| 20 µM primer forward | 1 µM | 160 nM |
| 20 µM primer reverse | 1 µM | 160 nM |
| DNA template | 1 µl | 20 ng |
| Polymerase | 2.5 U | 1U |
| **Total volume** | **25 µl** | **25 µl** |

The PCR reactions were performed in a T3000 Thermocycler (Biometra, Jena). An outline of the PCR program is given below. Annealing temperatures were chosen according to the temperature determined from primer lengths, base composition, and individual optimization.

| | Cycles | Temperature | Time |
|---|---|---|---|
| Denaturation | 1x | 96°C | 3 min |
| Denaturation | | 96°C | 30 sec |
| Annealing | 30x | 55-66°C | 30 sec |
| Extension | | 72°C | 1 min |
| Final extension | 1x | 72°C | 10 min |
| Cooling | 1x | 4°C | ∞ |

PCR results were analyzed by agarose gel electrophoresis (see **section 10.1.3**). For further cloning, the fragments were purified using the Qiagen® PCR-purification kit (Qiagen, Hilden) as described in the manual.

### 10.1.2. Restriction Enzyme Digestion

Amplified PCR products or plasmid vectors were treated with restriction enzymes in the corresponding buffers provided by the companies (Fermentas, St. Leon-Rot, and New England Biolabs, Frankfurt am Main). The digestion reactions were performed for 4 hours at 37°C, if not

indicated otherwise in the manuals of the enzymes. The digestion created DNA fragments with "sticky" overhang ends.

### 10.1.3. Gel Electrophoresis

Following restriction enzyme digestion, the fragments were separated and analyzed by gel electrophoresis. The gel was prepared, solving 1% agarose gel in 1x TAE buffer. The DNA fragments were prepared adding 1x DNA loading buffer, were applied on the gel, and separated at 100 V for 1 hour. As a size standard, GeneRuler™ 1 kb DNA ladders were applied in one lane on the same gel. DNA fragments were visualized using UV light at 265 nm with a Gel Stick "Touch" (INTAS, Göttingen). For further cloning, the required fragments were excised from the gel using a scalpel.

### 10.1.4. Cloning DNA Fragments into Plasmid Vectors

DNA insert fragments and vector DNA were digested (see **section 10.1.2**), and the vector ends were de-phosphorylated using FastAP™ alkaline phosphatase (Fermentas, St. Leon-Roth) to prevent religation during cloning. Digested vectors and inserts were purified using QIAquick® Gel Extraction Kit (Qiagen, Hilden). Inserts were introduced into the plasmid vector by using T4 DNA Ligase (Thermo Scientific, Schwerte). A ratio of linearized vector and DNA insert of 1:3 to 1:5 was used. 100 ng of vector DNA was used and the amount of insert calculated accordingly. The ligation was done in 20 µl total volume using 1 µl of T4 DNA Ligase. The ligation mix was incubated for 1 hour at 22°C and further for 10 min at 65°C to stop ligation. 1.5 µl of the ligation mix was then electroporated into XL-1 Blue as described in **section 10.1.6**.

### 10.1.5. Production of Electro-Competent Bacteria and Transformation

E. coli XL-1 Blue bacteria from the stock were inoculated in 10 ml LB-medium containing tetracylin and incubated at 37°C overnight while shaking at 220 rpm. The next day, 3 x 1L LB medium were inoculated with the pre-culture. Incubation was stopped, when optical density reached 0.5 – 0.6 at 600 nm. Suspension was incubated 15 min on ice and centrifuged for 10 min at 4,000 rpm. The pellet was resolved in 50 ml bi-distilled water, centrifuged for 10 min at 5,000 rpm, and washed in 50 ml bi-distilled water again. After the final centrifugation for 10 min at 5,000 rpm, the pellet was resuspended in 20 ml cold glycerol (10% v/v). Aliquots of 50 µl were stored at – 80°C.

Transformation efficiency of the generated bacteria was tested. Electro-competent bacteria were transformed with 1 ng of a defined plasmid (procedure see **section 10.1.6**). 1, 10, and 100 µl of the transformation was plated and incubated overnight at 37°C. 24 hours later, the colonies were counted and the transformation efficiency calculated using the following formula:

Transformation efficiency = (colony / [ng] transformed DNA) x (total volume / plated volume)

For electro-competent E. coli XL-1 Blue the reference transduction efficiency was $1.0 \times 10^9$ µg.

### 10.1.6. Transformation by Electroporation

Plasmids were transformed into electro-competent E. coli XL-1 Blue.

For each sample, 50 µl of competent bacteria were thawed on ice. 1-50 ng of a plasmid for re-transformation in 1-2 µl or 2-3 µl of a ligation mix were added to the bacteria. The mix was incubated on ice for one minute. Then, the samples were transferred into pre-chilled electroporation cuvettes. A cuvette was placed in an electroporator and pulsed at 2.5 kV for 4.5 - 5.5 milliseconds. Immediately

after transformation, the celled were transferred into 1 ml of SOC medium. After shaking at 37 °C for 30 min, 500 µl, 200 µl, and 100 µl of the bacteria solution were spread on LB agar dishes containing the relevant antibiotic for selection. Plates were incubated overnight at 37°C. Single colonies were picked about 15 hours later.

### 10.1.7. Homoglogous Recombination

In order to modify the adenoviral genome, homologous recombination between a shuttle plasmid (pShuttle or pfiber) and the viral backbone plasmids (pVKs) was performed via homologous recombination.

4 µg of the respective shuttle plasmid was linearized by PmeI and backbone plasmids. For homologous recombinations with pfiber plasmids, pVKs were digested with SwaI in 50 µl. Both reactions were performed for 4 hours at 37°C. Afterwards, 2 µl of FastAP™ alkaline phosphatase (Fermentas, St. Leon-Roth) were added and samples were incubated for another 45 min at 37°C. Then, DNA was purified by precipitation. Lithium chloride to a final concentration of 500 mM and afterwards 2.5-fold volumes of 100% ethanol were added. The samples were centrifuged at 13,000 rpm for 20 min, the supernatant was aspirated, the pellets were washed in 0.5 ml of 70% EtOH, centrifuged again, and then resuspended in 30 µl of bi-distilled water. The protein concentration in the samples was determined by measurement with a NanoDrop ND-1000 UV/VIS spectrophotometer (Peqlab, Erlangen).

Homologous recombination was carried out using 100 ng of linearized pVK backbone plasmid, and 600 ng of linearized shuttle plasmid (pfiber or pShuttle). Both were mixed and added to 50 µl of electro-competent BJ5183 bacteria. The solution was transferred to a cooled cuvette, was placed in an electroporator, and pulsed at 2.5 kV for 4.5-5.5 milliseconds. Immediately after transformation, the celled were transferred into 1 ml of SOC medium. The solution was incubated at 30°C for 30 min and then spread on LB agar dishes containing the appropriate antibiotic. The plates were incubated at 30°C. Successfully recombined genomes were forming colonies, which started to appear 20 hours post-plating. Single clones were picked and analyzed via restriction enzyme digestion (see s**ection 10.1.2**) for correct sequence organization.

### 10.1.8. Isolation of Plasmid DNA for Analysis

Following generation of new constructs by cloning or homologous recombination, the correct genome organization was verified. Following transformation, single clones were picked from the agar plate and were inoculated in 5 ml LB medium supplemented with the relevant antibiotic and incubated overnight in a shaker at 180 rpm and 37°C (normal cloning) or 30°C (homologous recombination). Bacteria were harvested by centrifugation at 1,000 rpm for 10 min. For normal sized plasmids (<15 kb), DNA was isolated using the AxyPrep™ Plasmid Miniprep Kit (Axygen Biosciences, Union City, CA) according to the manufacturer's protocol.

Larger plasmids (>15 kb, e.g. adenoviral genomes) were purified by a column-free protocol using buffer solutions from the QIAprep® Plasmid Midi Kit (Qiagen, Hilden). After centrifugation, the pellets were resuspended in 250 µl of buffer P1 supplemented with RNase A (provided by the kit) and lysed by adding 250 µl buffer P2. Samples were incubated for 5 min at room temperature to allow lysis. Then, 350 µl of buffer P3 was added. Bacterial cell debris was removed by centrifugation at 13,000 rpm for 10 min and supernatants were mixed with 750 µl isopropanol. After mixing, precipitated DNA was pelleted at 13,000 rpm for 30 min at 4°C and washed with 70% (v/v) ethanol. Supernatants were aspirated and DNA was resuspended in 50 µl bi-distilled water.

The purified plasmids were subsequently characterized by restriction enzyme digestion (see **section 10.1.2**) with suited enzymes and buffers (Fermentas, St.Leon-Rot, and New England Biolabs, Frankfurt am Main) following gel electrophoresis (see **section 10.1.3**). The key viral genome segments of correct candidates were sequenced using the GATC Biotech Sanger service (GATC Biotech, Konstanz).

### 10.1.9. Quantitative Isolation of Plasmid DNA

For larger scale plasmid isolation regardless of plasmid size, correct single clones from a re-transformation or frozen stock were inoculated in 100 ml LB medium supplemented with the appropriate antibiotic and incubated overnight in a shaker at 180 rpm at 37°C (normal cloning) or 30°C (homologous recombination). Plasmid DNA was isolated using the QIAGEN® Plasmid Plus Midi Kit (Qiagen, Hilden) according to the manufacturer's instructions. DNA precipitates were dissolved in 200 - 500 µl bi-distilled water, characterized by restriction enzyme digestions as descried in **section 10.1.2**, and subsequently stored at -20°C.

## 10.2. Cell Culture

### 10.2.1. Maintenance of Cells

Human established pancreatic tumor cell lines MiaPaCa-2 and BxPc-3 (kindly provided by Ingrid Herr, University Hospital Heidelberg) were cultured in DMEM/5% (containing 5% heat-inactivated fetal bovine serum (FBS)). AsPc-1 and Panc-1 (provided by Celina Cziepluch, DKFZ, Heidelberg) were cultivated in RPMI/5%. A549 (lung carcinoma cell line) and HEK293 were cultivated in DMEM/5%. Absence of mycoplasma was confirmed every three months. Cells were used until passage 30.
JoPaca-1 and PacaDD-159 were cultures in PacaDD medium (see Materials **section 9.7**). JoPaca-1 cultures were used in passages 9 to 11 and PacaDD-159 cultures in passages 11 to13.
MSCs were provided and characterized by the group of Ingrid Herr (University Hospital Heidelberg). They were isolated from bone marrow of healthy patients, both male and female between 20 to 30 years old, by Ficoll's dense centrifugation and attachment to plastic surfaces. Further, they were characterized by their differentiation potential into chondrogenic, adipogenic, and osteogenic lineages [131, 133]. For about 3 passages, MSCs were expanded and then frozen by cryo-preservation, stored, and re-thawed prior to usage. The MSCs obtained from the group of Ingrid Herr were between passages 3-5 and were used until passage 9. They were cultured in NH medium.
All cells were grown at 37°C and 5% $CO_2$ humidified atmosphere. For splitting, the cells were once washed with 10 ml of PBS, detached with 4 ml of Trypsin-EDTA and then split 1:3 (for MSCs and low-passage pancreatic carcinoma cultures) or 1:10 (for established pancreatic cancer cell lines).

### 10.2.2. Cryo-Preservation and Thawing

Cells from a 10-cm plate were trypsinized, centrifuged at 1,000 rpm for 10 min, and resuspended in 4 ml of FBS containing 10% (v/v) DMSO. 1 ml aliquots in Cryo tubes (Nunc, Thermo Fisher Scientific, Schwerte) were stored NALGENE™ Cryo 1°C Freezing Container (Nunc, Thermo Fisher Scientific, Schwerte) overnight before moving to long-term storing at -196°C in liquid nitrogen.

### 10.2.3. Cell Number Determination

Viable Cells were counted using a Neubauer chamber. After trypsinization, cells were diluted and stained with trypan blue solution and applied into the chamber. At least 4 big squares were counted and the number of vital cells calculated using the following formula:
cells/ml = average of cell number in large squares x dilution factor x $10^4$.

## 10.3. Recombinant Adenoviruses

The cloning strategies were described in detail in Result **section 7.8.1**. **Ad5** has been described as Ad5Luc1 in Krasnykh et al. [67]. **Ad5/3** has been described as Ad5/3Luc1 in Krasnykh et al. [67]. **Ad5RGD** was described as Ad5lucRGD in [239]. **Ad-Luc** and **Ad-Δ19K-Luc** were described as Ad5/3.19K+.IL and Ad5/3.19K+.IL, respectively, in Rohmer et al. [81]. **Ad-CMV-GFP** was kindly provided by Igor Dmitriev and David Curiel. Prodrug convertase FCU1-encoding **Ad-CMV-FCU1** was described in Erbs et al. [106].
All other viruses were generated in the course of this study.
*GFP* from pEGFP-N1 (Clontech, Mountain View, CA) was cloned into pSΔ24 [161], generating pSΔ24-GFP. pSΔ24-GFP was recombined with pVK500 5/3 ΔE3 to generate **Ad-GFP** (for details see also Results **section 7.8.2**). **Ad-Luc-GFP** was generated by homologous recombination of pSΔ24-GFP and pVK500 5/3 ΔE3 IL (see Rohmer et al. [81] and Results **section 7.8.3**). In order to generate **Ad-Δ19K-Luc-GFP**, the *E1B19K* deletion from pSΔ24-E1B19K- [81] was introduced into pSΔ24-GFP, resulting in pSΔ24-E1B19K-GFP. The deletion of *E1B19K* had been generated by PCR with oligonucleotides 19K-5' (5'-CGA GGA CTT GCT TAA CGA GC-3') and 19K-3' (5'-GGA CGG AAG ACA ACA GTA GC-3') from Ad337 as described in Rohmer et al. [81]. pSΔ24-E1B19K-GFP was recombined with pVK500 5/3 ΔE3 IL to generate Ad-Δ19K-Luc-GFP (see also Results **section 7.8.4**).
Full-length *TRAIL* was provided by Ingrid Herr (University Hospital Heidelberg) and cloned into pGL3-IRES-Luc [93] replacing the luciferase gene. The resulting pGL3-IRES-TRAIL plasmid was subcloned into pfiber5/3 ΔE3 IRES Luc to obtain pfiber5/3 ΔE3 IRES TRAIL. Homologous recombination with pVK500 Δ24 resulted in the genome of **Ad-TRAIL** (see also Results **section 7.8.5**). Homologous recombination of pSΔ24-GFP and pVK500 5/3 ΔE3 IRES TRAIL (both generated above) resulted in the genome of **Ad-TRAIL-GFP** (see also Results **section 7.8.6**).
Recombination of pVK500 5/3 d24 IRES FCU1 and pSΔ24-GFP generated the genome for **Ad-FCU1-GFP** (see also Results **section 7.8.7**).
Viruses were PacI digested and transfected with Lipofectamin (Invitrogen, Karlsruhe) into A549 cells (see also **section 10.3.1**). The viruses were amplified in A549 cells and subsequently purified by CsCl equilibrium density gradient ultracentrifugation (see also **sections 10.3.2** and **10.3.3**). Accuracy of genome sequences was confirmed by PCR. Viral particles concentration was determined by optical density measurement at 260 nm (see also **section 10.3.4**). Infectious virus particles were determined by $TCID_{50}$ assay on A549 or HEK293 cells for replication-competent or -deficient viruses, respectively (see also **section 10.3.5**).

### 10.3.1. Preparation of Virus DNA and Transfection

6 µg of modified pVK plasmid containing the full adenovirus genome was digested with PacI overnight at 37°C in 150 µl. 2 µl were used for a control agarose gel separation, to check the excision of a 3kb fragment. The linearized DNA was precipitated by adding 3.5x volumes of Isopropanol. After centrifugation at 13,000 rpm for 20 min at 4°C, 3.3x volumes of EtOH (70%) were added and samples

were centrifuged again with 13,000 rpm for 10 min at 4°C. The DNA was resuspended in 30 µl bi-distilled water. 2500 ng of linearized DNA was mixed with 250 µl of OptiMEM and 1 µl of Plus Reagent (Solution A) and incubated for 15 min at room temperature. Another 250 µl of OptiMEM was supplied with 20 µl of Lipofectamine (Invitrogen) (Solution B) and incubated for 15 min as well. Solutions A and B were mixed and incubated for another 20 min at room temperature.
The day before transfection, 1.5 x $10^6$ A549 cells were seeded in a T25 flask. Prior to transfection, the cells were washed once with PBS, 250 µl OptiMEM were added, the transfection solution was added, and incubated for 4 hours. Then, the transfection solution was removed and 5 ml of DMEM/2% were added.

### 10.3.2. Virus Propagation

After transfection (see **section 10.3.1**), half of the medium in the T25 flask was removed every two days and replenished with fresh medium. This was repeated until a cytopathic effect was observed. When cells were lysed, cells and supernatant were harvested and subjected to three freeze-thaw cycles. The cell debris was removed by centrifugation at 13,000 rpm for 10 min at 4°C. From the obtained 5 ml of virus-containing medium, 4 x 1 ml were aliquoted and frozen at -80°C. 1 ml was distributed on one 14-cm plate with A549 cells (70% confluent) in DMEM/2%. After 48 hours, when cells were detached, the cells were harvested in 5 ml of supernatant and the described freeze-thaw cycle was repeated. In the next steps the amount of plates used for infection was scaled up to 5 x and finally to 20 x 10-cm plates, following the same infection and harvesting procedure as described above. 48 hours-post infection of 20 plates of A549 cells, the cells were again harvested in 5 ml of supernatant, freeze-thawed three times, and the obtained 5 ml of virus solution were used for purification.
The 48 hour post-infection time point for harvesting the infected A549 cells was crucial. The cells had detached, but the virus was not released. However, for the viruses containing two transgenes, a longer replication cycle was observed and the harvesting time point was delayed to 3 days post-infection.

### 10.3.3. Virus Purification

Two ultracentrifuge tubes (Herolab, Wiesloch) were prepared for density centrifugation. A gradient was loaded containing 3 ml of CsCL, 1.4 g/$cm^3$ at the bottom, 5ml of CsCl 1.27 g/$cm^3$ on top and finally 2.5 ml of the virus solution was added. The tubes were centrifuged (Sorvall WX Ultra 80, Thermo Scientific, Schwerte) for 4h at 32,000 U at 4°C.
Afterwards, the viral band was harvested and purified using a PD-10 column (GE Healthcare, Little Chalfont, UK). Prior to the purification steps, the column was equilibrated with 25 ml of PBS. The harvested viral band was filled up to 2.5 ml with PBS and applied on the column. Another 500 µl of PBS was added. All the throw-flow liquid up to this point was discarded. The virus was eluted with 2 ml PBS and collected in a tube containing 200 µl of glycerol. The virus was mixed with the glycerol, aliquoted, and stored at –80°C.

### 10.3.4. OD260 Measurement for Physical Viral Particle Determination

To determine the physical viral particles concentration, the virus was diluted 1:5, 1:10 and 1:20 in viral lysis buffer, containing 0.5% SDS. The viruses were inactivated by incubation at 56°C for 10 min. Then, OD260 was measured at 260 nm using a NanoDrop ND-1000 UV/VIS spectrophotometer

(Peqlab, Erlangen) and the viral particles concentration was calculated by using the formula as reported by [240, 241]: vp/ml = OD260 x 20 x viral dilution x 1.1 x $10^{12}$.

### 10.3.5. 50% Tissue Culture Infectious Dose 50 ($TCID_{50}$) Assay

In order to determine infectious viral particle titers, the tissue culture dose 50 ($TCID_{50}$) assay was performed. 10,000 A549 cells or HEK293 cells were plated in 96-wells in 100 µl DMEM/2%. A549 cells were used for replication-competent viruses. HEK293 cells were used for replication-deficient viruses, as they are stably transformed with sheared Ad5 genome and therefore substitute the missing *E1* gene and allow viral replication. The day after plating, the cells were infected with 100 µl of serial diluted virus in 10-fold replicates. The virus was diluted $10^{-5}$ to $10^{-12}$ $TCID_{50}$/cell in DMEM/2%. On each plate, the remaining wells were used as uninfected controls. 14 days post-infection, the number of wells showing cytopathic effect through plaque formation was assessed by bright-field microscopy. The $TCID_{50}$ titer was calculated by the reported formula [242]:

$TCID_{50}/ml = 10^{1 + 1 \times (\text{sum of positive wells}-0.5)}$

The ratios of physical virus particles to infectious virus particles were between 13 and 65. This ratio provided information about the quality of the virus preparation. High ratio numbers mean that a higher amount of physical viral particles is needed to obtain the same number of infectious viral particles compared to lower ratio numbers. The calculations for infections were mostly based on the $TCID_{50}$ titers. However, high amounts of physical, but uninfectious viral particles can themselves induce a cytopathic effect. Therefore, in order to compare different viruses tested in one experiment, the ratios should be similar. Therefore, if the ratio exceeded 80, the virus preparation was repeated.

### 10.3.6. Genome and Transgene Expression Verification of Generated Viruses

Virus genome organization was verified by control PCRs. *E1A*, *E3*, fiber, the deletion of *E1B19K*, and the inserted transgenes *GFP* and *TRAIL* were analyzed (see for pipetting scheme **section 10.1.1** and for primer sequences Materials **section 9.11**). Gene modifications were verified by PCRs under the following conditions:

| Analyzed modification/ transgene insertion | Primers | Annealing temperature | Fragment sizes | |
|---|---|---|---|---|
| E1AΔ24 | Delta 24<br>SeqITR | 60°C | Wild type E1A:<br>Δ24: | 630 bp<br>no band |
| ΔE1B19K | E1B-rev<br>SeqITR | 60°C | Wild type E1B19K:<br>ΔE1B19K: | 1829 bp<br>1684 bp |
| ΔE3 | E3-rev<br>E3-for | 60°C | Wild type E3:<br>ΔE3: | 2836 bp<br>156/207 bp |
| 3 knob | 3knob<br>Seq Mfe Fiber | 62°C | | 489 bp |
| 5 knob | 5knob<br>Seq Mfe Fiber | 62°C | | 521 bp |
| GFP | GFP-N1 f2<br>3' pShuttle rv | 58°C | | 1007 bp |
| TRAIL | hTRAIL fw<br>hTRAIL rv2 | 58°C | | 858 bp |

Further, transgene expression was confirmed by luciferase assay (see **section 10.5.1**), visual GFP expression, or immunoblots (GFP, TRAIL, FCU1, see **section 10.5.2 - 10.5.6**)

## 10.4. Recombinant Virus Techniques

### 10.4.1. Transduction with Replication-Deficient Capsid-Modified Viruses

Cells were seeded in 48-well plates (50,000 for established pancreatic cell lines, 25,000 for low-passage pancreatic cell cultures, and 10,500 cells for MSCs) in normal maintenance medium. 24 hours later, they were transduced in 100 µl DMEM/2% or 100 µl NH medium with replication deficient viruses (established and low-passage pancreatic cancer cells: 100 vp/cell, MSCs: 1,000 vp/cell) in triplicates. 2 hours post-infection, cells were washed twice with PBS and 500 µl DMEM/5% or 500 µl NH medium were added. 48 hours post-infection, cells were lysed for a subsequent luciferase activity assay (see **section 10.5.1**).

### 10.4.2. Burst Assay in MSCs

10,500 MSCs were seeded in 48-well plates in 500 µl NH medium. 24 hours later, the cells were infected with a virus titer of 1,000 $TCID_{50}$/cell in 100 µl NH medium in triplicates. 2 hours post-infection cells were washed twice with PBS and 500 µl NH medium were added to each well. After 2, 4, 6, and 8 days supernatant and cells were harvested separately. The total 500 µl of supernatant were harvested and centrifuged at 1,000 rpm for 10 min to remove residual, floating cells. Supernatant and cell pellet were separated. The remaining cells in the well were scraped and reunited with the floating cells obtained before. The cells were washed twice with PBS and finally resuspended in 250 µl NH medium. Cells and supernatant were freeze-thawed three times. Cell samples were subsequently centrifuged at 15,000 rpm for 10 min to precipitate cell debris. Total virus amount in cells and supernatant were titrated by $TCID_{50}$ assay on A549 cells as described in **section 10.3.5**.

### 10.4.3. Cytotoxicity Assay in MSCs

10,500 MSCs were seeded in 48-well plates in 500 µl in NH medium. 24 hours later the cells were infected with serial dilutions between 100 and 0.001 $TCID_{50}$/cell of virus in 100 µl NH medium. After incubation at 37°C for 2 hours, 400 µl fresh NH medium were added. 14 days post-infection, the plates were stained with a crystal violet solution. The medium was removed and 50 µl of crystal violet solution was added to each well. Plates were incubated at room temperature for 30 min and subsequently the plates were rinsed under tub water until all unbound dye was removed. The plates were dried and scanned using a Perfection V500 Photo scanner (Epson, Meerbusch).

### 10.4.4. Infection of MSCs with Ad-GFP with and without Polybrene

10,500 MSCs were plated in a 48-well plate in 500 µl NH medium. 24 hours later, the cells were infected with Ad-GFP between 100 and 10,000 $TCID_{50}$/cell in 100 µl of NH medium or NH medium containing 8 ng/ml Polybrene (Sigma-Aldrich, Taufkirchen). 2 hours post-infection, the medium was removed and 500 µl of NH medium were added. The cells were incubated 48 hours at 37°C. Afterwards, the medium was aspirated, 200 µl of 4% Formaldehyde in PBS was added to each well, and incubated for 10 min at room temperature for fixation. Then, 200 µl of 0.5% (v/v) Triton X-100 in

bi-distilled water was added for permeabilization and incubated for 10 min at room temperature. Finally, the cells were stained with 200 µl Hoechst 33258 (1:2000 in bi-distilled water) for 10 min at room temperature. The dye was removed, the wells were washed once with 500 µl of bi-distilled water, and 500 µl of bi-distilled water/well were added. Fluorescence pictures were taken using a BIOREVO BZ-9000 fluorescence microscope (KEYENCE, Neu-Isenburg).
In pre-experiments, MSCs were transduced with Ad-GFP in medium containing 2, 4, 8, and 16 ng/ml Polybrene. 8 ng/ml was determined as the lowest concentration mediating optimized transduction.

### 10.4.5. Burst Assay in MSCs with Medium Containing Polybrene

10,500 MSCs were seeded in 48-well plates in 500 µl NH medium. 24 hours later, the cells were infected with a virus titer of 1,000 $TCID_{50}$/cell in 100 µl NH medium or with 100 $TCID_{50}$/cell in 100 µl NH medium containing 8 ng/ml Polybrene in triplicates.
In order to obtain the input titer two hours post infection, the supernatant was removed, cells were washed twice with PBS, scraped, transferred to a new tube, centrifuged, and resuspended in 250 µl NH medium. The wells, which were meant to be harvested at day 4 post-infection, were washed twice with PBS at 2 hours post-infection and 500 µl of NH medium were added. Cells and supernatant samples at day 4 were harvested as described in **section 10.4.2**. The samples were freeze-thawed three times. Cell samples were subsequently centrifuged at 15,000 rpm for 10 min to precipitate cell debris. Total virus amount in cells and supernatant were titrated by $TCID_{50}$ assay on A549 cells as described in **section 10.3.5**.

### 10.4.6. Infection of MiaPaCa-2 with Supernatant from Infected MSCs for XTT assay

10,000 MiaPaCa-2 cells were plated in 96-well plates in 100 µl DMEM/5%. 24 hours later the medium was removed and the cells were infected either with titrated virus-containing supernatant from infected MSC or purified virus. From the burst assay (see **section 10.4.5**), supernatant from Donor 4/day 4 were titrated by $TCID_{50}$ assay on A549 and then serial dilutions between 1.0 and 0.0001 $TCID_{50}$/cell in 100 µl DMEM/2% were used for infection of MiaPaCa-2. Further, MiaPaCa-2 cells were infected with the same $TCID_{50}$ titers of purified virus. All infections were done in triplicates.

### 10.4.7. Migration Assay of Virus-Infected MSCs

**Staining**

24 hours before the start of migration, the MSCs were stained red with PKH26 red-fluorescent dye (Sigma-Aldrich, Taufkirchen) in suspension. 4 x $10^6$ MSCs were washed one in serum-free medium, centrifuged with 800 rpm for 5 min and then resuspended in 750 µl Diluent C (provided by the kit). The cells were immediately mixed with dye solution (3 µl dye in 750 µl Diluent C) and incubated for 2 min. Then, 1.5 ml of FBS were added. After centrifugation (800 rpm, 5 min), the cells were resuspended in DMEM/10%, washed once in DMEM/10%, and were finally resuspended in DMEM/2%FBS. The cells were counted and 7.6 x $10^5$ cells/well were plated in 5 wells of a 12-well plate.

**Infection / Start Migration**

The next day, the 5 wells with MSCs were infected with 2,500 $TCID_{50}$/cell in 2 ml DMEM/2% with either one of the modified virus or mock-infected with DMEM/2%. After 2 hours of incubation at 37°C, the cells were washed twice with PBS. The cells were trypsinized and washed with DMEM/2%. The cells from each of the 5 infections (4 viruses + 1 mock) were resuspended in 1.8 ml of DMEM/2%.

For analysis of migration of virus-transduced MSCs, CytoSelect™ 24-Well Cell Migration Assay (12 µm, Colorimetric Format, Cell Biolabs, San Diego, CA) was used. Transwells were prepared by pipetting 500 µl DMEM/10% into the lower well of the 24-well plate. 1 x $10^5$ MSCs in 300 µl DMEM/2% were added into the upper well. As controls, 0.5 x $10^5$ MSCs/well for every infection condition (4 viruses + 1 mock) were plated in a 24-well plate. All transwell and control conditions were done in triplicates.

**Stop Migration / Fluorescence Pictures**

38 hours after the start of migration, the cells from the upper side of the transwell membrane were scraped with a cotton swab. Fluorescent pictures of the migrated cells at the lower side of the membrane were taken with a BIOREVO BZ-9000 fluorescence microscope (KEYENCE, Neu-Isenburg). Additionally, fluorescent images of the 24-well controls were taken. For all insert and control well samples, three images were taken following an identical pattern.

**Membrane Staining**

The transwell membranes were stained with crystal violet as described in the manual and bright-field pictures were taken. The membranes were incubated for 10 min with 400 µl of the staining solution. Afterwards, the inserts were washed in a beaker of water and were air-dried. Bright-field pictures of the crystal violet stained, migrated cells on the lower side of the transwell membranes were taken with a BIOREVO BZ-9000 fluorescence microscope (KEYENCE).

Each insert was transferred to a clean well and 200 µl of extraction solution were added. The inserts were incubated for 10 min at room temperature. Afterwards, 100 µl of the extracted solutions were transferred to a new 96-well plate and the dye intensity was measured at OD560 with a SPECTROstar Nano microplate reader (BMG Labtech, Ortenberg). The means of measured OD 560 values of the triplicates of each of the 5 conditions (4 viruses + mock) were blotted.

### 10.4.8. Infection of MiaPaCa-2 for Western blot Sample Generation

50,000 MiaPaCa-2 cells were plated in 6-wells in 3 ml DMEM/5%. 24 hours later transduced with 10 $TCID_{50}$/cell of the respective virus in 1 ml DMEM/2%. 2 hours post-infection 2 ml of medium containing 5% were added. 48 hours post-infection cells were scraped and centrifuged (800 rpm, 5 min). Preparation of cell lysates is further described in **sections 10.5.2** and **10.5.3**.

### 10.4.9. Virus Infection Testing AraC as Virus Genome Replication Inhibitor

50,000 A549 cells were seeded in DMEM/2% in 500 µl in 48-wells. One day later, they were transfected with 100 $TCID_{50}$/cell in DMEM/2% in 100 µl. The infection was stopped two hours later by adding DMEM/5% or DMEM/5% containing 25 µg/ml AraC. AraC was replenished every 12 hours by adding AraC into the wells, without changing the medium. 30 hours post-infection, GFP was monitored by fluorescence imaging using Leica DFC 350 FX (Leica Microsystems, Wetzlar).

### 10.4.10. Cytotoxicity Assay in Established and Low-Passage Pancreatic Cancer Cells

50,000 (established pancreatic cancer cells) or 25,000 cells (low-passage pancreatic cancer cultures) were seeded in 48-well plates in 500 µl in the respective medium (MiaPaCa-2, BxPc-3: DMEM/5%; Panc-1, AsPc-1: RPMI/5%; JoPaca-1: IMDM/10%; PacaDD-159: PacaDD medium). 24 hours later the cells were infected with serial diluted virus between 100 and 0.001 $TCID_{50}$/cell in media containing 2%FBS. After incubation at 37°C for 2 hours, 400 µl fresh medium were added (MiaPaCa-2, BxPc-3: DMEM/5%; Panc-1, AsPc-1: RPMI/5%; JoPaca-1: IMDM/10%; PacaDD-159: PacaDD medium). 5 days prior to staining 5-FC and 5-FU at final concentration between 10 mM and 0.1 µM were added in 100

µl DMEM/2%. 100 µl medium were added to untreated wells for volume adjustment. 6 days (MiaPaCa-2 and AsPc-1), 8 days (BxPc-3 and Panc-1), or 12 days (JoPaca-1, PacaDD-159) post-infection plates were stained with crystal violet as described in **section 10.4.3**.

#### 10.4.11. Infection of Low-Passage Pancreatic Tumor Cell Lines with Ad-GFP

25,000 JoPaca-1 and PacaDD-159 cells were seeded in 500 µl IMDM/2% and PacaDD medium, respectively. 24 hours post-plating, cells were infected with serial dilutions between 1 and 1,000 $TCID_{50}$/cell of Ad-GFP in IMDM/2% or PacaDD medium. 2 hours post-infection, the infection solution was removed and 500 µl of IMDM/10% or PacaDD medium were added. 48 hours post-infection, the medium was aspirated, 200 µl of 4% Formaldehyde in PBS was added to each well, and incubated for 10 min at room temperature for fixation. Then, 200 µl of 0.5% (v/v) Triton X-100 in bi-distilled water was added for permeabilization and incubated for 10 min at room temperature. Finally, the cells were stained with 200 µl Hoechst 33258 (1:2000 in bi-distilled water) for 10 min at room temperature. The staining solution was removed and the wells were washed once with 500 µl of bi-distilled water. Fluorescence pictures were taken using a BIOREVO BZ-9000 fluorescence microscope (KEYENCE, Neu-Isenburg).

#### 10.4.12. Spheroid Infection and GFP Monitoring

5,000 MiaPaCa-2 cells were seeded in a round-bottom 96-well plate in 100 µl DMEM/2%FBS/1%HEPES containing 0.5% methylcellulose. The spheroids were provided by the group of Ingrid Herr (University Hospital Heidelberg). 24 hours post-seeding, the cells had cumulated at the bottom of the well and only wells with proper formation of a single spheroid were used for infection. The spheroids were infected with virus in 100 µl DMEM/2%FBS/1%HEPES or mock-infected with DMEM/2%FBS/1%HEPES in triplicates. The virus spread in the spheroids was monitored via observation of GFP expression. Pictures were taken 0, 2, 4, 6, and 8 day post-infection with a BIOREVO BZ-9000 microscope (KEYENCE, Neu-Isenburg).

### 10.5. Biochemical and Immunological Protein Methods

#### 10.5.1. Luciferase Assay

48 hours post-infection (see **section 10.4.1**), medium was removed, and cells were washed once with PBS. 100 µl of cell culture lysis buffer (Promega, Madison, WI) was added and incubated at room temperature for 20 min. 20 µl (established pancreatic cancer cell lines) or 50 µl (low-passage pancreatic cancer cultures and MSCs) of cell lysates were transferred to a solid white 96-well flat-bottom polystyrene microplate (Thermo Scientific Nunc, Schwerte). Luciferase activity in relative luminescence units (RLU) was determined by using a reporter assay system (Promega). Utilizing the injection system of a Synergy2 microplate reader (BioTek, Bad Friedrichshall), 50 µl of luciferase substrate were added. After a delay of 2 sec, luciferase activity was measured for 10 sec. Wells containing only lysis buffer were used as background controls.

### 10.5.2. Preparation of Protein Lysates for TRAIL, FCU1, and GFP Immunoblots

48 hours post-infection (see **section 10.4.8**) cells were scraped, transferred to a tube, centrifuged (800 rpm, 5 min), and the pellets were subsequently lysed in 100 µl of RIPA buffer. After incubation on ice for 30 min, the samples were centrifuged again (15,000 rpm, 5 min) and the supernatant transferred to a new tube.

### 10.5.3. Preparation of Protein Lysates for Fiber/Hexon Immunoblots

For generation of protein lysates for fiber/hexon protein detection, the cells were scraped, transferred to a tube, centrifuged (800 rpm, 5 min), and subsequently 100 mM tris (stock 1 M) was added. The tubes were shaken for 30 min at 4°C. Subsequently, 3 µl of 5 M NaCl and the samples were centrifuged (5 min, 1,000 rpm, 4°C). The supernatants was transferred to new tubes and the samples were strictly kept at 4°C for further steps.

### 10.5.4. Measuring Protein Concentration

Protein concentration in the protein lysate samples were determined by the Bradford method. The lysate samples were diluted 1:4 in bi-distilled water. For a standard curve, a series of 10-fold dilutions of BSA was prepared ranging from 1.0 to 0.1 µg/µl.

In a semi-micro F-bottom cuvette (greiner bio-one, Frickenhausen) the diluted samples were mixed with 100 µl of Solution A (Dc Protein Assay, Bio-Rad, Munich) and vortexed. Next, 800 µl of Solution B were added, vortexed, and the cuvettes were incubated for 30 min at room temperature. Protein concentrations were measured at 750 nm by using a 4050 Ultrospec II UV/Vis Spectrophotometer (LKB Biochrom, Cambridge, UK). The protein concentrations of the samples were calculated based on the standard curve.

### 10.5.5. SDS PAGE

Lysates containing 30 µg (fiber/hexon) or 50 µg (others) total protein were mixed with 4x SDS sample buffer. Proteins were incubation at 96°C for 10 min for denaturation. After cooling, the samples were shortly centrifuged. They were loaded on a polyacrylamide gels comprised of a 12.5% separating gel and a 4% stacking gel. For a size standard, 5 µl of the PageRuler™ Prestained Protein ladder were added in a separate lane on the same gel. Electrophoresis was performed in 1x running buffer at 100 V until the bromophenol blue front had reached the bottom of the gel or, for proteins with large sizes like fiber/hexon, until the marker bands corresponding to the expected sizes had reached the middle of the gel.

### 10.5.6. Western Blot Analysis

After protein separation, the acrylamide gel was stacked with a nitrocellulose membrane between Whatman filter papers (Whatman, Dassel) in a wet blot chamber (Bio-Rad, Munich). All components were soaked in 1x transfer buffer before. The proteins were allowed to be transferred to the nitrocellulose membrane for 1 hour at 0.8 mA/cm$^2$.

After blotting, the membrane was incubated in Western blot blocking solution overnight at 4°C (for y-CD western blot) or for 1 hour at room temperature (all others) on a rocking platform. The blot was afterwards washed three times for 10 min with Western blot washing buffer. Afterwards membranes were incubated with primary antibody diluted in Western blot washing buffer for 1 hour at room

temperature. For dilutions see Materials **section 9.10**. Afterwards, membranes were again washed three times for 10 min with Western blot washing buffer and then incubated with HRP-coupled secondary antibody diluted in Western blot washing buffer for 1 hour at room temperature. For dilutions see Materials **section 9.10**. Finally, the blots were washed again as described above and the chemoluminometric reaction was initiated by adding Pierce ECL Western Blotting Substrate (Thermo Fisher Scientific, Schwerte). Super RX Fuji Medical X-Ray Films (Fujifilm Corporation, Tokyo, Japan) were exposed to the blots for various time spans and subsequently developed using a Curix 60 processor (AGFAR HealthCare, Bonn, Germany)
Subsequently, each membrane was subjected to staining for β-actin as loading control. Therefore, the membranes were washed three times with Western blot washing buffer and subsequently incubated with diluted antibody against β-actin for 1 hour at room temperature. Afterwards, the procedure was followed as described above.

### 10.5.7. XTT Assay

Infected MiaPaCa-2 cells (see **section 10.4.6**) were analyzed 8 days post-infection by XTT assay. The assay was performed using the Cell Titer 96® AQueous One Solution Cell Proliferation Assay System (Promega, Madison, WI).
The reagent solution was prepared as described in the manufacturer's protocol by mixing buffer and substrate solution. 25 µl of the mix were added to each well and the plates were incubated for 2 hours at 37°C in a humidified atmosphere. Afterwards, the plates were read out at 477 nm and 620 nm (reference wavelength). Background absorption measured in wells with medium only was subtracted from each value. Further, values measured at 620 nm were subtracted from values at 477 nm for each well. Blots showing measured absorbance units were generated. Mock-infected cells were used as control for maximal cell vitality.

### 10.5.8. LDH Assay

Spheroids were infected in triplicates with the modified viruses or mock-infected as described in **section 10.4.12** and cultured over 8 days. After 4 and 6 days an LDH assay was performed using the CytoTox96® Non-Radioactive Cytotoxicity Assay (Promega, Madison, WI). At day 4 and day 6 post-infection, 30 µl of spheroid supernatant was withdrawn from each infected and mock-infected well. After every withdrawal, the volume was replenished with 30 µl DMEM/2%FBS/1%HEPES.
For every time point, 3 additional mock-infected spheroids were used as positive complete lysis control. To these complete lysis control wells, 10 µl of lysis solution buffer supplied by the assay kit was added and the cells were incubated for 30 min at 37°C to allow complete lysis. Then 30 µl of of the total lysis control as well as 30 µl of supernatant from the infected and mock-infected spheroids were transferred to a 96-well plate. Further, 3 wells containing only medium were used for background absorbance determination. 30 µl of substrate (supplied by the kit) were added to each well as described in the manufacturer's protocol and incubated for 30 min at room temperature. Afterwards, 30 µl of stop solution was added and absorbance measured at 592 nm. The background values were subtracted from all values and the percentage of dead cells were calculated by setting total lysis control as 100% dead cells.

### 10.5.9. Spheroid size determination

Spheroid sizes were determined using the program Histo®, which was generated and provided by Dr. Wolfgang Groß (group Ingrid Herr, University Hospital Heidelberg). The bright-field pictures taken from infected or mock-infected spheroids at day 6 were loaded and an “Area, free hand border” drawn around the outer spheroid border. By subsequent selection of the inner area, the program determined the spheroid surface area in pixels. Area determinations were done for three spheroids for every condition and means and standard deviations were calculated.

## 10.6. Statistical Analysis

All statistical analyses were performed using GraphPad Prism 5.0 software (GraphPad Software, La Jolla, CA). One-way analysis of variance (1way ANOVA) and subsequent Bonferroni’s Multiple Comparison Test was used to compare multiple means with each other.

# 11. References


1. Longley, DB, Harkin, DP, and Johnston, PG (2003). 5-fluorouracil: mechanisms of action and clinical strategies. *Nature reviews Cancer* **3**: 330-338.
2. Hegyi, P, and Petersen, OH (2013). The exocrine pancreas: the acinar-ductal tango in physiology and pathophysiology. *Reviews of physiology, biochemistry and pharmacology* **165**: 1-30.
3. Ashcroft, FM, and Rorsman, P (2012). Diabetes mellitus and the beta cell: the last ten years. *Cell* **148**: 1160-1171.
4. Siegel, R, Naishadham, D, and Jemal, A (2013). Cancer statistics, 2013. *CA: a cancer journal for clinicians* **63**: 11-30.
5. Lowy, AM, Leach, Steven D., Philip, Philip (Eds.) (2008). Molecular Genetics of Pancreatic Cancer. *Pancreatic Cancer*.
6. Hezel, AF, Kimmelman, AC, Stanger, BZ, Bardeesy, N, and Depinho, RA (2006). Genetics and biology of pancreatic ductal adenocarcinoma. *Genes & development* **20**: 1218-1249.
7. Johns Hopkins Medicine, U (2014). Types of Pancreas Tumors.
8. Institute, NC (2014). Pancreatic Neuroendocrine Tumors (Islet Cell Tumors) Treatment. vol. 2014.
9. Almoguera, C, Shibata, D, Forrester, K, Martin, J, Arnheim, N, and Perucho, M (1988). Most human carcinomas of the exocrine pancreas contain mutant c-K-ras genes. *Cell* **53**: 549-554.
10. Scarpa, A*, et al.* (1993). Pancreatic adenocarcinomas frequently show p53 gene mutations. *The American journal of pathology* **142**: 1534-1543.
11. Whelan, AJ, Bartsch, D, and Goodfellow, PJ (1995). Brief report: a familial syndrome of pancreatic cancer and melanoma with a mutation in the CDKN2 tumor-suppressor gene. *The New England journal of medicine* **333**: 975-977.
12. Tempero, MA*, et al.* (2010). Pancreatic adenocarcinoma. *Journal of the National Comprehensive Cancer Network : JNCCN* **8**: 972-1017.
13. Raimondi, S, Maisonneuve, P, and Lowenfels, AB (2009). Epidemiology of pancreatic cancer: an overview. *Nature reviews Gastroenterology & hepatology* **6**: 699-708.
14. American Cancer Society, I (2014). Treating pancreatic cancer by stage.
15. Thota, R, Pauff, JM, and Berlin, JD (2014). Treatment of metastatic pancreatic adenocarcinoma: a review. *Oncology (Williston Park)* **28**: 70-74.
16. Burris, HA, 3rd*, et al.* (1997). Improvements in survival and clinical benefit with gemcitabine as first-line therapy for patients with advanced pancreas cancer: a randomized trial. *Journal of clinical oncology : official journal of the American Society of Clinical Oncology* **15**: 2403-2413.
17. Kizilbash, SH, Ward, KC, Liang, JJ, Jaiyesimi, I, and Lipscomb, J (2014). Survival outcomes in patients with early stage, resected pancreatic cancer - a comparison of gemcitabine- and 5-fluorouracil-based chemotherapy and chemoradiation regimens. *International journal of clinical practice*.
18. Kvols, LK (2005). Radiation sensitizers: a selective review of molecules targeting DNA and non-DNA targets. *Journal of nuclear medicine : official publication, Society of Nuclear Medicine* **46 Suppl 1**: 187S-190S.
19. Rao, S, and Cunningham, D (2002). Advanced pancreatic cancer--5 years on. *Annals of oncology : official journal of the European Society for Medical Oncology / ESMO* **13**: 1165-1168.
20. Nowell, PC (1976). The clonal evolution of tumor cell populations. *Science* **194**: 23-28.
21. Reya, T, Morrison, SJ, Clarke, MF, and Weissman, IL (2001). Stem cells, cancer, and cancer stem cells. *Nature* **414**: 105-111.
22. Short, JJ, and Curiel, DT (2009). Oncolytic adenoviruses targeted to cancer stem cells. *Mol Cancer Ther* **8**: 2096-2102.
23. Dorado, J, Lonardo, E, Miranda-Lorenzo, I, and Heeschen, C (2011). Pancreatic cancer stem cells: new insights and perspectives. *Journal of gastroenterology* **46**: 966-973.
24. Dean, M, Fojo, T, and Bates, S (2005). Tumour stem cells and drug resistance. *Nature reviews Cancer* **5**: 275-284.
25. Moore, N, and Lyle, S (2011). Quiescent, slow-cycling stem cell populations in cancer: a review of the evidence and discussion of significance. *Journal of oncology* **2011**.
26. Ribacka, C, and Hemminki, A (2008). Virotherapy as an approach against cancer stem cells. *Current gene therapy* **8**: 88-96.
27. Li, C*, et al.* (2011). c-Met is a marker of pancreatic cancer stem cells and therapeutic target. *Gastroenterology* **141**: 2218-2227 e2215.
28. Li, C*, et al.* (2007). Identification of pancreatic cancer stem cells. *Cancer research* **67**: 1030-1037.
29. Hermann, PC*, et al.* (2007). Distinct populations of cancer stem cells determine tumor growth and metastatic activity in human pancreatic cancer. *Cell stem cell* **1**: 313-323.
30. Suzuki, A, Nakauchi, H, and Taniguchi, H (2004). Prospective isolation of multipotent pancreatic progenitors using flow-cytometric cell sorting. *Diabetes* **53**: 2143-2152.
31. Hage, C*, et al.* (2013). The novel c-Met inhibitor cabozantinib overcomes gemcitabine resistance and stem cell signaling in pancreatic cancer. *Cell death & disease* **4**: e627.

32. Baccelli, I, and Trumpp, A (2012). The evolving concept of cancer and metastasis stem cells. *The Journal of cell biology* **198**: 281-293.
33. Everts, B, and van der Poel, HG (2005). Replication-selective oncolytic viruses in the treatment of cancer. *Cancer Gene Ther* **12**: 141-161.
34. Atherton, MJ, and Lichty, BD (2013). Evolution of oncolytic viruses: novel strategies for cancer treatment. *Immunotherapy* **5**: 1191-1206.
35. Garber, K (2006). China approves world's first oncolytic virus therapy for cancer treatment. *Journal of the National Cancer Institute* **98**: 298-300.
36. Robert Hans Ingemar Andtbacka, FAC, Thomas Amatruda, Neil N. Senzer, Jason Chesney, Keith A. Delman, Lynn E. Spitler, Igor Puzanov, Susan Doleman, Yining Ye, Ari M. Vanderwalde, Robert Coffin and Howard Kaufman (2013). OPTiM: A randomized phase III trial of talimogene laherparepvec (T-VEC) versus subcutaneous (SC) granulocyte-macrophage colony-stimulating factor (GM-CSF) for the treatment (tx) of unresected stage IIIB/C and IV melanoma. *Journal of Clinical Oncology* **31**: LBA9008.
37. Sheridan, C (2013). Amgen announces oncolytic virus shrinks tumors. *Nature biotechnology* **31**: 471-472.
38. Saito, Y*, et al.* (2006). Oncolytic replication-competent adenovirus suppresses tumor angiogenesis through preserved E1A region. *Cancer Gene Ther* **13**: 242-252.
39. Angarita, FA, Acuna, SA, Ottolino-Perry, K, Zerhouni, S, and McCart, JA (2013). Mounting a strategic offense: fighting tumor vasculature with oncolytic viruses. *Trends in molecular medicine* **19**: 378-392.
40. Liu, TC, Hwang, T, Park, BH, Bell, J, and Kirn, DH (2008). The targeted oncolytic poxvirus JX-594 demonstrates antitumoral, antivascular, and anti-HBV activities in patients with hepatocellular carcinoma. *Mol Ther* **16**: 1637-1642.
41. Bartlett, DL*, et al.* (2013). Oncolytic viruses as therapeutic cancer vaccines. *Molecular cancer* **12**: 103.
42. Liikanen, I*, et al.* (2013). Oncolytic adenovirus with temozolomide induces autophagy and antitumor immune responses in cancer patients. *Mol Ther* **21**: 1212-1223.
43. Kaufman, HL, Kim, DW, DeRaffele, G, Mitcham, J, Coffin, RS, and Kim-Schulze, S (2010). Local and distant immunity induced by intralesional vaccination with an oncolytic herpes virus encoding GM-CSF in patients with stage IIIc and IV melanoma. *Annals of surgical oncology* **17**: 718-730.
44. Heo, J*, et al.* (2013). Randomized dose-finding clinical trial of oncolytic immunotherapeutic vaccinia JX-594 in liver cancer. *Nat Med* **19**: 329-336.
45. Modrow, S, Falke, D, Truyen, U, and Schätzl, H (2010). *Molekulare Virologie*, Spektrum Akademischer Verlag: Heidelberg.
46. Wang, H*, et al.* (2011). Desmoglein 2 is a receptor for adenovirus serotypes 3, 7, 11 and 14. *Nat Med* **17**: 96-104.
47. Gaggar, A, Shayakhmetov, DM, and Lieber, A (2003). CD46 is a cellular receptor for group B adenoviruses. *Nat Med* **9**: 1408-1412.
48. Roelvink, PW*, et al.* (1998). The coxsackievirus-adenovirus receptor protein can function as a cellular attachment protein for adenovirus serotypes from subgroups A, C, D, E, and F. *Journal of virology* **72**: 7909-7915.
49. Vetrini, F, and Ng, P (2010). Gene therapy with helper-dependent adenoviral vectors: current advances and future perspectives. *Viruses* **2**: 1886-1917.
50. Grana, X, Garriga, J, and Mayol, X (1998). Role of the retinoblastoma protein family, pRB, p107 and p130 in the negative control of cell growth. *Oncogene* **17**: 3365-3383.
51. Whyte, P*, et al.* (1988). Association between an oncogene and an anti-oncogene: the adenovirus E1A proteins bind to the retinoblastoma gene product. *Nature* **334**: 124-129.
52. Martin, ME, and Berk, AJ (1998). Adenovirus E1B 55K represses p53 activation in vitro. *Journal of virology* **72**: 3146-3154.
53. Yew, PR, and Berk, AJ (1992). Inhibition of p53 transactivation required for transformation by adenovirus early 1B protein. *Nature* **357**: 82-85.
54. Yin, XM, Oltvai, ZN, and Korsmeyer, SJ (1994). BH1 and BH2 domains of Bcl-2 are required for inhibition of apoptosis and heterodimerization with Bax. *Nature* **369**: 321-323.
55. Han, J, Sabbatini, P, Perez, D, Rao, L, Modha, D, and White, E (1996). The E1B 19K protein blocks apoptosis by interacting with and inhibiting the p53-inducible and death-promoting Bax protein. *Genes & development* **10**: 461-477.
56. Elsing, A, and Burgert, HG (1998). The adenovirus E3/10.4K-14.5K proteins down-modulate the apoptosis receptor Fas/Apo-1 by inducing its internalization. *Proceedings of the National Academy of Sciences of the United States of America* **95**: 10072-10077.
57. Chiou, SK, and White, E (1997). p300 binding by E1A cosegregates with p53 induction but is dispensable for apoptosis. *Journal of virology* **71**: 3515-3525.
58. Putzer, BM, Stiewe, T, Parssanedjad, K, Rega, S, and Esche, H (2000). E1A is sufficient by itself to induce apoptosis independent of p53 and other adenoviral gene products. *Cell death and differentiation* **7**: 177-188.
59. Tollefson, AE, Scaria, A, Hermiston, TW, Ryerse, JS, Wold, LJ, and Wold, WS (1996). The adenovirus death protein (E3-11.6K) is required at very late stages of infection for efficient cell lysis and release of adenovirus from infected cells. *Journal of virology* **70**: 2296-2306.
60. Freeman, AE, Black, PH, Vanderpool, EA, Henry, PH, Austin, JB, and Huebner, RJ (1967). Transformation of primary rat embryo cells by adenovirus type 2. *Proceedings of the National Academy of Sciences of the United States of America* **58**: 1205-1212.

61. Graham, FL, and van der Eb, AJ (1973). Transformation of rat cells by DNA of human adenovirus 5. *Virology* **54**: 536-539.
62. Yamamoto, M, and Curiel, DT (2010). Current issues and future directions of oncolytic adenoviruses. *Mol Ther* **18**: 243-250.
63. Liu, TC, Galanis, E, and Kirn, D (2007). Clinical trial results with oncolytic virotherapy: a century of promise, a decade of progress. *Nature clinical practice Oncology* **4**: 101-117.
64. Hemmi, S, Geertsen, R, Mezzacasa, A, Peter, I, and Dummer, R (1998). The presence of human coxsackievirus and adenovirus receptor is associated with efficient adenovirus-mediated transgene expression in human melanoma cell cultures. *Hum Gene Ther* **9**: 2363-2373.
65. Korn, WM*, et al.* (2006). Expression of the coxsackievirus- and adenovirus receptor in gastrointestinal cancer correlates with tumor differentiation. *Cancer Gene Ther* **13**: 792-797.
66. Kanerva, A*, et al.* (2002). Targeting adenovirus to the serotype 3 receptor increases gene transfer efficiency to ovarian cancer cells. *Clin Cancer Res* **8**: 275-280.
67. Krasnykh, VN, Mikheeva, GV, Douglas, JT, and Curiel, DT (1996). Generation of recombinant adenovirus vectors with modified fibers for altering viral tropism. *Journal of virology* **70**: 6839-6846.
68. Volk, AL*, et al.* (2003). Enhanced adenovirus infection of melanoma cells by fiber-modification: incorporation of RGD peptide or Ad5/3 chimerism. *Cancer biology & therapy* **2**: 511-515.
69. Liu, Y, Ye, T, Sun, D, Maynard, J, and Deisseroth, A (2004). Conditionally replication-competent adenoviral vectors with enhanced infectivity for use in gene therapy of melanoma. *Hum Gene Ther* **15**: 637-647.
70. Yamamoto, M*, et al.* (2003). Infectivity enhanced, cyclooxygenase-2 promoter-based conditionally replicative adenovirus for pancreatic cancer. *Gastroenterology* **125**: 1203-1218.
71. Whyte, P, Williamson, NM, and Harlow, E (1989). Cellular targets for transformation by the adenovirus E1A proteins. *Cell* **56**: 67-75.
72. Heise, C*, et al.* (2000). An adenovirus E1A mutant that demonstrates potent and selective systemic anti-tumoral efficacy. *Nat Med* **6**: 1134-1139.
73. Fueyo, J*, et al.* (2000). A mutant oncolytic adenovirus targeting the Rb pathway produces anti-glioma effect in vivo. *Oncogene* **19**: 2-12.
74. Bauerschmitz, GJ*, et al.* (2002). Treatment of ovarian cancer with a tropism modified oncolytic adenovirus. *Cancer research* **62**: 1266-1270.
75. Bischoff, JR*, et al.* (1996). An adenovirus mutant that replicates selectively in p53-deficient human tumor cells. *Science* **274**: 373-376.
76. Leitner, S*, et al.* (2009). Oncolytic adenoviral mutants with E1B19K gene deletions enhance gemcitabine-induced apoptosis in pancreatic carcinoma cells and anti-tumor efficacy in vivo. *Clin Cancer Res* **15**: 1730-1740.
77. Sauthoff, H, Heitner, S, Rom, WN, and Hay, JG (2000). Deletion of the adenoviral E1b-19kD gene enhances tumor cell killing of a replicating adenoviral vector. *Hum Gene Ther* **11**: 379-388.
78. Liu, TC*, et al.* (2004). An E1B-19 kDa gene deletion mutant adenovirus demonstrates tumor necrosis factor-enhanced cancer selectivity and enhanced oncolytic potency. *Mol Ther* **9**: 786-803.
79. Liu, TC*, et al.* (2005). Functional interactions of antiapoptotic proteins and tumor necrosis factor in the context of a replication-competent adenovirus. *Gene Ther* **12**: 1333-1346.
80. Oberg, D*, et al.* (2010). Improved potency and selectivity of an oncolytic E1ACR2 and E1B19K deleted adenoviral mutant in prostate and pancreatic cancers. *Clin Cancer Res* **16**: 541-553.
81. Rohmer, S*, et al.* (2009). Transgene expression by oncolytic adenoviruses is modulated by E1B19K deletion in a cell type-dependent manner. *Virology* **395**: 243-254.
82. Cherubini, G*, et al.* (2011). The oncolytic adenovirus AdDeltaDelta enhances selective cancer cell killing in combination with DNA-damaging drugs in pancreatic cancer models. *Gene Ther* **18**: 1157-1165.
83. Tollefson, AE, Ryerse, JS, Scaria, A, Hermiston, TW, and Wold, WS (1996). The E3-11.6-kDa adenovirus death protein (ADP) is required for efficient cell death: characterization of cells infected with adp mutants. *Virology* **220**: 152-162.
84. Rasheed, ZA, Matsui, W, and Maitra, A (2012). Pathology of pancreatic stroma in PDAC. In: Grippo, PJ and HG Munshi (eds). *Pancreatic Cancer and Tumor Microenvironment*: Trivandrum (India).
85. Lopez, MV*, et al.* (2009). Tumor associated stromal cells play a critical role on the outcome of the oncolytic efficacy of conditionally replicative adenoviruses. *PloS one* **4**: e5119.
86. Sauthoff, H*, et al.* (2003). Intratumoral spread of wild-type adenovirus is limited after local injection of human xenograft tumors: virus persists and spreads systemically at late time points. *Hum Gene Ther* **14**: 425-433.
87. Cattaneo, R, Miest, T, Shashkova, EV, and Barry, MA (2008). Reprogrammed viruses as cancer therapeutics: targeted, armed and shielded. *Nature reviews Microbiology* **6**: 529-540.
88. Falschlehner, C, Emmerich, CH, Gerlach, B, and Walczak, H (2007). TRAIL signalling: decisions between life and death. *The international journal of biochemistry & cell biology* **39**: 1462-1475.
89. Dimberg, LY, Anderson, CK, Camidge, R, Behbakht, K, Thorburn, A, and Ford, HL (2013). On the TRAIL to successful cancer therapy? Predicting and counteracting resistance against TRAIL-based therapeutics. *Oncogene* **32**: 1341-1350.
90. Griffith, TS, Anderson, RD, Davidson, BL, Williams, RD, and Ratliff, TL (2000). Adenoviral-mediated transfer of the TNF-related apoptosis-inducing ligand/Apo-2 ligand gene induces tumor cell apoptosis. *Journal of immunology* **165**: 2886-2894.

91. Mao, L*, et al.* (2014). Replication-competent adenovirus expressing TRAIL synergistically potentiates the antitumor effect of gemcitabine in bladder cancer cells. *Tumour biology : the journal of the International Society for Oncodevelopmental Biology and Medicine*.
92. Rivera, AA*, et al.* (2004). Mode of transgene expression after fusion to early or late viral genes of a conditionally replicating adenovirus via an optimized internal ribosome entry site in vitro and in vivo. *Virology* **320**: 121-134.
93. Quirin, C*, et al.* (2011). Selectivity and efficiency of late transgene expression by transcriptionally targeted oncolytic adenoviruses are dependent on the transgene insertion strategy. *Hum Gene Ther* **22**: 389-404.
94. Jin, F, Kretschmer, PJ, and Hermiston, TW (2005). Identification of novel insertion sites in the Ad5 genome that utilize the Ad splicing machinery for therapeutic gene expression. *Mol Ther* **12**: 1052-1063.
95. Guedan, S, Rojas, JJ, Gros, A, Mercade, E, Cascallo, M, and Alemany, R (2010). Hyaluronidase expression by an oncolytic adenovirus enhances its intratumoral spread and suppresses tumor growth. *Mol Ther* **18**: 1275-1283.
96. Lamfers, ML*, et al.* (2005). Tissue inhibitor of metalloproteinase-3 expression from an oncolytic adenovirus inhibits matrix metalloproteinase activity in vivo without affecting antitumor efficacy in malignant glioma. *Cancer research* **65**: 9398-9405.
97. Zhang, Q*, et al.* (2004). Effective gene-viral therapy for telomerase-positive cancers by selective replicative-competent adenovirus combining with endostatin gene. *Cancer research* **64**: 5390-5397.
98. Cerullo, V*, et al.* (2010). Oncolytic adenovirus coding for granulocyte macrophage colony-stimulating factor induces antitumoral immunity in cancer patients. *Cancer research* **70**: 4297-4309.
99. Cody, JJ, and Douglas, JT (2009). Armed replicating adenoviruses for cancer virotherapy. *Cancer Gene Ther* **16**: 473-488.
100. Lawrence, TS, Rehemtulla, A, Ng, EY, Wilson, M, Trosko, JE, and Stetson, PL (1998). Preferential cytotoxicity of cells transduced with cytosine deaminase compared to bystander cells after treatment with 5-flucytosine. *Cancer research* **58**: 2588-2593.
101. Miller, CR, Williams, CR, Buchsbaum, DJ, and Gillespie, GY (2002). Intratumoral 5-fluorouracil produced by cytosine deaminase/5-fluorocytosine gene therapy is effective for experimental human glioblastomas. *Cancer research* **62**: 773-780.
102. Etienne, MC*, et al.* (1995). Response to fluorouracil therapy in cancer patients: the role of tumoral dihydropyrimidine dehydrogenase activity. *Journal of clinical oncology : official journal of the American Society of Clinical Oncology* **13**: 1663-1670.
103. Koyama, F*, et al.* (2000). Adenoviral-mediated transfer of Escherichia coli uracil phosphoribosyltransferase (UPRT) gene to modulate the sensitivity of the human colon cancer cells to 5-fluorouracil. *European journal of cancer* **36**: 2403-2410.
104. Kanai, F*, et al.* (1998). Adenovirus-mediated transduction of Escherichia coli uracil phosphoribosyltransferase gene sensitizes cancer cells to low concentrations of 5-fluorouracil. *Cancer research* **58**: 1946-1951.
105. Oonuma, M*, et al.* (2002). Gene therapy for intraperitoneally disseminated pancreatic cancers by Escherichia coli uracil phosphoribosiltransferase (UPRT) gene mediated by restricted replication-competent adenoviral vectors. *International journal of cancer Journal international du cancer* **102**: 51-59.
106. Erbs, P*, et al.* (2000). In vivo cancer gene therapy by adenovirus-mediated transfer of a bifunctional yeast cytosine deaminase/uracil phosphoribosyltransferase fusion gene. *Cancer research* **60**: 3813-3822.
107. Dias, JD*, et al.* (2010). Targeted chemotherapy for head and neck cancer with a chimeric oncolytic adenovirus coding for bifunctional suicide protein FCU1. *Clin Cancer Res* **16**: 2540-2549.
108. Cohen, EE, and Rudin, CM (2001). ONYX-015. Onyx Pharmaceuticals. *Current opinion in investigational drugs* **2**: 1770-1775.
109. Hecht, JR*, et al.* (2003). A phase I/II trial of intratumoral endoscopic ultrasound injection of ONYX-015 with intravenous gemcitabine in unresectable pancreatic carcinoma. *Clin Cancer Res* **9**: 555-561.
110. Khuri, FR*, et al.* (2000). a controlled trial of intratumoral ONYX-015, a selectively-replicating adenovirus, in combination with cisplatin and 5-fluorouracil in patients with recurrent head and neck cancer. *Nat Med* **6**: 879-885.
111. Nemunaitis, J*, et al.* (2001). Intravenous infusion of a replication-selective adenovirus (ONYX-015) in cancer patients: safety, feasibility and biological activity. *Gene Ther* **8**: 746-759.
112. Reid, T*, et al.* (2002). Hepatic arterial infusion of a replication-selective oncolytic adenovirus (dl1520): phase II viral, immunologic, and clinical endpoints. *Cancer research* **62**: 6070-6079.
113. Alemany, R, Suzuki, K, and Curiel, DT (2000). Blood clearance rates of adenovirus type 5 in mice. *The Journal of general virology* **81**: 2605-2609.
114. Jonsson, MI, Lenman, AE, Frangsmyr, L, Nyberg, C, Abdullahi, M, and Arnberg, N (2009). Coagulation factors IX and X enhance binding and infection of adenovirus types 5 and 31 in human epithelial cells. *Journal of virology* **83**: 3816-3825.
115. Shayakhmetov, DM, Gaggar, A, Ni, S, Li, ZY, and Lieber, A (2005). Adenovirus binding to blood factors results in liver cell infection and hepatotoxicity. *Journal of virology* **79**: 7478-7491.
116. Smith, TA*, et al.* (2003). Receptor interactions involved in adenoviral-mediated gene delivery after systemic administration in non-human primates. *Hum Gene Ther* **14**: 1595-1604.
117. Russell, SJ, Peng, KW, and Bell, JC (2012). Oncolytic virotherapy. *Nature biotechnology* **30**: 658-670.
118. Fisher, KD, Stallwood, Y, Green, NK, Ulbrich, K, Mautner, V, and Seymour, LW (2001). Polymer-coated adenovirus permits efficient retargeting and evades neutralising antibodies. *Gene Ther* **8**: 341-348.

119. Wu, H, Dmitriev, I, Kashentseva, E, Seki, T, Wang, M, and Curiel, DT (2002). Construction and characterization of adenovirus serotype 5 packaged by serotype 3 hexon. *Journal of virology* **76**: 12775-12782.
120. Alcayaga-Miranda, F, Cascallo, M, Rojas, JJ, Pastor, J, and Alemany, R (2010). Osteosarcoma cells as carriers to allow antitumor activity of canine oncolytic adenovirus in the presence of neutralizing antibodies. *Cancer Gene Ther* **17**: 792-802.
121. Willmon, C, Harrington, K, Kottke, T, Prestwich, R, Melcher, A, and Vile, R (2009). Cell carriers for oncolytic viruses: Fed Ex for cancer therapy. *Mol Ther* **17**: 1667-1676.
122. Ahmed, AU*, et al.* (2011). A comparative study of neural and mesenchymal stem cell-based carriers for oncolytic adenovirus in a model of malignant glioma. *Molecular pharmaceutics* **8**: 1559-1572.
123. Muthana, M*, et al.* (2011). Use of macrophages to target therapeutic adenovirus to human prostate tumors. *Cancer research* **71**: 1805-1815.
124. Komarova, S, Kawakami, Y, Stoff-Khalili, MA, Curiel, DT, and Pereboeva, L (2006). Mesenchymal progenitor cells as cellular vehicles for delivery of oncolytic adenoviruses. *Mol Cancer Ther* **5**: 755-766.
125. Sonabend, AM, Ulasov, IV, Tyler, MA, Rivera, AA, Mathis, JM, and Lesniak, MS (2008). Mesenchymal stem cells effectively deliver an oncolytic adenovirus to intracranial glioma. *Stem Cells* **26**: 831-841.
126. Stoff-Khalili, MA*, et al.* (2007). Mesenchymal stem cells as a vehicle for targeted delivery of CRAds to lung metastases of breast carcinoma. *Breast cancer research and treatment* **105**: 157-167.
127. Cole, C*, et al.* (2005). Tumor-targeted, systemic delivery of therapeutic viral vectors using hitchhiking on antigen-specific T cells. *Nat Med* **11**: 1073-1081.
128. Spaeth, E, Klopp, A, Dembinski, J, Andreeff, M, and Marini, F (2008). Inflammation and tumor microenvironments: defining the migratory itinerary of mesenchymal stem cells. *Gene Ther* **15**: 730-738.
129. Hass, R, Kasper, C, Bohm, S, and Jacobs, R (2011). Different populations and sources of human mesenchymal stem cells (MSC): A comparison of adult and neonatal tissue-derived MSC. *Cell communication and signaling : CCS* **9**: 12.
130. Dwyer, RM, and Kerin, MJ (2010). Mesenchymal stem cells and cancer: tumor-specific delivery vehicles or therapeutic targets? *Hum Gene Ther* **21**: 1506-1512.
131. Apel, A*, et al.* (2009). Suitability of human mesenchymal stem cells for gene therapy depends on the expansion medium. *Experimental cell research* **315**: 498-507.
132. Pittenger, MF*, et al.* (1999). Multilineage potential of adult human mesenchymal stem cells. *Science* **284**: 143-147.
133. Barry, FP, and Murphy, JM (2004). Mesenchymal stem cells: clinical applications and biological characterization. *The international journal of biochemistry & cell biology* **36**: 568-584.
134. Hodgkinson, CP, Gomez, JA, Mirotsou, M, and Dzau, VJ (2010). Genetic engineering of mesenchymal stem cells and its application in human disease therapy. *Hum Gene Ther* **21**: 1513-1526.
135. Dvorak, HF (1986). Tumors: wounds that do not heal. Similarities between tumor stroma generation and wound healing. *The New England journal of medicine* **315**: 1650-1659.
136. Pereboeva, L, Komarova, S, Mikheeva, G, Krasnykh, V, and Curiel, DT (2003). Approaches to utilize mesenchymal progenitor cells as cellular vehicles. *Stem Cells* **21**: 389-404.
137. Loebinger, MR, Eddaoudi, A, Davies, D, and Janes, SM (2009). Mesenchymal stem cell delivery of TRAIL can eliminate metastatic cancer. *Cancer research* **69**: 4134-4142.
138. Loebinger, MR, Sage, EK, Davies, D, and Janes, SM (2010). TRAIL-expressing mesenchymal stem cells kill the putative cancer stem cell population. *British journal of cancer* **103**: 1692-1697.
139. Tang, XJ*, et al.* (2014). TRAIL-engineered bone marrow-derived mesenchymal stem cells: TRAIL expression and cytotoxic effects on C6 glioma cells. *Anticancer research* **34**: 729-734.
140. Studeny, M, Marini, FC, Champlin, RE, Zompetta, C, Fidler, IJ, and Andreeff, M (2002). Bone marrow-derived mesenchymal stem cells as vehicles for interferon-beta delivery into tumors. *Cancer research* **62**: 3603-3608.
141. Dembinski, JL*, et al.* (2010). Reduction of nontarget infection and systemic toxicity by targeted delivery of conditionally replicating viruses transported in mesenchymal stem cells. *Cancer Gene Ther* **17**: 289-297.
142. Komarova, S, Roth, J, Alvarez, R, Curiel, DT, and Pereboeva, L (2010). Targeting of mesenchymal stem cells to ovarian tumors via an artificial receptor. *Journal of ovarian research* **3**: 12.
143. Xia, X*, et al.* (2011). Mesenchymal stem cells as carriers and amplifiers in CRAd delivery to tumors. *Molecular cancer* **10**: 134.
144. Yong, RL*, et al.* (2009). Human bone marrow-derived mesenchymal stem cells for intravascular delivery of oncolytic adenovirus Delta24-RGD to human gliomas. *Cancer research* **69**: 8932-8940.
145. Treacy, O*, et al.* (2012). Adenoviral transduction of mesenchymal stem cells: in vitro responses and in vivo immune responses after cell transplantation. *PloS one* **7**: e42662.
146. Stolzing, A, Jones, E, McGonagle, D, and Scutt, A (2008). Age-related changes in human bone marrow-derived mesenchymal stem cells: consequences for cell therapies. *Mechanisms of ageing and development* **129**: 163-173.
147. Garcia-Castro, J*, et al.* (2010). Treatment of metastatic neuroblastoma with systemic oncolytic virotherapy delivered by autologous mesenchymal stem cells: an exploratory study. *Cancer Gene Ther* **17**: 476-483.
148. Conget, PA, and Minguell, JJ (2000). Adenoviral-mediated gene transfer into ex vivo expanded human bone marrow mesenchymal progenitor cells. *Experimental hematology* **28**: 382-390.
149. Hakkarainen, T*, et al.* (2007). Human mesenchymal stem cells lack tumor tropism but enhance the antitumor activity of oncolytic adenoviruses in orthotopic lung and breast tumors. *Hum Gene Ther* **18**: 627-641.
150. Miller, CR*, et al.* (1998). Differential susceptibility of primary and established human glioma cells to adenovirus infection: targeting via the epidermal growth factor receptor achieves fiber receptor-independent gene transfer. *Cancer research* **58**: 5738-5748.

151. Mizuguchi, H, Sasaki, T, Kawabata, K, Sakurai, F, and Hayakawa, T (2005). Fiber-modified adenovirus vectors mediate efficient gene transfer into undifferentiated and adipogenic-differentiated human mesenchymal stem cells. *Biochemical and biophysical research communications* **332**: 1101-1106.
152. Felix Rückert, CP (2012). Immunohistological analysis of six new primary pancreatic adenocarcinoma cell lines.
153. Fredebohm, J*, et al.* (2012). Establishment and characterization of a highly tumourigenic and cancer stem cell enriched pancreatic cancer cell line as a well defined model system. *PloS one* **7**: e48503.
154. Rao, L, Modha, D, and White, E (1997). The E1B 19K protein associates with lamins in vivo and its proper localization is required for inhibition of apoptosis. *Oncogene* **15**: 1587-1597.
155. Arcasoy, SM, Latoche, JD, Gondor, M, Pitt, BR, and Pilewski, JM (1997). Polycations increase the efficiency of adenovirus-mediated gene transfer to epithelial and endothelial cells in vitro. *Gene Ther* **4**: 32-38.
156. Zhao, C*, et al.* (2014). Adenovirus-mediated gene transfer in mesenchymal stem cells can be significantly enhanced by the cationic polymer polybrene. *PloS one* **9**: e92908.
157. Yin, T*, et al.* (2011). Cancer stem-like cells enriched in panc-1 spheres possess increased migration ability and resistance to gemcitabine. *International journal of molecular sciences* **12**: 1595-1604.
158. Mehta, G, Hsiao, AY, Ingram, M, Luker, GD, and Takayama, S (2012). Opportunities and challenges for use of tumor spheroids as models to test drug delivery and efficacy. *Journal of controlled release : official journal of the Controlled Release Society* **164**: 192-204.
159. Quint, K*, et al.* (2012). Pancreatic cancer cells surviving gemcitabine treatment express markers of stem cell differentiation and epithelial-mesenchymal transition. *International journal of oncology* **41**: 2093-2102.
160. He, TC, Zhou, S, da Costa, LT, Yu, J, Kinzler, KW, and Vogelstein, B (1998). A simplified system for generating recombinant adenoviruses. *Proceedings of the National Academy of Sciences of the United States of America* **95**: 2509-2514.
161. Suzuki, K, Alemany, R, Yamamoto, M, and Curiel, DT (2002). The presence of the adenovirus E3 region improves the oncolytic potency of conditionally replicative adenoviruses. *Clin Cancer Res* **8**: 3348-3359.
162. Nokisalmi, P*, et al.* (2010). Oncolytic adenovirus ICOVIR-7 in patients with advanced and refractory solid tumors. *Clin Cancer Res* **16**: 3035-3043.
163. Russell, SJ (1994). Replicating vectors for cancer therapy: a question of strategy. *Seminars in cancer biology* **5**: 437-443.
164. Lieber, A, He, CY, Kirillova, I, and Kay, MA (1996). Recombinant adenoviruses with large deletions generated by Cre-mediated excision exhibit different biological properties compared with first-generation vectors in vitro and in vivo. *Journal of virology* **70**: 8944-8960.
165. Koski, A*, et al.* (2010). Treatment of cancer patients with a serotype 5/3 chimeric oncolytic adenovirus expressing GMCSF. *Mol Ther* **18**: 1874-1884.
166. Thaci, B*, et al.* (2012). Pharmacokinetic study of neural stem cell-based cell carrier for oncolytic virotherapy: targeted delivery of the therapeutic payload in an orthotopic brain tumor model. *Cancer Gene Ther* **19**: 431-442.
167. Ahmed, AU*, et al.* (2010). Bone marrow mesenchymal stem cells loaded with an oncolytic adenovirus suppress the anti-adenoviral immune response in the cotton rat model. *Mol Ther* **18**: 1846-1856.
168. Hung, SC, Lu, CY, Shyue, SK, Liu, HC, and Ho, LL (2004). Lineage differentiation-associated loss of adenoviral susceptibility and Coxsackie-adenovirus receptor expression in human mesenchymal stem cells. *Stem Cells* **22**: 1321-1329.
169. Sotiropoulou, PA, Perez, SA, Salagianni, M, Baxevanis, CN, and Papamichail, M (2006). Characterization of the optimal culture conditions for clinical scale production of human mesenchymal stem cells. *Stem cells* **24**: 462-471.
170. Doebis, C, Ritter, T, Brandt, C, Schonberger, B, Volk, HD, and Seifert, M (2002). Efficient in vitro transduction of epithelial cells and keratinocytes with improved adenoviral gene transfer for the application in skin tissue engineering. *Transplant immunology* **9**: 323-329.
171. Jacobsen, F*, et al.* (2006). Polybrene improves transfection efficacy of recombinant replication-deficient adenovirus in cutaneous cells and burned skin. *J Gene Med* **8**: 138-146.
172. Lin, P, Correa, D, Lin, Y, and Caplan, AI (2011). Polybrene inhibits human mesenchymal stem cell proliferation during lentiviral transduction. *PloS one* **6**: e23891.
173. Bang, OY, Lee, JS, Lee, PH, and Lee, G (2005). Autologous mesenchymal stem cell transplantation in stroke patients. *Annals of neurology* **57**: 874-882.
174. Hare, JM*, et al.* (2009). A randomized, double-blind, placebo-controlled, dose-escalation study of intravenous adult human mesenchymal stem cells (prochymal) after acute myocardial infarction. *Journal of the American College of Cardiology* **54**: 2277-2286.
175. Le Blanc, K*, et al.* (2008). Mesenchymal stem cells for treatment of steroid-resistant, severe, acute graft-versus-host disease: a phase II study. *Lancet* **371**: 1579-1586.
176. Bramante, S*, et al.* (2013). Serotype chimeric oncolytic adenovirus coding for GM-CSF for treatment of sarcoma in rodents and humans. *International journal of cancer Journal international du cancer*.
177. Pesonen, S*, et al.* (2012). Integrin targeted oncolytic adenoviruses Ad5-D24-RGD and Ad5-RGD-D24-GMCSF for treatment of patients with advanced chemotherapy refractory solid tumors. *International journal of cancer Journal international du cancer* **130**: 1937-1947.
178. Zheng, S, Ulasov, IV, Han, Y, Tyler, MA, Zhu, ZB, and Lesniak, MS (2007). Fiber-knob modifications enhance adenoviral tropism and gene transfer in malignant glioma. *J Gene Med* **9**: 151-160.
179. Subramanian, T, Vijayalingam, S, and Chinnadurai, G (2006). Genetic identification of adenovirus type 5 genes that influence viral spread. *Journal of virology* **80**: 2000-2012.

180. Gros, A*, et al.* (2008). Bioselection of a gain of function mutation that enhances adenovirus 5 release and improves its antitumoral potency. *Cancer research* **68**: 8928-8937.
181. van den Hengel, SK, de Vrij, J, Uil, TG, Lamfers, ML, Sillevis Smitt, PA, and Hoeben, RC (2011). Truncating the i-leader open reading frame enhances release of human adenovirus type 5 in glioma cells. *Virology journal* **8**: 162.
182. Henderson, S, Huen, D, Rowe, M, Dawson, C, Johnson, G, and Rickinson, A (1993). Epstein-Barr virus-coded BHRF1 protein, a viral homologue of Bcl-2, protects human B cells from programmed cell death. *Proceedings of the National Academy of Sciences of the United States of America* **90**: 8479-8483.
183. Neilan, JG, Lu, Z, Afonso, CL, Kutish, GF, Sussman, MD, and Rock, DL (1993). An African swine fever virus gene with similarity to the proto-oncogene bcl-2 and the Epstein-Barr virus gene BHRF1. *Journal of virology* **67**: 4391-4394.
184. Ruggeri, B, Zhang, SY, Caamano, J, DiRado, M, Flynn, SD, and Klein-Szanto, AJ (1992). Human pancreatic carcinomas and cell lines reveal frequent and multiple alterations in the p53 and Rb-1 tumor-suppressor genes. *Oncogene* **7**: 1503-1511.
185. Yasutome, M, Gunn, J, and Korc, M (2005). Restoration of Smad4 in BxPC3 pancreatic cancer cells attenuates proliferation without altering angiogenesis. *Clinical & experimental metastasis* **22**: 461-473.
186. Alemany, R (2014). Oncolytic Adenoviruses in Cancer Treatment *Biomedicines* **2**: 36-49.
187. Kagawa, S*, et al.* (2001). Antitumor activity and bystander effects of the tumor necrosis factor-related apoptosis-inducing ligand (TRAIL) gene. *Cancer research* **61**: 3330-3338.
188. Stuckey, DW, and Shah, K (2013). TRAIL on trial: preclinical advances in cancer therapy. *Trends in molecular medicine* **19**: 685-694.
189. Kelley, SK*, et al.* (2001). Preclinical studies to predict the disposition of Apo2L/tumor necrosis factor-related apoptosis-inducing ligand in humans: characterization of in vivo efficacy, pharmacokinetics, and safety. *The Journal of pharmacology and experimental therapeutics* **299**: 31-38.
190. Szegezdi, E*, et al.* (2009). Stem cells are resistant to TRAIL receptor-mediated apoptosis. *Journal of cellular and molecular medicine* **13**: 4409-4414.
191. Secchiero, P*, et al.* (2008). Tumor necrosis factor-related apoptosis-inducing ligand promotes migration of human bone marrow multipotent stromal cells. *Stem Cells* **26**: 2955-2963.
192. van Dijk, M, Halpin-McCormick, A, Sessler, T, Samali, A, and Szegezdi, E (2013). Resistance to TRAIL in non-transformed cells is due to multiple redundant pathways. *Cell death & disease* **4**: e702.
193. Dong, F*, et al.* (2006). Eliminating established tumor in nu/nu nude mice by a tumor necrosis factor-alpha-related apoptosis-inducing ligand-armed oncolytic adenovirus. *Clin Cancer Res* **12**: 5224-5230.
194. Jimenez, JA*, et al.* (2010). Antitumor activity of Ad-IU2, a prostate-specific replication-competent adenovirus encoding the apoptosis inducer, TRAIL. *Cancer Gene Ther* **17**: 180-191.
195. Sova, P*, et al.* (2004). A tumor-targeted and conditionally replicating oncolytic adenovirus vector expressing TRAIL for treatment of liver metastases. *Mol Ther* **9**: 496-509.
196. Zhou, W*, et al.* (2011). Treatment of patient tumor-derived colon cancer xenografts by a TRAIL gene-armed oncolytic adenovirus. *Cancer Gene Ther* **18**: 336-345.
197. Ibrahim, SM*, et al.* (2001). Pancreatic adenocarcinoma cell lines show variable susceptibility to TRAIL-mediated cell death. *Pancreas* **23**: 72-79.
198. Khanbolooki, S*, et al.* (2006). Nuclear factor-kappaB maintains TRAIL resistance in human pancreatic cancer cells. *Mol Cancer Ther* **5**: 2251-2260.
199. Matsuzaki, H*, et al.* (2001). Combination of tumor necrosis factor-related apoptosis-inducing ligand (TRAIL) and actinomycin D induces apoptosis even in TRAIL-resistant human pancreatic cancer cells. *Clin Cancer Res* **7**: 407-414.
200. Zhang, L, and Fang, B (2005). Mechanisms of resistance to TRAIL-induced apoptosis in cancer. *Cancer Gene Ther* **12**: 228-237.
201. Wang, W, Abbruzzese, JL, Evans, DB, Larry, L, Cleary, KR, and Chiao, PJ (1999). The nuclear factor-kappa B RelA transcription factor is constitutively activated in human pancreatic adenocarcinoma cells. *Clin Cancer Res* **5**: 119-127.
202. Kallifatidis, G*, et al.* (2009). Sulforaphane targets pancreatic tumour-initiating cells by NF-kappaB-induced antiapoptotic signalling. *Gut* **58**: 949-963.
203. Sayers, TJ, and Murphy, WJ (2006). Combining proteasome inhibition with TNF-related apoptosis-inducing ligand (Apo2L/TRAIL) for cancer therapy. *Cancer immunology, immunotherapy : CII* **55**: 76-84.
204. Dieterle, A*, et al.* (2009). The Akt inhibitor triciribine sensitizes prostate carcinoma cells to TRAIL-induced apoptosis. *International journal of cancer Journal international du cancer* **125**: 932-941.
205. Shenoy, K, Wu, Y, and Pervaiz, S (2009). LY303511 enhances TRAIL sensitivity of SHEP-1 neuroblastoma cells via hydrogen peroxide-mediated mitogen-activated protein kinase activation and up-regulation of death receptors. *Cancer research* **69**: 1941-1950.
206. Kaliberov, SA*, et al.* (2006). Combination of cytosine deaminase suicide gene expression with DR5 antibody treatment increases cancer cell cytotoxicity. *Cancer Gene Ther* **13**: 203-214.
207. Shi, X, Liu, S, Kleeff, J, Friess, H, and Buchler, MW (2002). Acquired resistance of pancreatic cancer cells towards 5-Fluorouracil and gemcitabine is associated with altered expression of apoptosis-regulating genes. *Oncology* **62**: 354-362.
208. Tsujie, M*, et al.* (2007). Human equilibrative nucleoside transporter 1, as a predictor of 5-fluorouracil resistance in human pancreatic cancer. *Anticancer research* **27**: 2241-2249.

209. MacMillan, WE, Wolberg, WH, and Welling, PG (1978). Pharmacokinetics of fluorouracil in humans. *Cancer research* **38**: 3479-3482.
210. Schilsky, RL (1998). Biochemical and clinical pharmacology of 5-fluorouracil. *Oncology (Williston Park)* **12**: 13-18.
211. Perry, M (2008). *The Chemotherapy Source Book*, Lippincott Williams & Wilkins.
212. Vermes, A, Guchelaar, HJ, and Dankert, J (2000). Flucytosine: a review of its pharmacology, clinical indications, pharmacokinetics, toxicity and drug interactions. *The Journal of antimicrobial chemotherapy* **46**: 171-179.
213. Mesnil, M, Piccoli, C, Tiraby, G, Willecke, K, and Yamasaki, H (1996). Bystander killing of cancer cells by herpes simplex virus thymidine kinase gene is mediated by connexins. *Proceedings of the National Academy of Sciences of the United States of America* **93**: 1831-1835.
214. Yang, L*, et al.* (1998). Intercellular communication mediates the bystander effect during herpes simplex thymidine kinase/ganciclovir-based gene therapy of human gastrointestinal tumor cells. *Hum Gene Ther* **9**: 719-728.
215. Diallo, JS, Roy, D, Abdelbary, H, De Silva, N, and Bell, JC (2011). Ex vivo infection of live tissue with oncolytic viruses. *Journal of visualized experiments : JoVE*.
216. Kurata, N*, et al.* (2011). Predicting the chemosensitivity of pancreatic cancer cells by quantifying the expression levels of genes associated with the metabolism of gemcitabine and 5-fluorouracil. *International journal of oncology* **39**: 473-482.
217. Eggenhofer, E*, et al.* (2012). Mesenchymal stem cells are short-lived and do not migrate beyond the lungs after intravenous infusion. *Frontiers in immunology* **3**: 297.
218. Schrepfer, S, Deuse, T, Reichenspurner, H, Fischbein, MP, Robbins, RC, and Pelletier, MP (2007). Stem cell transplantation: the lung barrier. *Transplantation proceedings* **39**: 573-576.
219. Crop, MJ*, et al.* (2010). Inflammatory conditions affect gene expression and function of human adipose tissue-derived mesenchymal stem cells. *Clinical and experimental immunology* **162**: 474-486.
220. Curcio, E, Salerno, S, Barbieri, G, De Bartolo, L, Drioli, E, and Bader, A (2007). Mass transfer and metabolic reactions in hepatocyte spheroids cultured in rotating wall gas-permeable membrane system. *Biomaterials* **28**: 5487-5497.
221. Lin, RZ, and Chang, HY (2008). Recent advances in three-dimensional multicellular spheroid culture for biomedical research. *Biotechnology journal* **3**: 1172-1184.
222. Grill, J*, et al.* (2002). The organotypic multicellular spheroid is a relevant three-dimensional model to study adenovirus replication and penetration in human tumors in vitro. *Mol Ther* **6**: 609-614.
223. Wang, L, Mezencev, R, Bowen, NJ, Matyunina, LV, and McDonald, JF (2012). Isolation and characterization of stem-like cells from a human ovarian cancer cell line. *Molecular and cellular biochemistry* **363**: 257-268.
224. Lam, JT*, et al.* (2007). A three-dimensional assay for measurement of viral-induced oncolysis. *Cancer Gene Ther* **14**: 421-430.
225. Huszthy, PC*, et al.* (2008). Oncolytic herpes simplex virus type-1 therapy in a highly infiltrative animal model of human glioblastoma. *Clin Cancer Res* **14**: 1571-1580.
226. Baek, SJ, Kang, SK, and Ra, JC (2011). In vitro migration capacity of human adipose tissue-derived mesenchymal stem cells reflects their expression of receptors for chemokines and growth factors. *Experimental & molecular medicine* **43**: 596-603.
227. Ponte, AL*, et al.* (2007). The in vitro migration capacity of human bone marrow mesenchymal stem cells: comparison of chemokine and growth factor chemotactic activities. *Stem Cells* **25**: 1737-1745.
228. Liu, H*, et al.* (2010). Hypoxic preconditioning advances CXCR4 and CXCR7 expression by activating HIF-1alpha in MSCs. *Biochemical and biophysical research communications* **401**: 509-515.
229. Kim, SM*, et al.* (2010). Irradiation enhances the tumor tropism and therapeutic potential of tumor necrosis factor-related apoptosis-inducing ligand-secreting human umbilical cord blood-derived mesenchymal stem cells in glioma therapy. *Stem Cells* **28**: 2217-2228.
230. Klopp, AH*, et al.* (2007). Tumor irradiation increases the recruitment of circulating mesenchymal stem cells into the tumor microenvironment. *Cancer research* **67**: 11687-11695.
231. Zielske, SP, Livant, DL, and Lawrence, TS (2009). Radiation increases invasion of gene-modified mesenchymal stem cells into tumors. *International journal of radiation oncology, biology, physics* **75**: 843-853.
232. Kidd, S*, et al.* (2009). Direct evidence of mesenchymal stem cell tropism for tumor and wounding microenvironments using in vivo bioluminescent imaging. *Stem Cells* **27**: 2614-2623.
233. Kidd, S, Spaeth, E, Klopp, A, Andreeff, M, Hall, B, and Marini, FC (2008). The (in) auspicious role of mesenchymal stromal cells in cancer: be it friend or foe. *Cytotherapy* **10**: 657-667.
234. Djouad, F*, et al.* (2003). Immunosuppressive effect of mesenchymal stem cells favors tumor growth in allogeneic animals. *Blood* **102**: 3837-3844.
235. El-Haibi, CP*, et al.* (2012). Critical role for lysyl oxidase in mesenchymal stem cell-driven breast cancer malignancy. *Proceedings of the National Academy of Sciences of the United States of America* **109**: 17460-17465.
236. Houghton, J*, et al.* (2004). Gastric cancer originating from bone marrow-derived cells. *Science* **306**: 1568-1571.
237. Mader, EK*, et al.* (2013). Optimizing patient derived mesenchymal stem cells as virus carriers for a phase I clinical trial in ovarian cancer. *Journal of translational medicine* **11**: 20.
238. Welch, DR*, et al.* (1991). Characterization of a highly invasive and spontaneously metastatic human malignant melanoma cell line. *International journal of cancer Journal international du cancer* **47**: 227-237.
239. Dmitriev, I*, et al.* (1998). An adenovirus vector with genetically modified fibers demonstrates expanded tropism via utilization of a coxsackievirus and adenovirus receptor-independent cell entry mechanism. *Journal of virology* **72**: 9706-9713.

240. Lawrence, WC, and Ginsberg, HS (1967). Intracellular uncoating of type 5 adenovirus deoxyribonucleic acid. *Journal of virology* **1**: 851-867.
241. Maizel, JV, Jr., White, DO, and Scharff, MD (1968). The polypeptides of adenovirus. I. Evidence for multiple protein components in the virion and a comparison of types 2, 7A, and 12. *Virology* **36**: 115-125.
242. Karber, G (1931). 50% end-point calculation. *Arch Exp Pathol Pharmak* **162**: 480-483.

# 12. Publications

Hammer K, Kaczorowski A, Liu L, Schemmer P, Herr I, Nettelbeck D (2014). Engineered Adenoviruses Combine Enhanced Oncolysis with Improved Virus Production by Mesenchymal Stromal Carrier Cells. Submitted.

Fernandez-Ulibarri I, Hammer K, Arndt M, Dorer D, Engelhardt S, Kontermann R, Hess J, Allgayer H, Krauss J, Nettelbeck D (2014). Genetic Delivery of an ImmunoRNAse by an Oncolytic Adenovirus Enhances Anticancer Activity. Submitted.

Boehme KW, Hammer K, Tollefson WC, Konopka-Anstadt JL, Kobayashi T, Dermody TS (2013). Nonstructural protein σ1s mediates reovirus-induced cell cylce arrest and apoptosis. J Virol 87(23): 12967-79.

Zeller E, Hammer K, Kirschnick M, Braeuning A (2013). Mechanisms of Ras/β-Catenin interactions. Arch Toxicol. 87(4):611-32.

# 13. Acknowledgments

My sincere thanks go to Dirk Nettelbeck for giving me the opportunity to work on this exciting project and for his committed support in all matters connected to the scientific work.

Further, I would like to thank the former lab members of the Nettelbeck group and especially Inés Fernández Ulibarri, for helpful advice and enjoyable company. I also would like to single out Sarah Engelhardt and would like to thank her for her helping hand and good humor.

I would like to thank Ingrid Herr and Adam Kaczorowski for the collaboration on this project, for sharing their expertise in working with MSCs and low-passage cultures, and for providing MSCs, spheroids, and other material for the project. I would especially like to thank Li Liu from the group of Ingrid Herr for the help with the establishing of the migration assay.

I would further like to thank Martin Müller, Dirk Grimm, and Suat Özbek for evaluation of my thesis.

Finally my deepest thanks go to my parents for their guidance, support, and advice, to my sister Maria, and especially to Andreas Wiedemann for his patience, support, and humor at all times.